SEMICLASSICAL QUANTIZATION
IN MANY DIMENSIONS

thesis by

Roy David Williams

In Partial Fulfillment of the Requirements
For the Degree of
Doctor of Philosophy

California Institute of Technology
Pasadena, California
1983

(Submitted: April 25, 1983)

Acknowledgements

Abstract

We examine the semiclassical limit of the quantum energy spectrum in many dimensions: by means of a WKB-like ansatz leading to Einstein-Brillouin-Keller (EBK) quantization, by means of a path integral, hence associating a bound state with a particular classical periodic trajectory, and by the Birkhoff-Gustavson (BG) transformation to action-angle variables. We extend the EBK method to many-fermion systems using coherent states; and apply both EBK using surfaces of section, and the BG transformation to an SU(3) schematic nuclear shell model. We describe a new algorithm for finding periodic trajectories of a Lagrangian system with polynomial potential. It is applied to the Henon-Heiles system with good results, and these trajectories are used to quantize the system. The EBK and BG methods have some success, while periodic trajectory quantization fails. We discuss possible reasons for this failure and future approaches to these problems.

Contents

Tables

Figures

§1. Introduction

It took classical mechanics 100 years to find a clear mathematical framework, from Newton's Principia Mathematica in 1687 to Lagrange's Mechanique Analytique in 1788. Another 100 years elapsed before serious doubts appeared about the universal applicability of classical concepts. The main difficulties had to do with the existence of energy levels in atoms and molecules. Balmer's formula for the frequencies of the hydrogen spectrum was published in 1885. This particular puzzle found a preliminary resolution in Bohr's model of 1912, but the definitive answer was given by Schrödinger in 1926, and was found to be totally satisfactory in all applications to atomic, molecular, and solid-state physics.

This complete success has led most physicists to neglect further inquiry into the transition from classical to quantum mechanics. Bohr's atom and the more general results of Sommerfeld and others are presented in all textbooks on quantum mechanics as satisfactory explanations for the way in which classical mechanics is able to give good answers when properly modified. The argument is always based on the method of Wentzel, Kramers, and Brillouin and it is always applied either to problems of one degree of freedom, or to problems where the variables can be separated by the appropriate choice of coordinate system. This creates the illusion of being a generally valid condition, and induces not only the reader, but also the author, into believing that all interesting cases have been covered. However, it was soon realized that often these quantization rules are insufficient, for example in the case of the helium atom, and in 1917 Einstein (Ei17) found the most general conditions which a mechanical system must satisfy for the applicability of the Bohr-Sommerfeld rules. With modifications by Brillouin and Keller, this was

the basis of the EBK quantization method, (Ei17, Ke58), discussed in §3.

This thesis is concerned with the behavior of a non-relativistic quantum-mechanical system in the limit $\hbar \to 0$. Of course $\hbar$ is a fixed and measurable constant which does not vary; the meaning of the limit is that the parameters of the problem vary in such a way as to simulate a change in $\hbar$. For example, in the Schrödinger equation,

$$\left[-\frac{\hbar^2}{2m} \nabla^2 + V(x) \right] \psi(x) = E\,\psi(x) \ , \tag{1.1}$$

if we increase the mass by some large factor B^2, we make the system more classical, or equivalently we can decrease $\hbar$ by the factor B.

Classical mechanics is the approximation obtained when $\hbar$ is set identically to zero, and semiclassical mechanics is a power series in $\hbar$ for the quantum observables. The series is only asymptotically convergent (see for example Ba79) since it ultimately depends on a stationary phase approximation. Thus the series can be made arbitrarily accurate only by taking small enough $\hbar$, rather than by taking sufficiently many terms. In spite of this problem, we hope to extract some useful quantum properties, in particular the bound-state energies.

Classical mechanics itself has advanced during the twentieth century, particularly in regard to the global structure of the phase space (Li83, He80 are good reviews). The most notable achievement is the celebrated Kolmogorov-Arnold-Moser (KAM) theorem of 1953 (Ko53), stating that when several analytically soluble systems are combined with sufficiently weak coupling, then the motion has the same smooth structure as the integrable motion with no coupling. Classical mechanics has also gained a whole new vocabulary, with transitions to chaos, strange

attractors, bifurcations, and entropy (Li83). It would be fruitful indeed to find how these concepts manifest themselves in the underlying quantum mechanics.

In addition to the EBK quantization method, there is a method based on the path integral. The use of the path integral in quantum mechanics was pioneered by Feynman (Fe56), and the quantization method formulated by Gutzwiller (Gu73). The path integral approach consists of writing down a formal expression for quantum observables in terms of classical concepts such as the Lagrangian function, and from this expression one can derive the complete apparatus of quantum mechanics, or alternatively use the stationary phase approximation to derive classical mechanics. In addition, using the same approximation in a different way, one can obtain a quantization rule, quite different from the EBK method. In one dimension both methods reduce to the familiar WKB approximation, which works very well, because the phase space of a system of one degree of freedom is so simple. Other quantization methods have been suggested, which are perturbation expansions about a stable fixed point of the potential. The Birkhoff-Gustavson transformation (Bi66) is an algebraic method of finding a power-series expression for the action-angle variables, which is divergent, but still useful close to the fixed point. Another method, suggested by Born and used by Chapman, Garrett, and Miller (Ch76), uses a Fourier series for the action-angle variables instead of a power series.

In addition to the intrinsic interest in the connection between quantum and classical mechanics, there would be much practical utility in such an understanding. For example, intramolecular dynamics is the study of the motion of objects large enough to have definite classical

motion, but with quantum properties also. For a good review of the extensive literature, see Rice, (Ri80). Another example is nuclear physics, where the large number of identical particles and the coherent interaction between them causes the system to behave classically (i.e., collectively), yet the many-body wave-function contains so much information that extracting useful properties is often very difficult, ambiguous, and arbitrary. Classical mechanics, however, is a minimal description of the system, and generally much more tractable. The phenomenologically successful Time-Dependent Hartree-Fock approximation and other mean-field theories (Ne82, Ko81, and references therein) are classical theories, and offer hope of achieving tractable descriptions of a variety of properties of the nucleus. Among these are bound-state energies (Kl77, Le80), the nuclear partition function, spontaneous and induced fission lifetimes (Ke81), and elements of the many-body S-matrix (Al81). Periodic trajectory quantization has been suggested for TDHF (Ka79), and the WKB method has been used successfully in a schematic two-level shell model (Le80, Sh80, Ka79), and in certain Interacting Boson Hamiltonians (Di80). The full EBK quantization in two dimensions has been applied to a schematic three-level shell model, with some success (Wi82 and §12). In addition to bound states, it may be that a classical description can offer novel insights into level densities, collectivity, doorway states, and giant resonances.

Each quantization method has drawbacks. The EBK method, as pointed out by Einstein, can only be used when the classical trajectories in phase space are regular in the sense of KAM, that is for sufficiently small excitation energies. The path-integral method associates a particular periodic orbit of the system with a bound state, and is shown in §13 to

fail for a particular system. Another formulation, by Berry and Tabor (Be76, Ta83), associates the whole set of periodic orbits with the whole spectrum, and has had some success, although the method is extremely difficult to implement. There has also been much practical work on quantization, mostly with the EBK method, which is easier to use than the periodic trajectory method (Ca77, Ea74). The EBK method gives good results when the system under investigation is well-behaved, but for our example, the SU(3) schematic nuclear shell model, the method fails when the potential ceases to be harmonic. Quantization by periodic trajectories has been used successfully by Balian and Bloch (Ba77), and by Berry (Be81), on systems which consist of a particle bouncing freely within some arrangement of hard walls, and also by Tabor for a simple map of the plane to itself, which can be made to look like a quantum or classical dynamical system (Ta83). Gutzwiller (Gu77) makes an isomorphism between the periodic trajectories of the anisotropic Kepler problem and periodic binary sequences, and has thereby quantized this system with good results. This is completely contrary to our attempt with the Henon-Heiles potential, §13, which gives nonsensical results. All previous work uses an analytic method of reducing the numerical problem of finding periodic orbits to one dimension, or of analytically calculating the orbits themselves. There has been no attempt until now, as far as we know, to test the method in the more general case, where no such analytical aids are available. We find that the set of periodic trajectories is very complex, much more so than a previous study of the same problem indicates, and feel that it is only the choice of a system that can be analytically reduced that makes this quantization method work.

This thesis is thus an attempt to quantitatively test quantization methods. Section 2 discusses the classical mechanics that we shall need. We introduce the concept of an isolating constant of the motion, and show that the existence of a complete set of these constants is equivalent to a solution for all time of Hamilton's equations. Furthermore, the KAM theorem is stated and made plausible: that the system retains a complete set of isolating constants under sufficiently small perturbations.

Sections 3 and 4 derive the theory and technique of EBK quantization. We show that approximating of the bound-state wave-function by a slowly changing amplitude and phase is self-consistent, and that separating the Schrödinger equation in powers of $\hbar$ leads to the Hamilton-Jacobi equation and to Liouville's theorem. The quantization condition then arises from demanding that the wave-function be single valued. We can view the phase space of the classical system using surfaces of section, and we discuss the example of the Henon-Heiles potential. In addition, we can use the areas of closed curves on the section to implement EBK quantization. Section 5 generalizes the EBK method to many-fermion systems, by converting the second-quantized Hamiltonian to a partial differential operator in a space of coherent states. The many-fermion problem then resembles a Schrödinger equation, and is accessible to the EBK quantization method.

In section 6 we derive the path-integral expression for the quantum propagator in Hamiltonian form, and reduce it to Lagrangian form. Section 7 proves the stationary phase approximation in one and then in many dimensions. Section 8 derives in detail a new algorithm for finding periodic trajectories of a Lagrangian system with polynomial potential. The algorithm can move along the continuous families of periodic

trajectories, and calculate the stability index and its rate of change along the family. Section 9 brings together the ideas of the preceeding three sections, and uses them to obtain the prescription for quantization by periodic trajectories. This prescription involves the stability index, its rate of change with period, and the Maslov index, which is shown to be equal to the number of conjugate points on the trajectory modulo 4. Section 10 discusses a partial unification of the two methods, and their drawbacks. EBK fails in the chaotic part of phase space, and the periodic trajectory method ignores the "topology" of the periodic trajectories. Section 11 develops the algebraic Birkhoff-Gustavson quantization method. The system is assumed to be a set of coupled harmonic oscillators, and to have action-angle variables. The energy is developed as a power series in the putative action variables, so that the quantization is then trivial. The method only works if the original oscillators have incommensurate frequencies, and the power series is always divergent, but still useful if treated as an asymptotic series.

Section 12 describes the application of the methods of sections 5, 3, and 4, and also 11 to the SU(3) schematic nuclear shell-model, with results that indicate that EBK quantization only works if the system is close to harmonic, and that the same is true of the Birkhoff-Gustavson method. Section 13 deals with the Henon-Heiles potential. We calculate the exact quantum energies by perturbation theory of a potential which is the same as the Henon-Heiles in the region of interest, and describe the computation and results from the periodic trajectory algorithm of section 8. We find a large number of periodic trajectories, and period-multiplying bifurcations of two types. We find that the quantization prescription developed in section 9 gives incorrect results.

Section 14, which contains the conclusions, gives possible reasons for the partial failure of EBK quantization and the complete failure of quantization by periodic trajectories. We also suggest some possible approaches for further work.

§2. Integrable and Non-Integrable Systems.

Most scientists appear to be under the impression that classical mechanics is straightforward. With few exceptions (e.g., Ar78, Li83) the textbooks consider only those dynamical systems with one degree of freedom, or systems that can be separated into several such; in these cases all quantities of interest can be computed by quadrature. In fact the phase space of most systems is dotted or even filled with chaotic regions, in which the time-evolution of the deterministic system satisfies essentially all known tests for randomness (Ra74), even for a system of only two degrees of freedom. These chaotic regions were known to Poincaré, (Po92), and to Einstein, (Ei17), but the physics community seems to have been more excited by quantum mechanics for the last sixty years. While the existence of chaotic regions may be pleasing to those in statistical mechanics, who have assumed them all along, it is frightening to the designers of extensive mechanical systems, for example the intersecting storage rings of high energy physics. Before we embark on a study of semiclassical quantization, we ought to know what complexities await us in the classical description of a quantum system. In particular, we will see in §3 that the EBK quantization method works only when the phase space is regular, in a sense defined below.

Given a Hamiltonian dynamical system of N degrees of freedom,

$$\dot{q} = \partial H(q,p)/\partial p \qquad (2.1)$$

$$\dot{p} = -\partial H(q,p)/\partial q$$

and the initial conditions q^0 and p^0, the values of q and p can be found for any time t,

$$q = q(t,q^0,p^0) \quad \text{and} \quad p = p(t,q^0,p^0) , \tag{2.2}$$

and can, in principle, be solved for the initial conditions q^0 and p^0, giving $2N$ functions of the phase space variables which are constant along any trajectory of the system. Elimination of the time leaves $2N-1$ constants C_j which completely determine the system trajectory in phase space. Finding these constants, however is a nasty problem, and can only be done for very simple systems; the only obvious such constant is the conserved energy.

Fixing one of these constants defines a $2N-1$ dimensional hypersurface in phase space, and so each constant can be one of two types. Some are isolating, in the sense that the domain of phase space to which they restrict the trajectory is compact and readily partitioned from the rest of phase space. Others, apparently the vast majority, are nonisolating. The energy is isolating, since it is not difficult to find its contours in phase space. The distinction between these two classes of constant is evident from the example of two harmonic oscillators of frequencies ω_1, ω_2. The cooordinates and momenta satisfy

$$p_i \cos \omega_i t + \omega_i q_i \sin \omega_i t = p_i^0 , \tag{2.3}$$

$$\omega_i q_i \cos \omega_i t - p_i \sin \omega_i t = \omega_i q_i^0 , \text{ for } i = 1, 2 .$$

We can eliminate t for each i to get two energy integrals, and eliminate t between $i = 1$ and 2, to obtain a third integral C_3. The nature of C_3 depends on the ratio $\sigma = \omega_1/\omega_2$: for rational σ, the trajectory is a closed curve, and C_3 is a multivalued function with a finite number of branches. On the other hand, if the σ is irrational, the trajectory densely fills the phase space which is available by conservation of the two energies, i.e., a

rectangle in the q_1, q_2 plane, and the integral C_3 is a pathological function, with an infinite number of branches. For rational σ, C_3 is an isolating integral of the motion, but not when σ is irrational.

An alternative view of dynamics is given by Hamilton-Jacobi theory. This representation is based on finding a canonical transformation to action-angle variables (I, ϑ), so that the Hamiltonian is only a function of the action variables. In that case, the motion is trivially integrable, so the actions are constant, and the angles increase linearly with time at a rate $\omega \equiv \partial H / \partial I$. The action variables are then a complete set of isolating constants of the motion. They are isolating because it easy to identify the hyperplanes of constant action given $H(I)$, yet the hyperplanes of constant initial condition (solutions of (2.2)) become arbitrarily contorted after long enough evolution time. The motion is then topologically equivalent to a set of uncoupled harmonic oscillators: incommensurate frequencies cause the phase space to be densely filled.

We can generalize this idea of filling phase space as follows. Suppose we follow the motion of single point for an unlimited period of time, and think of the corresponding trajectory traced out in phase space. There are two possibilities, either that there is a $2N$-dimensional subspace such that the trajectory comes arbitrarily close to every point of the subspace, or that the trajectory stays within a space of less than $2N$ dimensions. The resulting manifold is then called an invariant submanifold. If it is true that the trajectory stays on a submanifold of the whole phase space, then that submanifold must have the topology of a torus, as is clear from the "hairy-coconut" theorem: the Hamiltonian velocity is always in the tangent space of the submanifold, and is nowhere zero or infinite, so the topology cannot be spherical. In other words, it is impossible to comb the

hair on a spherical topology without a singularity.

Let us now consider a system which is almost integrable. For small ε,

$$H_\varepsilon(I,\vartheta) = H_0(I) + \varepsilon H_1(I,\vartheta) \ . \tag{2.4}$$

The traditional view was that in general the system is no longer integrable for any non-zero ε. This is not true, though, and the system is still integrable for sufficiently small ε. This is the content of the monumental Kolmogorov-Arnold-Moser theorem (Ko53), one of the few really general and powerful results concerning the global behavior of the trajectories. We must suppose that the frequencies ω serve as a local coordinate system:

$$\det \frac{\partial^2 H_0}{\partial I^2} \neq 0 \tag{2.3}$$

and that the frequencies are not "too rational": there must be constants $C > 0$, $\mu > 0$ so that for all integer vectors $\vec{k}$, $|\vec{\omega} \cdot \vec{k}| > C |\vec{k}|^{-\mu}$. Under these conditions, and for sufficiently small $|\varepsilon|$, most of phase space is filled with invariant tori which are continuous deformations of the original $\varepsilon = 0$ tori. In other words a canonical transformation exists from the action-angle variables for H_0 to action-angle variables for H_ε, although the transformation may not exist throughout phase space.

We can make the theorem plausible as follows. Suppose that H_ε is expanded in a Fourier series, and one term dominates:

$$H = H_0(I) + \varepsilon f_{mn}(I) \cos(m\vartheta_1 + n\vartheta_2) + \cdots \tag{2.5}$$

Then we can remove the angle-dependent term by a canonical transformation to variables J, φ with generating function,

$$F_2(I,\varphi) = I_1\varphi_1 + I_2\varphi_2 + \varepsilon B_{mn}(I)\sin(m\varphi_1 + n\varphi_2) \ , \qquad (2.6)$$

$$\text{so} \quad J_1 = \partial F_2/\partial\varphi_1 = I_1 + \varepsilon B_{mn}m\cos(m\varphi_1 + n\varphi_2)$$

$$J_2 = \partial F_2/\partial\varphi_2 = I_2 + \varepsilon B_{mn}n\cos(m\varphi_1 + n\varphi_2)$$

so the new Hamiltonian K is given by

$$K(J,\varphi) = H_0(J) + \varepsilon[f_{mn} - B_{mn}(m\omega_1 + n\omega_2)]\cos(m\varphi_1 + n\varphi_2)$$

$$+ O(\varepsilon^2) \ , \qquad (2.7)$$

where the ω's are the unperturbed frequencies. Thus we can solve for B_{mn} to make K integrable,

$$B_{mn} = \frac{f_{mn}}{m\omega_1 + n\omega_2} \ , \qquad (2.8)$$

and we conclude that B_{mn} is small only if the frequencies are incommensurable.

The phase space of a non-integrable system thus splits into regular regions filled with invariant tori, and the rest is generally chaotic. If there is an elliptic fixed point, that is, a stable equilibrium point, then the infinitesimal variations around it will be harmonic, and the motion will be regular (He80). As the non-linearity increases, the motion gradually becomes chaotic. In the case of a particle in a potential well, this non-linearity parameter is the excitation energy. In general there are regular regions containing chaotic regions, which in turn contain regular regions, and so on in an infinite hierarchy (Ar78), and in addition there are periodic orbits sprinkled liberally around the whole phase space.

One of the conditions for the applicability of the KAM theorem is the

absence of resonances, i.e., the unperturbed frequencies must have a frequency ratio that is "far" from rational. This is the old problem of "small divisors", inherited from nineteenth century celestial mechanics. A Fourier series (more correctly, a Poisson series) for the gravitational force between two planets in Kepler orbits is a sum of terms $c_{\vec{k}}\exp(i\vec{k}\cdot\omega)$ over all integer vectors $\vec{k}$, and so a time-integral of this series, which is the velocity perturbation, will be divergent if $\vec{k}\cdot\omega = 0$. Since the rational numbers are dense in the reals, this problem threatens for all combinations of frequencies and is the reason for the complexity of many-dimensional classical mechanics. Of course, in the one-dimensional case, there is only one frequency, so this difficulty vanishes.

§3. Einstein-Brillouin-Keller Quantization.

In this section we shall derive and generalize the WKB method (Fr65) to many dimensions, and show that it works only when the phase space is smooth in the sense of KAM. The generalized method, formulated by Einstein, Brillouin, and Keller (Ei17, Ke58, Li83), associates a particular invariant torus with a quantum bound state, and clearly such tori must exist (which satisfy the quantization condition) for the method to work.

We start with a Schrödinger equation in an N dimensional space, written in terms of "coordinate" and "momentum" operators q and $p = -i\hbar\partial/\partial q$, which are each N-dimensional vectors in the space and its dual respectively. The time-dependent Schrödinger equation is

$$i\hbar\frac{\partial}{\partial t}\psi(q) = H(q,p)\,\psi(q) \tag{3.1}$$

where ψ is the wave-function. We make a WKB-like ansatz,

$$\psi(q) = A(q)\,\exp(iS(q)/\hbar) \ , \tag{3.2}$$

with A and S real functions which are assumed to vary smoothly. The Schrödinger equation becomes

$$i\hbar\frac{\partial A}{\partial t} - A\frac{\partial S}{\partial t} = e^{-iS/\hbar}\,H(q,p)\,A\,e^{iS/\hbar} \ . \tag{3.3}$$

Now $e^{-iS/\hbar}$ is a unitary linear operator, which leaves q unchanged, and transforms p as follows,

$$e^{-iS/\hbar}p\,e^{iS/\hbar} = p + \partial S/\partial q \ , \tag{3.4}$$

so that (3.3) becomes

$$i\hbar\frac{\partial A}{\partial t} - A\frac{\partial S}{\partial t} = H(q,p + \frac{\partial S}{\partial q})\,A \tag{3.5}$$

When $\hbar$ is identically zero, p is zero, since it is $-i\hbar\partial/\partial q$ and has a factor $\hbar$ and (3.5) becomes

$$-\frac{\partial S}{\partial t} = H(q, \frac{\partial S}{\partial q}) \tag{3.6}$$

which is the Hamilton-Jacobi equation of classical mechanics. It allows S to be real, and shows that the WKB ansatz does not lead to an inconsistency. We now take the first order terms in $\hbar$ in order to extract the equation satisfied by the amplitude A. A direct evaluation of these terms is awkward for a general H, and is easiest (Di58) by multiplying first by Af, where f is an arbitrary real function and integrating over the space. In bra-ket notation, with $<A|B> = \int d^N q\, A(q)\, B(q)$,

$$<Af \mid i\hbar\frac{\partial A}{\partial t} - A\frac{\partial S}{\partial t}> = <Af \mid H(q,p + \frac{\partial S}{\partial q})\, A> \ . \tag{3.7}$$

Subtracting the complex conjugate equation gives

$$2i\hbar<Af \mid \frac{\partial A}{\partial t}> = <A\, [f,H]\, A> \tag{3.8}$$

where [] represents the commutator. Expanding the commutator,

$$[f,H] = i\hbar\frac{\partial f}{\partial q} H_p \ , \tag{3.9}$$

$$\text{where} \quad H_p \equiv \left[\frac{\partial H(q,p)}{\partial p}\right]_{p\,=\,\partial S/\partial q}$$

meaning that we substitute $\partial S/\partial q$ for p in the derivative of H. Thus (3.8) becomes

$$<f\frac{\partial A^2}{\partial t}> = <A^2\, \frac{\partial f}{\partial q} H_p> = -<f\, \frac{\partial}{\partial q}(A^2 H_p)> \ , \tag{3.10}$$

where we have integrated by parts. Since this holds for an arbitrary function f, we conclude that

$$\frac{\partial A^2}{\partial t} = -\frac{\partial}{\partial q}[A^2 H_p] \tag{3.11}$$

which states physically that the square amplitude A^2 is the density of a fluid of velocity H_p, whose total mass is conserved, or in other words it is a statement of Liouville's theorem that a closed volume of phase-space has constant volume during its (classical) evolution.

Consider the problem of finding a bound state of the quantum system from the semiclassical equations (3.6) and (3.11). For a stationary state the time dependence must be simply exponential, so we can separate the Hamilton-Jacobi equation to obtain

$$H(q, \frac{\partial S}{\partial q}) = E \tag{3.12}$$

where E is the bound-state energy.

We now take the one-dimensional harmonic oscillator as a prototype, to illustrate the quantization procedure. The Hamiltonian is simply $H(q,p) = \frac{1}{2}p^2 + \frac{1}{2}q^2$, so the Hamilton-Jacobi equation can be solved directly:

$$\frac{1}{2}(\partial S/\partial q)^2 + \frac{1}{2}q^2 = E$$

$$\rightarrow \quad S = S_0 \pm (\frac{1}{2}q(2E - q^2)^{\frac{1}{2}} + E\arcsin\frac{q}{\sqrt{2E}}) \tag{3.13}$$

where S_0 is an arbitrary constant. S is multivalued in two senses, both because of the $\pm$ sign, and because arcsin is a multivalued function. The amplitude can be found from (3.11), and since we are looking for a

stationary state, the time-derivative is zero,

$$\frac{\partial}{\partial q}[A^2 p] = 0$$

$$\rightarrow \quad A = C \, (2E - q^2)^{-1/4} \tag{3.14}$$

for some arbitrary constant C.

In the general case, we can solve the Hamilton-Jacobi equation by the method of characteristics. We parametrize the coordinate q and the value of $p \equiv \dfrac{\partial S}{\partial q}$ by a variable t, and obtain part of the solution for $S(q)$. Notice that the quantum operator p has been replaced by its classical equivalent, which is a number. The solution of (3.12) by characteristics yields a one-dimensional submanifold of the original N-dimensional space, where the submanifold and the solution are given by Hamilton's equations:

$$\dot{q} = \partial H / \partial p \tag{3.15}$$

$$\dot{p} = -\partial H / \partial q$$

so that $S(q(t)) = \int_0^t p \cdot \dot{q} \; dt$. The solutions of these equations are precisely the subject of §2. We found that the trajectory may be either chaotic or regular (KAM tori), or periodic for a given initial condition. If the trajectory is chaotic, there are somewhere between zero and infinity values of p and hence S for each value of q, and we cannot use this approach to quantize the system. If the trajectory is periodic, then the solution, and hence the wave-function, is unphysically confined to a line. However, if the trajectory lies on a KAM torus, then the one-dimensional manifold of q-values becomes an N-dimensional manifold in the limit $t \rightarrow \infty$, and there

are a finite number of values of p for a given q. This manifold is called a Lagrangian submanifold. We can extend the original WKB ansatz to a sum of such terms, one for each branch of $S(q)$. For the harmonic oscillator, we write S_+ for the (still multivalued) function using the +ve sign in (3.13), and similarly S_- for the -ve sign. The WKB ansatz is then replaced by

$$\psi(q) = A_+(q) \, e^{iS_+(q)/\hbar} + A_-(q) \, e^{iS_-(q)/\hbar}$$

$$= A(q) \, (e^{iS_+(q)/\hbar} + e^{iS_-(q)/\hbar}) \; , \qquad (3.16)$$

where $A_+ = A_-$ because they both satisfy (3.14) and the wave-function ψ is real for the oscillator. Notice that the arbitrary constant S_0 of (3.13) may be different for the two branches of S, and we shall need more input from the quantum mechanics to calculate this difference, in order to get the correct quantization condition.

If γ is a path on the Lagrangian submanifold whose q-projections at the endpoints are q and q', then

$$S(q') - S(q) = \int_\gamma p \cdot dq = \int_\gamma \nabla S \cdot dq \; . \qquad (3.17)$$

Suppose the path has equal endpoints. Then if this closed path is not continuously deformable to a point, each sheet of S will be infinitely multivalued, where the difference between sheets is the above integral evaluated for the closed curve. For the harmonic oscillator, the submanifold is a circle, and the multivaluedness is that from the arcsin function in the expression for S_+ and S_-. The quantization condition is then just the condition that the wave-function be single valued: since A is the same for each branch, and single valued, the condition is that each branch of S

be single valued modulo $2\pi\hbar$, so that when the endpoints of γ are the same, then the integral should be a multiple of $2\pi\hbar$. Since the submanifold has the topology of a torus, there are N topologically independent paths on it, and thus N quantum numbers. For the harmonic oscillator example, we can see directly that the difference between values of S_+ or S_- is $2\pi E$, from the arcsin function, so the bound-state energies are integers. However, although the spacings are correct, we know the ground state has energy $\frac{1}{2}$, and this discrepancy is remedied below.

One of the underlying assumptions of the above analysis is that the amplitude A is slowly varying, and this assumption breaks down at the edge of the classically allowed region, where A is infinite. In quantum mechanics this does not happen, and instead the wave-function takes a form charactaristic of the type of caustic (or catastrophe: see Maslov, Ma81, Berry, Be76) present. The simplest such catastrophe is the fold, which is the generic case and was analyzed by Airy (Ai38), where the classical edge takes the form of a linear hill. This is the case for the harmonic oscillator example. Let us examine the wave-function close to the classical edge, at $q = \sqrt{2\bar{E}}$. The Schrödinger equation is

$$(-\frac{\hbar^2}{2}\frac{d^2}{dq^2} + \frac{1}{2}q^2)\psi = E\psi(q)$$

$$\rightarrow (-\frac{\hbar^2}{2}\frac{d^2}{dq^2} + \frac{1}{2}(q - \sqrt{2\bar{E}})^2 + \sqrt{2\bar{E}}(q - \sqrt{2\bar{E}}))\psi = 0 \qquad (3.18)$$

and neglecting the term $(q - \sqrt{2\bar{E}})^2$ since we are close to the edge, we can solve (3.18) to get an Airy function (Ab64),

$$\psi(q) = \text{Ai}\left[\left[\frac{2\sqrt{2\bar{E}}}{\hbar^2}\right]^{1/3}(\sqrt{2\bar{E}} - q)\right]$$

$$\sim K \, (q \, - \, \sqrt{2\bar{E}})^{-1/4} \, \sin\left[\frac{2\sqrt{2}\sqrt{2\bar{E}}}{3\hbar}(q \, - \, \sqrt{2\bar{E}})^{3/2} + \frac{\pi}{4}\right] \, , \quad (3.19)$$

where K is an irrelevant constant. We recognize the amplitude of (3.19) as the amplitude defined by (3.14) in the limit $q \rightarrow \sqrt{2\bar{E}}$, and the two exponentials that make up the sin function can be identified with the two branches S_+ and S_-. Clearly, only the difference $S_+ - S_-$ is physically meaningful, since the wave-function ψ is only defined to within an arbitrary phase. From (3.19), this difference between the two sheets of S must be $\pi/2$. In general, the difference between sheets is $\pi/4$ multiplied by an integer, the Maslov index, which is defined modulo 4. The derivation of the Maslov index for higher order caustics involves the full machinery of catastrophe theory (see Maslov and Fedoriuk, Ma81), and we will not consider it further.

We have found that S discontinuously gains a phase $\pi/2$ at each classical edge, so that the quantization condition derived above is

$$\int_\gamma p \cdot dq \, = 2\pi\hbar(n \, + \, \tfrac{1}{2}) \, . \qquad (3.20)$$

For the harmonic oscillator example (3.20) is the ordinary WKB method, and the quantization is an integral around a circle,

$$2\pi\hbar(n \, + \, \tfrac{1}{2}) = \int_{-\sqrt{2\bar{E}}}^{\sqrt{2\bar{E}}} \sqrt{2\bar{E} - q^2} \, (dq) \, + \int_{\sqrt{2\bar{E}}}^{-\sqrt{2\bar{E}}} \sqrt{2\bar{E} - q^2} \, (-dq) = 2\pi E \quad (3.21)$$

which are the exact energy levels.

This quantization method works only in the regular part of the phase space, since it demands the existence of invariant KAM tori. Its implementation for a system of two degrees of freedom is straightforward and

is explained in the next section, although it is extremely difficult to use for systems of three or more freedoms (No80).

§4. Surfaces of Section.

Given a classical Hamiltonian system of 2 degrees of freedom, it is hard to visualize trajectories in the four-dimensional phase space. If we restrict initial conditions to one value of the energy, E, there are only 3 independent coordinates left over, since $H(q_1, q_2, p_1, p_2) = E$. Since three-dimensional space is still difficult to draw, we can plot only intersection points of the orbit with a plane, in particular, only those intersections which pass through the plane in one of the two possible senses. This plane may be either the q_1, p_1 plane, with $q_2 = 0$ and $p_2 > 0$, or the q_2, p_2 plane, with $q_1 = 0$ and $p_1 > 0$, or it may be some more general plane.

In Figure 1, we illustrate the procedure schematically. The left and right sides of the figure represent the situations when p_2 or p_1 respectively is omitted in favor of the energy, and the same invariant torus is shown in the two projections. The section plane is defined by setting some rotated coordinate (written q_A or q_B) to zero, and plotting the other rotated variables. Thus the torus is cut in the plane AA' or BB', and the resulting figure shown. The particular canonical transformation is of the F_2 type (Go80),

$$F_2(p_A, q) = p_A^T R\, q \ ,$$

so $\quad q_A = R\, q$,and $\quad p_A = R^{-T} p = R\, p$.

where R is the 2×2 rotation matrix.

Although the surface of section technique is applicable to any Hamiltonian system of 2 freedoms, for simplicity we restrict ourselves to a Lagrangian system and apply no rotation,

$$L = \tfrac{1}{2}(p_1^2 + p_2^2) - V(q_1, q_2) \ . \tag{4.2}$$

The trajectory defined by the solution to the equations of motion induces a mapping of the section plane to itself, since, for example, if we know q_1, p_1, and the energy, and that $p_2 > 0$, $q_2 = 0$, then the initial conditions are completely specified, and the value of the mapping is the values of q_1, p_1 the next time these conditions occur. The set of intersection points is clearly restricted to an area defined by one of the inequalities,

$$\tfrac{1}{2}p_1^2 + V(q_1, 0) \leq E \qquad \text{for } q_1, p_1 \text{ section,} \tag{4.3}$$

$$\tfrac{1}{2}p_2^2 + V(0, q_2) \leq E \qquad \text{for } q_2, p_2 \text{ section.}$$

For example, if the system is a pair of uncoupled oscillators, then the left sides of these inequalities are the individually conserved energies, and are thus constant. If the frequency ratio is irrational, then the sections are circles, and if it is rational, each section is a finite number of points lying on a circle, where the number of points is the denominator of the rational frequency ratio.

In Figures 3-6 we illustrate surfaces of section for the Henon-Heiles system (He64) of §13,

$$V(q_1, q_2) = \tfrac{1}{2}(q_1^2 + q_2^2) + q_1^2 q_1 - q_2^3 / 3 \tag{4.4}$$

illustrated in the contour map of Figure 2. Figures 3-6(a) show the q_1, p_1 section, and Figures 3-6(b) show the q_2, p_2 section. We only show the $p_1 > 0$ or $p_2 > 0$ part of the surface, and the other halves can be obtained by the symmetry operations $q_1, p_1 \rightarrow -q_1, -p_1$, or $q_2, p_2 \rightarrow q_2, -p_2$. This symmetry exists because the potential is even in q_1. If the section mapping for some value of E takes the point q_1, p_1 to the point $\bar{q}_1, \bar{p}_1$, then the point $-\bar{q}_1, -\bar{p}_1$ is taken to $-q_1, -p_1$. Similarly, if $q_2, p_2 \rightarrow \bar{q}_2, \bar{p}_2$, then $\bar{q}_2, -\bar{p}_2 \rightarrow q_2, -p_2$. Thus any structure in the surface, such as an invariant

torus or chaos, is repeated, but reflected in the q_2-axis, or rotated by π, for the q_2, p_2 or q_1, p_1 section, respectively.

In order to calculate the sections, we used a fifth-order Runge-Kutta procedure to integrate the differential equations, and quadratic inverse interpolation to obtain the time at which the trajectory intersects the plane, then quadratic interpolation to get the section point. It is a good test of numerical accuracy that when the trajectory lies on a torus, the section really looks like a curve, with no spread around it. In the chaotic regions, two initially close trajectories separate exponentially, and no numerical method can accurately follow the motion. In the regular part of phase space, however, we found that integrating forward for a long time, then back for the same time reproduces the initial conditions well. After these calculations were complete, we discovered an elegant method due to Henon (He82) for calculating surfaces of section, which is to integrate until a crossing is discovered, manifested by a change in sign of some variable q, then change the independent variable from time to the variable q, and integrate from the previous value of q to $q = 0$. The implementation is surprisingly easy, and the results better than the complicated interpolation method.

Figure 3 is the section for a low energy, 0.02, which is the nonlinear coupling constant of KAM, so we might expect invariant tori. However, the low-energy sections do not look like the circles characteristic of irrationally related oscillators, since the KAM theorem does not apply for rationally related frequencies. For this low value of the energy, the system is very similar to a pair of harmonic oscillators of equal frequency, in which case the section map would be the trivial map $q, p \to q, p$, and indeed the section point does move very slowly. Nevertheless, the phase space is

smoothly filled with invariant tori, whose intersections with the plane are closed curves. No chaotic regions are visible although, of course, such regions may exist on an extremely small scale. The central point of a set of concentric curves (the minimax if it were a contour plot) represents a periodic orbit, which is a fixed point of the section mapping. Figure 4 shows a higher energy, 0.08, which is still mostly regular, but with perhaps a very small chaotic region, at center left. Figure 5, at energy 0.10, has a well developed chaotic region, but still mostly regular. There are "island chains", and the centers of the islands represent periodic orbits, but with iterations of the section mapping jumping from one to another in sequence, rather than being a fixed point of the map. The Henon-Heiles potential, as with any cubic potential, has a dissociation energy, in this case at $E = 1/6$, at the vertices of the equilateral triangle in the contour map, above which the trajectory is energetically capable of escaping to infinity ("the phase-space becomes non-compact"). There is a saddle-point in the potential at this energy, and if the energy is slightly less than dissociation, then the particle has almost zero velocity near the saddle, and two initially close trajectories will rapidly diverge, and "forget" their initial conditions. This is the reason for the widespread chaos in Figure 6, for energy 0.166. Even so, a few invariant tori can be seen, and in addition, there must be large numbers of periodic orbits, albeit unstable, as the results of §13 show.

The surfaces of section are not only a useful qualitative way of viewing the phase space of a classical system. We have seen in §2 that the EBK quantization method relies on being able to calculate the loop integrals of $\vec{p} \cdot d\vec{q}$ around paths on the KAM tori, which are precisely the areas of the closed curves on the surface of section. The area of a closed curve on the

q_1, p_1 section is $\int p_1 \, dq_1$, and since q_2 is zero, this is equal to $\int \vec{p} \cdot d\vec{q}$, and similarly for the other section. The trick is to make sure that the two sections represent independent topological paths, which can be fairly easily done by viewing the trajectory in q_1, q_2 space then choosing by how much to rotate the coordinates: the trajectory traces a distorted Lissajous figure, and we want the sections parallel to the axes of the enclosing distorted rectangle. This is explained more fully in §12, when we quantize the SU(3) schematic nuclear shell model.

It is possible to extend the surface of section technique to paraboloidal or cylindrical sections (Ea74) in order to quantize systems whose tori have these geometries when projected into three-dimensional space. It is also possible to extend the procedure to a system of three degrees of freedom, by calculating when the trajectory in the five-dimensional energy shell is on the two-dimensional section, which is as difficult as calculating when a three-dimensional trajectory lies on a line. This has been done with prodigious amounts of computer time by Noid and Marcus (No80) with some success.

§5. Semiclassical Dynamics of a Many-Fermion System.

In §3, we showed how to approximate the bound-state wave-functions which satisfy a Schrödinger equation when $\hbar$ is very small. In that case we were guided by knowledge of classical mechanics, and reassured to see the Hamilton-Jacobi equation and Liouville's theorem. In the mechanics of a many-fermion system such as an atomic nucleus, it is empirically clear that there is classical behavior, as can be seen by the success of the liquid drop model for example, but even the identification of a small parameter analogous to $\hbar$ is not easily justifiable. A good choice, however, is the reciprocal of the number of particles, since we know that collective properties are much more obvious in very heavy nuclei than in light nuclei. If there are many "similar" single-particle states in each shell, one can approximate the system as a small set of states (shells), each of which can be occupied by a large number N of fermions. In that case, the collective states are well approximated by the coherent states defined below, and the quantity N^{-1} appears in place of $\hbar$ in the semiclassical dynamics (Ya82).

We consider a system of fermions interacting through a Hamiltonian $H = K + V$, where K is the one-body kinetic energy operator and V the two-body effective potential operator. In second-quantized notation,

$$H = \sum_{rs} a_r^+ <r\,|\,K\,|\,s> a_s \; + \; \tfrac{1}{2} \sum_{rstu} a_r^+ a_s^+ <rs\,|\,V\,|\,tu> a_u a_t \;\; . \qquad (5.1)$$

For the unperturbed system with Hamiltonian K, there are n_h occupied or hole orbitals, and n_p unoccupied or particle orbitals: this state is the unperturbed fermion ground state $|0>$, which is a Slater determinant of the hole states made from the zero-particle vacuum $|->$,

$$| 0 > = \prod_h a_h^+ |- > \qquad (5.2)$$

There are four sets of bifermion operators, which preserve the number of particles in the system, $a_p^+ a_h$, $a_h^+ a_p$, $a_p^+ a_{p'}$, and $a_h^+ a_{h'}$, with $p, p' = 1, \ldots, n_p$ and $h, h' = 1, \ldots, n_h$. The bifermion operators have commutation relations,

$$[a_i^+ a_j, a_k^+ a_l] = a_i^+ a_l \, \delta_{jk} - a_k^+ a_j \, \delta_{il} \qquad (5.3)$$

where i, j, k, l may label any of the $n_p + n_h$ single particle states. For our semiclassical treatment we use coherent states (Bl81) described by an $n_p \times n_h$ matrix z_{ph} of complex numbers, and generated by a Thouless transformation of the unperturbed ground state,

$$|z> = \exp \sum_{ph} (z_{ph} a_p^+ a_h) \, |0> \; . \qquad (5.4)$$

We can calculate the overlap of two coherent states $<z | z'>$ as follows. Using (5.3), we can see that the bifermion operators $a_p^+ a_h$ commute among themselves, so the exponential of the sum on ph can be split into a product of exponentials,

$$|z> = \prod_h \exp(\sum_p z_{ph} \, a_p^+ a_h) \, |0> \; , \qquad (5.5)$$

and each exponential expanded into a power series. The squares and higher powers of the argument all contain squares and higher powers of a_h, and are thus zero. So

$$|z> = \prod_h (1 + \sum_p z_{ph} \, a_p^+ a_h) \, |0> \; . \qquad (5.6)$$

In terms of the zero-particle vacuum,

$$| z > = \prod_{h} (1 + \sum_{p} z_{ph} \, a_p^+ a_h) \, a_h^+ \, |\text{-} >$$

$$= \prod_{h} (a_h^+ + \sum_{p} z_{ph} \, a_p^+) \, |\text{-} > \qquad (5.7)$$

$$= \prod_{h} \alpha_h^+ \, |\text{-} > \ .$$

Thus $|z>$ is a Slater determinant of quasiparticle states $\alpha_h^+ \, |\text{-} >$, and the overlap of two such Slater determinants is the determinant of the overlaps of the single-particle states:

$$< z \, | z'> = \det < \text{-} | \alpha_h \cdot \alpha_h^+ | \text{-} >$$

$$= \det (\delta_{h'h} + \sum_{p} z_{ph'}^* \, z_{ph}')$$

$$= \det (1 + z^+ z') \ . \qquad (5.8)$$

It can also be shown (Bl81) that the coherent states have a completeness relation,

$$\int \prod_{ph} \frac{d z_{ph} \, d z_{ph}^*}{2\pi i} \, |z> \mu(z,z^*) <z| = 1 \qquad (5.9)$$

$$\mu(z,z^*) = [\det(1 + z^+ z)]^{-(n_p + n_h + 1)} \ .$$

Now we write a many-body wave-function for the system in terms of the coherent-state wave function ψ,

$$|\Psi> = \int d\mu(z) \, \psi^*(z) \, |z> \qquad (5.10)$$

where the measure $d\mu(z)$ is the same as that used in (5.9), and ψ is an analytic function of z,

$$\psi(z) = <\Psi|z> \ . \tag{5.11}$$

We will try to express the second-quantized operators as differential operators on this wave-function. Since the operators $a_p^+ a_h$ commute among themselves,

$$a_p^+ a_h \ |z> = \partial/\partial z_{ph} \ |z> \ . \tag{5.12}$$

We can construct similar relations for the other three sets of bifermion operators using the identity (Do81)

$$X \, e^C = e^C \, (X + \sum_{m=1}^{\infty} \frac{(-)^m}{m!} [C,[C,\cdots,[C,X]\cdots]]_m) \tag{5.13}$$

which yield, with summation convention implied,

$$a_h^+ a_p \ |z> = (z_{ph} - z_{p'h} \, z_{ph'} \, \partial/\partial z_{p'h'}) |z> \ ,$$

$$a_p^+ a_{p'} \ |z> = z_{p'h} \partial/\partial z_{ph} \ |z> \ , \tag{5.14}$$

$$a_h^+ a_{h'} \ |z> = (\delta_{hh'} - z_{ph} \partial/\partial z_{ph'}) \ |z> \ .$$

Let $\tilde{H}$ be the partial differential operator on analytic functions obtained from H by the replacement of bifermion operators by z and $\partial/\partial z$ given by (5.12) and (5.14). Also suppose that $|\Psi>$ is an eigenstate of H of energy E,

$$\left[\sum_{rs} a_r^+ <r|K|s> a_s + \sum_{rstu} a_r^+ a_s^+ <rs|V|tu> a_u a_t \right] |\Psi> = E \ |\Psi> \ , \tag{5.15}$$

and $\psi(z)$ its overlap with the coherent states given by (5.11). Then

$$\tilde{H}\psi(z) = \tilde{H} <\Psi|z> = <\Psi|H|z> = <\Psi|E|z> = E\psi(z) \ , \tag{5.16}$$

so we have found a Schrödinger equation with Hamiltonian $\tilde{H}$ which is

equivalent to the original many-fermion problem.

We now make the ansatz referred to at the beginning of this section; that the single particle levels split into "shells" of N members each, where N is some large number. A single-particle state can thus be labelled $|p,n>$ or $|h,n>$, where $p=1,\ldots,n_p$, $h=1,\ldots,n_h$, and $n=1,\ldots,N$. The N members of each shell are "identical" in the sense that all matrix elements of these states are assumed independent of n, except for the orthogonality factor $\delta_{nn'}$. Furthermore, we consider only collective states, in which the occupation probability is the same for each member of a shell. The semiclassical quantization of the Schrödinger equation (5.16) can then be accomplished in a similar manner to the configuration space analysis of §3. In the shell-model Hamiltonian (5.1), the one-body term is multiplied by the number of states in each shell, N, and the two-body term by the number of pairs $N(N-1)/2 \approx \frac{1}{2} N^2$. The one-body term contains first derivatives, and the two-body term second derivatives of the coherent state wave-functions, so that derivatives always appear in the combination $N \, \partial/\partial z_{ph}$. Thus we can approximate the behavior for large N by making the WKB ansatz $\psi = A e^{iNS}$ and solve the resulting Hamilton-Jacobi equation for S by the method of characteristics, replacing $\dfrac{\partial}{\partial z_{ph}}$ in $\tilde{H}$ by a new "momentum" variable $\bar{z}_{ph} \equiv \partial S/\partial z_{ph}$. If the metric of the coherent state space were flat, then the $\bar{z}_{ph}$ would be just the complex conjugate of z_{ph}. However, the metric given in (5.9) is not constant, so we need a change of variables to make it so. These new variables are, from Blaizot and Orland (Bl81),

$$\beta_{ph} = z_{ph} \cdot [(1+z^+z)^{-\frac{1}{2}}]_{h'h} \tag{5.17}$$

and there are coherent states $|\beta>$ constructed from the states $|z>$ by

making the transformation (5.17) and normalizing. The states $|\beta>$ have a completeness relation similar to (5.9), except that now the metric is unity, and the integration is restricted to the interior of the sphere $\beta^+\beta = 1$. We obtain the classical Hamiltonian in terms of these variables by replacing the bifermion operators by their expectation values,

$$<\beta|a_p^+a_h|\beta> = <\beta|a_h^+a_p|\beta>^* = [\beta(1-\beta^+\beta)^{\frac{1}{2}}]_{ph}$$

$$<\beta|a_p^+a_{p'}|\beta> = (\beta\beta^+)_{pp'} \tag{5.18}$$

$$<\beta|a_h^+a_{h'}|\beta> = \delta_{hh'} - (\beta^+\beta)_{hh'}$$

The resulting classical Hamiltonian is then the familiar TDHF Hamiltonian, which is the expectation of the shell-model Hamiltonian in the coherent state. The global minimum of such a classical Hamiltonian is the Hartree-Fock ground state, and the simplest quantization is the random-phase approximation (RPA), which assumes that the variations about the HF minimum are small, so one takes only the second degree terms in the β's, and obtains a set of harmonic oscillators, which are trivially easy to quantize.

§6: Path Integrals.

A path integral (Fe65, Sc81, De79, Ma80) is a mathematical device relating quantum-mechanical behavior to classical concepts, such as the Lagrangian. It takes the quantum propagator $G(q,q',T)$ to be the coherent sum of waves whose phase is the classical action. The sum is over all histories of the system (paths) which go from the initial point q to the final point q' in time T. This sum is not only infinite, but also uncountable, and the mathematical apparatus of measure theory on function spaces (Ka59) is needed to properly define the path integral, i.e., to make the various limit processes independent of the manner in which the limit is taken. Although the rigorous mathematics is difficult, much physical intuition can be gained from this osculation of classical and quantum mechanics. This section derives the path-integral expression for the propagator, which we shall use in §9 to develop a quantization method.

Let q be an N-dimensional vector of generalized coordinates with an associated orthonormal set of states $|q>$ which have a completeness relation,

$$\int dq \; |q><q| = 1 \; . \tag{6.1}$$

There is a Schrödinger equation expressing the evolution of the system, with units such that $\hbar = 1$,

$$[H(q,-i\frac{\partial}{\partial q}) - i\frac{\partial}{\partial t}]U(t) = -i\delta(t) \tag{6.2}$$

so that a wave-function $\varphi(q)$ evolved for time t becomes $U(t)\varphi(q)$. Notice that H has been assumed time independent, so that the evolution operator U is a function only of the difference between initial and final

times, not each of these independently. Solving (6.2), for $t > 0$,

$$<q''|U(t)|q'> = <q''|e^{-iHt}|q'>$$

$$= <q''|\lim_{J\to\infty}(1-iHt/J)^J|q'>$$

$$= \lim_{J\to\infty}\int dq_1 \cdots dq_{J-1} <q''|1-iHt/J|q_{J-1}><q_{J-1}| \cdots$$

$$|q_1><q_1|1-iHt/J|q'> , \qquad (6.3)$$

where the last part came from inserting a complete set of states at each time on a grid of J points. We now define "momentum" states which are also orthonormal and complete,

$$|p> = \int dq \ (2\pi)^{-N/2} e^{ipq} |q> \qquad (6.4)$$

$$\int dp \ |p><p| = 1 , \qquad (6.5)$$

and are eigenstates of the operator $-i\partial/\partial q$, since

$$<q|-i\partial/\partial q|p> = \int dq' <q|-i\partial/\partial q|q'>e^{ipq'}(2\pi)^{-N/2}$$

$$= \int dq' \ i\delta'(q-q')e^{ipq'}(2\pi)^{-N/2}$$

$$= \int dq' \ -i\delta(q-q')ipe^{ipq'}(2\pi)^{-N/2}$$

$$= p <q|p> . \qquad (6.6)$$

Since the states $|q>$ are complete, $-i\partial/\partial q|p> = p|p>$. Let us now examine a single matrix element from the product in the integrand of (6.3), insert a complete set of momentum states, and neglect all terms higher than first order in t/J,

$$<q_j \,|1 - iHt / J \,| \left[\int dp_j \,\, |p_j> <p_j|\right]\,|q_{j-1}>$$

$$= \int dp_j \,\, [1 - iH(q_j, p_j)t / J]\, <q_j|p_j>\, <p_j|q_{j-1}>$$

$$= \int dp_j \,\, [1 - iH(q_j, p_j)t / J]\, e^{ip_j(q_j - q_{j-1})}(2\pi)^{-N}$$

$$\approx \int dp_j \,\, (2\pi)^{-N} \exp i[p_j(q_j - q_{j-1}) - Ht / J] \qquad (6.7)$$

The propagator is thus

$$<q''|\,U(t)\,|q'> = \lim_{J \to \infty} \int \frac{dp_0}{(2\pi)^N} dq_1 \frac{dp_1}{(2\pi)^N} dq_2 \cdots dq_{J-1} \frac{dp_{J-1}}{(2\pi)^N}$$

$$\exp i \sum_{j=1}^{J} [p_{j-1}(q_j - q_{j-1}) - H(q_{j-1}, p_{j-1})t / J] \qquad (6.8)$$

It is now suggestive to make the large number of discrete integrations a single integral on "path space," which considerably simplifies the notation. We also put in $\hbar$ explicitly,

$$<q''|\,U(t)\,|q'> = \int D[q]\,D[p]\,e^{iS/\hbar}$$

$$\text{where} \qquad S = \int_0^t dt\,\,(p\dot{q} - H) \qquad (6.9)$$

which is the conventional representation of a path integral (Sc81). Note that q' and q'' appear in the boundary conditions of the allowed paths: $q(0) = q'$, $q(t) = q''$. However, it must be borne in mind that (6.9) is merely an abbreviation for the limit (6.8), and means neither more nor less; it is a convenient notation in which manipulations are less cumbersome.

Notice that the argument of the exponential is the ratio of the classical action for the path to the quantum of action. We will see later that the

semiclassical approximation consists essentially of reducing the integral over *all* paths to a sum over just classical trajectories. Thus if there are two distinct paths from a source to an observation point, quantum interference will occur if the difference in action is of order $\hbar$. The simplest illustration of this point is the double-slit experiment, explained in Feynman and Hibbs (Fe60).

If the Hamiltonian has the form $p^2/2m + V(q)$, i.e., quadratic in the momenta, we can easily derive a Lagrangian form of the path integral by explicitly integrating out the momenta. A typical momentum integral in (6.8) is then

$$\int \frac{dp_j}{2\pi} \exp i\left[p_j(q_{j+1}-q_j) - \frac{t}{J}\left[\frac{p_j^2}{2m} + V(q) \right] \right]$$

$$= \left[\frac{m}{2\pi i} \frac{J}{t} \right]^{\frac{1}{2}} \exp i\left[\frac{1}{2}m(q_{j+1}-q_j)^2 \frac{J}{t} - \frac{t}{J}V(q_j) \right] , \qquad (6.10)$$

or in continuum notation,

$$<q''| U(t) | q'> = \int D[q] \exp \frac{i}{\hbar} \int_0^t \frac{1}{2}m\dot{q}^2 - V(q)dt , \qquad (6.11)$$

so that the argument of the exponential is again the classical action, but in Lagrangian form. After all this work, we have a formal expression which is much more difficult to evaluate than the it is to solve the original Schrödinger equation. However, there is a natural way to make the semiclassical approximation, which is the subject of the next section.

It has been suggested (Bl81, Ku82, Kl78) that one can use a path integral over coherent-state histories in order to calculate the dynamics of a many-fermion system instead of the Schrödinger equation approach

of §5, and indeed it is found that the SPA on this path integral leads to the same TDHF Hamiltonian as the WKB method of §3 applied to the Schodinger equation. However, it is difficult to even define such an integral. In configuration space we have the infinitesimal propagator

$$<q_{j+1}| \ e^{-iH \ \delta t} \ |q_j> \ ,$$
(6.12)

which is for a one-dimensional free particle,

$$= \left[\frac{2\pi i \hbar \ \delta t}{m}\right]^{-\frac{1}{2}} \exp \frac{im(q_{j+1} - q_j)^2}{2\hbar \ \delta t}$$
(6.13)

representing an expanding Gaussian wave-packet. Since the phase varies very rapidly far from the source, q_{j+1} is kept close to q_j, and justifies the implicit assumption of (at worst) Brownian trajectories. It is on this basis that the Wiener measure is defined (see, for example Kac, Ka59, Berezin, Be80) and that the path integral is well-defined. For the coherent states, however, even the zero-time propagator connects states very far from each other, since they are not orthonormal, as (5.8) shows. Thus it would seem that there is no (Wiener) path integral expression for the coherent state propagator. We can, of course, leave the path-integral in the form of a limit as the time-mesh becomes infinitely fine, but we cannot be sure that different ways of taking the limit yield the same answer, nor can we "commute" the limit through the integral sign, or through the large number of stationary phase approximations. Neglecting these considerations, though, we can derive difference equations for the classical variables, instead of the usual differential equations, and there certainly is a solution close to the solution of the differential equations. But without the firm foothold of a well-defined measure, we cannot be sure that this continuous classical path is the only solution, and perhaps it is merely an

accident that coherent-state path integrals yield physically meaningful results. It is usually the case in mathematical physics that if the mathematics is not clear, then there is more than meets the eye in the physics. In any event, we have a bona fide classical limit for many-fermion systems from the method of §5, and we are justified in using path integrals for coordinate-space problems.

§7: The Stationary Phase Approximation

The expression (6.11) for the propagator is not easy to compute directly, although attempts have been made (Sc80) which took about 100 times as long as the solution of the ordinary Schrödinger equation, because of cancellation between positive and negative values of the integrand. Better results can be obtained (Ce79) if we are not interested in real-time dynamics, but in using the imaginary-time propagator $U(-i\tau)$ as a filter for the ground state,

$$\lim_{T \to \infty} e^{(E_0 - H)T} |\Psi> = |\Psi_0> \tag{7.1}$$

where $|\Psi>$ is a trial ground state, and $|\Psi_0>$ and E_0 are the exact ground state and energy respectively. We can thus find the ground-state energy by looking at the time development of $e^{-HT} |\Psi>$. The important paths are not the classical trajectories, which make the phase of the integrand stationary, but those which maximize the integrand, and also the cancellation problem is avoided because the integrand is always positive. This section, however, is concerned with analytical approximations to the path integral, of which there is only one: the stationary phase approximation and its extensions (Sc81).

Consider the integral

$$F(\lambda) = \int_{-\infty}^{\infty} dt \ e^{i\lambda f(t)} \tag{7.2}$$

as $\lambda \to 0$, where f is sufficiently smooth. We shall show that regions in which $f'(t) \neq 0$ contribute order λ^{-1} to the integral, and that the turning points of f contribute order $\lambda^{-\frac{1}{2}}$, which thus dominate for large λ. Suppose $f'(t) \neq 0$ in some interval $\alpha \leq t \leq \beta$. Then f must be monotonic in the

interval, and we can change variables to $z = f(t)$, so that the Jacobian is $\varphi(z) = 1/f'(f^{-1}(z))$:

$$\int_{\alpha}^{\beta} dt \; e^{i\lambda f(t)} = \int_{f(\alpha)}^{f(\beta)} e^{i\lambda z} \; \varphi(z) \; dz \; . \tag{7.3}$$

Integrating by parts, we obtain

$$\frac{-i}{\lambda} \Big[\varphi(z) \; e^{i\lambda z} \Big]_{f(\alpha)}^{f(\beta)} + \frac{i}{\lambda} \int_{f(\alpha)}^{f(\beta)} dz \; e^{i\lambda z} \; \varphi'(z) \tag{7.4}$$

which is of order λ^{-1}. Now we evaluate the contribution at a turning point t_0: $f'(t_0)=0$. Expand f in a Taylor series about the turning point, and integrate:

$$f(t-t_0) = f(t_0) + \tfrac{1}{2} f''(t_0)(t-t_0)^2 + \cdots$$

$$F(\lambda) = \int_{-\infty}^{\infty} \exp\Big[i\lambda f(t_0) + \tfrac{1}{2} i\lambda f''(t_0)(t-t_0)^2 \Big] \Big[1 + \frac{i}{6}\lambda f'''(t_0)(t-t_0)^3 + \cdots \Big]$$

$$= \sqrt{\frac{2\pi i}{\lambda f''(t_0)}} e^{i\lambda f(t_0)} \Big[1 - \frac{i}{8\lambda} \frac{f''''(t_0)}{f''(t_0)} + \cdots \Big] \tag{7.5}$$

$$\approx \sqrt{\frac{2\pi i}{\lambda f''(t_0)}} e^{i\lambda f(t_0)} \; . \tag{7.6}$$

Thus we can approximate the integral as a sum over such terms, one for each turning point in f. The phase of the approximant is $e^{i\pi/4}$ for the case $f''(t_0) > 0$, and $e^{-i\pi/4}$ for $f''(t_0) < 0$, as can be seen by adding a convergence factor $i0^+$ to $f''(t_0)$ in the integral (7.5). We can also use the stationary phase approximation for a many-dimensional integral,

$$F(\lambda) = \int d^N x \; e^{i\lambda f(x_1, \ldots, x_N)} \; . \tag{7.7}$$

We again demand that f be stationary with respect to $\mathbf{x}$, and approximate f as a quadratic form (given by the Taylor series) near the stationary point $\mathbf{x}_0$. Making a coordinate transformation to diagonalize the quadratic form, and doing each integral separately, the f'' term in (7.6) becomes the product of the eigenvalues of the quadratic form, which is just the determinant of the form. The SPA then becomes

$$\int dx_1 \cdots dx_N \; e^{i\lambda f(\mathbf{x})} \approx e^{i\lambda f(\mathbf{x}_0)} \left[\frac{2\pi i}{\lambda} \right]^{m/2} |\det f''(\mathbf{x}_0)|^{-\frac{1}{2}} e^{-iM\pi/2} \quad (7.8)$$

where M is the number of negative eigenvalues of the Hessian (second derivative) matrix of f at $\mathbf{x}_0$.

In semiclassical expansions, the large parameter λ is either $\hbar^{-1}$, for configuration space problems, or the number of particles, for many-body problems (Ya82). We shall use the stationary phase approximation on the path-integrals of §6 to derive the prescription for quantization by periodic trajectories in §9.

§8. Computation of Periodic Trajectories

In this section we shall develop a method of generating a large class of periodic trajectories of a time-independent Lagrangian system whose potential is polynomial in the coordinates. We shall see in §9 that a quantization rule can be found by a stationary phase approximation on a certain path integral, and that the prescription associates a quantum bound state with a particular periodic trajectory. Previous work has found properties of these trajectories either in a very restricted region of phase space (Co80), or described the bifurcations found at the end of this section in general terms (Ch80). Sinai and Vul have found a rigorous numerical method of checking that an orbit really is periodic (Si80), although the method is complicated, and we have relied on somewhat more heuristic convergence criteria for our search (see §13). Some periodic orbits of the Henon-Heiles potential have been discussed qualitatively (Ch77), and Helleman and Bountis (He78) found a large class of periodic orbits which look very different from the class we have found (see §13)). It is possible that a complete picture will contain both classes.

As with the Helleman and Bountis algorithm, ours gives good results even for extremely unstable orbits, since it uses the (global) variational principle rather than the (local) differential equations of motion, but unlike theirs, we feel that ours is much easier to generalize to other Lagrangian systems than the Henon-Heiles. We consider only the two degree of freedom case here, although the method can easily be generalized. This method is used to generate periodic trajectories for the Henon-Heiles potential in §13, in order to test the quantization procedure of §9. We shall now describe the algorithm in detail.

Let the Lagrangian be

$$L = \tfrac{1}{2}(\dot{x}^2 + \dot{y}^2) - V(x,y) \tag{8.1}$$

$$V(x,y) = \sum_{n,m} c_{nm} x^n y^m$$

Following Helleman and Bountis, He78, we write an arbitrary periodic path, not necessarily a classical trajectory, as

$$x(t) = \sum_{-\infty}^{\infty} A_k e^{ik\omega t} \tag{8.2}$$

$$y(t) = \sum_{-\infty}^{\infty} B_k e^{ik\omega t}$$

where $T = 2\pi/\omega$ is the period of the path, and we stipulate $A_k^* = A_{-k}$, $B_k^* = B_{-k}$ to ensure reality of the coordinates. Hamilton's principle states that for a classical path the action functional $S[x(t),y(t)] = \int_0^T L[x(t),y(t)]\,dt$ is stationary with respect to small variations of the path. In terms of the Fourier coefficients A_k, B_k, the problem of finding periodic trajectories is thus reduced to a minimization. Evaluating the action S for the path (8.2) using the Lagrangian (8.1) we obtain

$$\frac{\omega S}{\pi} = \sum_{-\infty}^{\infty} k^2 \omega^2 (A_k A_{-k} + B_k B_{-k}) \tag{8.3}$$

$$-2 \sum_{n,m} c_{nm} \left[\sum_{\Sigma\alpha + \Sigma\beta = 0} A_{\alpha_1} \cdots A_{\alpha_n} B_{\beta_1} \cdots B_{\beta_m} \right]$$

where the α's and β's each range from $-\infty$ to $+\infty$. For a periodic trajectory, the derivatives of S with respect to the coefficients A, B must be

zero. The differentiation is straightforward, but messy, and is omitted.

We now investigate Newton's method for solving the stationarity conditions in some large but finite basis of Fourier coefficients, i.e., we truncate the sums (6.2). Let the vector $\vec{C}$ refer generically to the collection of A_k and B_k, so that $S = S(\vec{C})$. If $\vec{C}$ is an approximate solution, and $\vec{C} + \delta\vec{C}$ is the linear extrapolation to the solution, then

$$H_{ij}\,\delta C_j = -\frac{\partial S}{\partial C_{-i}} \tag{8.4}$$

where

$$H_{ij} \equiv \frac{\partial^2 S}{\partial C_{-i}\,\partial C_j},$$

with all derivatives evaluated at $\vec{C}$. Newton's method consists of solving these equations iteratively until $\delta\vec{C} = 0$. However, in order to make use of this simple and efficient method, we must make a crucial restriction: to impose reality of the Fourier coefficients. This means that the trajectories we find will have velocity zero at $t = 0$, and that they are even in time, so that the velocity is also zero at $t = \frac{1}{2}T$, and the motion for $t > \frac{1}{2}T$ is on the same path as for $t < \frac{1}{2}T$. The reason is as follows. Since the Lagrangian is time-independent, any point on the periodic trajectory can be treated as a time origin, so the transformation

$$A_k' = A_k e^{ik\omega\tau} \tag{8.5}$$

$$B_k' = B_k e^{ik\omega\tau}$$

produces another periodic trajectory for all values of τ, in particular for an infinitesimal τ:

$$A'_k = A_k + \omega \, \delta\tau \, a_k, \qquad a_k = ikA_k, \tag{8.6}$$

$$B'_k = B_k + \omega \, \delta\tau \, b_k, \qquad b_k = ikB_k.$$

Under this transformation $\partial S / \partial \vec{C}$ remains zero, so that $(\vec{a}, \vec{b})$ is an eigenvector of the Hessian matrix H_{ij}, with zero eigenvalue. H is thus not invertible at the solution, so Newton's method is unstable. However, in the space of real Fourier coefficients, the conditions for reality of the coordinates become $A_{-k} = A_k$, $B_{-k} = B_k$. Notice that the eigenvector $(\vec{a}, \vec{b})$ constructed above is pure imaginary, and so $a_k = a^*_{-k} = -a_k$, and similarly for $\vec{b}$. Therefore this vector is orthogonal to the space of real coefficients, and is not an eigenvector of the restricted H_{ij}. Thus H_{ij} is invertible, and Newton's method is stable. In addition the order of H_{ij} is halved.

Given a periodic trajectory, we shall construct a family of such, parametrized by frequency. The derivatives of (8.3) can be split into the sum of a term $\omega^2 k^2 C_k$ and a multinomial $D_k(\vec{C})$ which does not depend on ω:

$$\omega^2 k^2 C_k + D_k(\vec{C}) = 0 \quad . \tag{8.7}$$

Differentiating with respect to ω,

$$2\omega k^2 C_k + \omega^2 k^2 \frac{\partial C_k}{\partial \omega} + \frac{\partial D_k}{\partial C_m} \frac{\partial C_m}{\partial \omega} = 0, \tag{8.8}$$

which is a set of linear equations that may be solved for $\partial \vec{C} / \partial \omega$, and hence for a new pair of initial conditions that also yield a periodic trajectory. Thus there is a continuous family of periodic orbits parametrized by frequency (or equivalently period), with real Fourier coefficients. The trajectory is uniquely defined by its initial conditions and its frequency,

$$x_{\omega+\delta\omega}(0) = x_\omega(0) + \delta\omega\, u_\omega, \qquad u_\omega = \sum_{-\infty}^{\infty} \frac{\partial A_m}{\partial\omega}, \qquad (8.9)$$

$$y_{\omega+\delta\omega}(0) = y_\omega(0) + \delta\omega\, v_\omega, \qquad v_\omega = \sum_{-\infty}^{\infty} \frac{\partial B_m}{\partial\omega}.$$

The behavior of trajectories close to a given (not necessarily periodic) classical trajectory is described by the stability matrix $L(t)$. This is the 4×4 matrix of the linear transformation between infinitesimal changes in the initial conditions $x(0), y(0), \dot{x}(0), \dot{y}(0)$ and the resulting changes in $x(t), y(t), \dot{x}(t), \dot{y}(t)$:

$$\begin{bmatrix} \delta x(t) \\ \delta y(t) \\ \delta \dot{x}(t) \\ \delta \dot{y}(t) \end{bmatrix} = L \begin{bmatrix} \delta x(0) \\ \delta y(0) \\ \delta \dot{x}(0) \\ \delta \dot{y}(0) \end{bmatrix} \qquad (8.10)$$

If we define $V_x = \partial V / \partial x$, etc., the equations of motion for the Lagrangian system (8.1) can be written,

$$\frac{d}{dt}\begin{bmatrix} x \\ y \\ \dot{x} \\ \dot{y} \end{bmatrix} = \begin{bmatrix} \dot{x} \\ \dot{y} \\ -V_x \\ -V_y \end{bmatrix}. \qquad (8.11)$$

Differentiating (8.11) with respect to initial conditions yields the differential equation for $L(t)$,

$$\frac{dL(t)}{dt} = ML = \begin{bmatrix} & & 1 & 0 \\ & & 0 & 1 \\ -V_{xx} & -V_{xy} & & \\ -V_{yx} & -V_{yy} & & \end{bmatrix} L \qquad (8.12)$$

with the initial condition $L(0) = 1$, and the derivatives of V are evaluated at $x(t), y(t)$. Let

$$J = \begin{bmatrix} & & -1 & 0 \\ & & 0 & -1 \\ +1 & 0 & & \\ 0 & +1 & & \end{bmatrix} \qquad (8.13)$$

which is the symplectic inner product matrix. We shall show that $L(t)$ is a symplectic matrix, i.e., it preserves J,

$$L^T J L = J \ . \qquad (8.14)$$

We know that $L(0) = 1$ is symplectic, and differentiating (8.14),

$$\dot{L}^T J L + L^T J \dot{L} = \qquad (8.15)$$

$$L^T M^T J L + L^T J M L =$$

$$L^T (M^T J + J M) L = 0$$

since the Hessian matrix of V is symmetric. Thus L is symplectic. It is well-known (Ar78) that if λ is an eigenvalue of a symplectic matrix, then λ^*, λ^{-1}, and λ^{-1*} are also eigenvalues. Therefore $\det L = 1$, which shows that the linear transformation L preserves volume. Thus a closed volume of phase space keeps the same volume during its evolution, which is a statement of Liouville's theorem that flow in phase-space is incompressible. Consider now the stability matrix $L_\omega(T)$ of a periodic trajectory of period $T = 2\pi/\omega$. Examining the equations of motion (8.11), we see that this matrix has a unit eigenvalue whose eigenvector is the initial motion $\vec{r} \equiv (\dot{x}(0), \dot{y}(0), \ddot{x}(0), \ddot{y}(0))$ along the trajectory. Thus the matrix must be characterized by a real number ν, the stability index, and lies in one of two classes, either stable, with eigenvalues 1, 1, $e^{i\nu}$, $e^{-i\nu}$, or unstable, with eigenvalues 1, 1, $\pm e^\nu$, $\pm e^{-\nu}$. If ν were complex, then unity would not be in the list of eigenvalues, contradicting the periodicity assumption. We

can easily calculate ν, within its inherent sign ambiguity, by calculating the trace of the stability matrix $L_\omega(T)$, which is $2+2\cos\nu$ for stable trajectories, and $2\pm2\cosh\nu$ for unstable trajectories.

We now investigate the two-dimensional eigenspace of unit eigenvalue, which transforms into itself under L_ω. One basis vector can be taken to be the time evolution vector $\vec{r}_\omega$ and the other is the period-changing vector $\vec{s}_\omega = (u_\omega, v_\omega, 0, 0)$ from (8.9). The result of evolving $\vec{x}_\omega(0) + \delta\omega\vec{s}_\omega$ for time T, then evolving further for the time $\delta T = -(2\pi/\omega^2)\delta\omega$ is the initial condition $\vec{x}_\omega(0) + \delta\omega\vec{s}_\omega$ again, since by the definition of $\vec{s}_\omega$, this is a periodic trajectory of frequency $\omega + \delta\omega$. Thus

$$L_\omega\vec{s}_\omega - (2\pi/\omega^2)\vec{r}_\omega = \vec{s}_\omega \tag{8.16}$$

so the action of L on the subspace spanned by $\vec{r}_\omega$ and $\vec{s}_\omega$ is

$$L\begin{bmatrix} \vec{r}_\omega \\ \vec{s}_\omega \end{bmatrix} = \begin{bmatrix} 1 & 0 \\ -2\pi/\omega^2 & 1 \end{bmatrix}\begin{bmatrix} \vec{r}_\omega \\ \vec{s}_\omega \end{bmatrix}, \tag{8.17}$$

so that this subspace transforms into itself under L_ω, and has unit eigenvalue.

For the quantization prescription of §9, we shall need not only the stability angle ν, but also its rate of change with period. Varying the differential equation (8.12) gives

$$\frac{d}{dt}(L + \delta L) = (M + \delta M)(L + \delta L)$$

$$\rightarrow \quad \frac{d}{dt}\delta L = \delta M\, L + M\,\delta L\ . \tag{8.18}$$

Since we know the change in initial conditions $x(0)$, $y(0)$ with period, from (8.9), and thus the change in $x(t)$, $y(t)$ at an arbitrary time using

$L(t)$, we can compute $\delta M(t)$, and hence solve (8.18) for $\delta L(t)/\delta\omega$. In addition, we must remember to solve (8.18) for a time $2\pi/(\omega + \delta\omega)$ instead of $2\pi/\omega$. By solving these 32 simultaneous differential equations, we can thus calculate not only the stability angle but also its change with period.

Finally, we point out that the stability matrix for multiple cycles of the same trajectory is just a power of L_ω. Thus if the trajectory is stable and ν is a rational multiple of 2π, then the eigenvalues of $L_\omega^n = L_{\omega/n}$ are all 1, where n is the denominator of the rational. This means that to first order all initial conditions in the vicinity of $\vec{x}_\omega(0)$ produce periodic trajectories of frequency ω/n. We actually find that at these bifurcation points a new line of trajectories is formed, of the required frequency. The above first order analysis predicts not a one-dimensional, but a two-dimensional set of new trajectories: it is clear that a second-order analysis would make this restriction. Notice that bifurcations from a stable part of a family are extremely common; as common as the rationals are in the reals. Thus each stable periodic trajectory is covered in a dense "hair" of bifurcations, so that the periodic trajectories must be dense in phase space in some sense; at least dense enough, one may conjecture, to make the stationary phase approximation fail for the path integral (see §9).

We have presented an algorithm to find periodic solutions of a Lagrangian dynamical system. In applications other than a particle in a potential well, the classical approximation to the quantum system is described rather by the more general Hamiltonian formalism: for example in the quantization of a many-body system, §12, the classical Hamiltonian is quartic in the momenta. The crux of the above method is the expression of the action as a function of path by means of a complete set

of periodic basis functions, the cosines for example. The Hamiltonian formalism is more general than the Lagrangian precisely because the coordinate and momentum are independent variables in the description of the path. There are thus three methods of proceeding in the more general case; either to make the momentum dependent on the coordinate path by explicitly solving one of Hamilton's equations,

$$\dot{q} = \partial H / \partial p \qquad \rightarrow \qquad p = p(q, \dot{q}), \qquad (8.19)$$

or equivalently to make the coordinate dependent on the momentum path, or thirdly to keep coordinate and momentum separate and then minimize the action. If the function $p(q, \dot{q})$ or $q(p, \dot{p})$ is available explicitly, the the system can be made Lagrangian by a canonical transformation to $p = \dot{q}$ or $q = \dot{p}$ respectively, and we are done. Keeping the coordinate and momentum independent we can evaluate

$$S = \int\limits_{0}^{2\pi/\omega} (p\dot{q} - H) \, dt \qquad (8.20)$$

and carry on as before. Unfortunately it is no longer so easy to eliminate the zero eigenvalue from Newton's method. Naively one would proceed in analogy to the Lagrangian case, and let the q Fourier series be a sum of cosines, and the p series a sum of sines. But if this is to be self-consistent, $\dot{q} = \partial H / \partial p$ must be a sine series, and similarly for the $\partial H / \partial q$. This will not be so without certain constraints on the Hamiltonian function. In addition there are two Fourier series in place of one. Thus one is faced with not only a much larger basis set, but also a more stubborn instability in the numerical method.

§9. Path-Integral Quantization

For a system of one degree of freedom, all bounded orbits are periodic, so the eigenvalues of the stability matrix of §8 are exhausted by the two unit eigenvalues, and there is no stability angle. The WKB quantization condition is then equivalent to the quantization condition derived in this chapter, but of course the terms involving the stability angle are not present. Gutzwiller (Gu73), in a long series of papers, derived in detail the prescription for quantization by periodic trajectories for many degrees of freedom, and we shall give a less rigorous version of his analysis in this section, which consequently contains various infinite factors that we unjustifiably neglect. Nevertheless, the derivation presented here contains the essential steps. More details can be found in DeWitte-Morette, De79, Rajaraman, Ra75, or Dashen et. al., Da74.

We shall derive the prescription for quantization by periodic trajectories starting with a time-independent classical Hamiltonian $H(q,p)$ and the path-integral expression (6.9) for the quantum propagator,

$$G(q',q'',T) \equiv \langle q'|e^{-iHT}|q''\rangle = \int D[q]\, D[p]\, e^{iS[q,p]/\hbar} \qquad (9.1)$$

$$\text{where} \qquad S[q,p] \equiv \int_0^T p\dot{q} - H(q,p)\, dt$$

$$\text{and} \qquad q(0) = q' \quad \text{and} \quad q(T) = q'' \ .$$

We need to find a quantum representation for the bound states in terms of this propagator in order to use its path-integral representation. First we take the trace of $G(q',q'',T)$, to obtain

$$G(T) = \mathrm{Tr}\, e^{-iHT} = \sum_j e^{-iE_j T/\hbar} \ , \qquad (9.2)$$

where the E_j are bound-state energies, and the sum is over all eigenstates of the system. If we multiply by $e^{iET/\hbar}$ and integrate over T to find the Fourier transform of $G(T)$ (E has a small positive imaginary part to converge the integral), we have

$$\int\limits_{0}^{\infty} dT \; e^{iET/\hbar} \, G(T) = \sum_{j} \frac{i\hbar}{E - E_j} \; . \tag{9.3}$$

Hence, if we know $G(T)$, we can find the semiclassical energies by locating the poles of its Fourier transform.

In order to calculate the trace of $G(q',q'',T)$, we integrate (9.1) over trajectories with $q' = q''$. This just means that the range of the path integral in (9.1) is no longer just paths with specified endpoints, but over all paths with equal, but unspecified, endpoints. We now apply the stationary phase approximation, so we demand that S is stationary with respect to small variations in the path, which is precisely Hamilton's principle for classical trajectories. Since the trace involves an integral over the initial point of the path, we can use the SPA on it. The initial point is constrained to be the same as the final point, so that the stationarity condition is

$$0 = \frac{\partial S}{\partial q(0)} + \frac{\partial S}{\partial q(T)} = p(0) - p(T) \tag{9.4}$$

Thus both coordinate and momentum are equal at the ends, so the SPA paths are periodic classical trajectories. The SPA expression for $G(T)$ is then

$$G_{sc}(T) = \sum_{p.t.} e^{i\bar{S}/\hbar} \int D[\delta q] D[\delta p] \, e^{i\delta^2 S/\hbar} \tag{9.5}$$

where the boundary conditions on the path integral are periodic, and the

sum is over all the periodic trajectories of period T, and the action of one such is denoted $\overline{S}$. The second order change in action is given by

$$\delta^2 S = \int_0^T \delta p \, \delta \dot{q} - \frac{1}{2} \begin{bmatrix} \delta q \\ \delta p \end{bmatrix} \hat{H} \begin{bmatrix} \delta q \\ \delta p \end{bmatrix} dt$$

$$= \frac{1}{2} \int_0^T \begin{bmatrix} \delta q \\ \delta p \end{bmatrix} J \frac{d}{dt} - \hat{H} \begin{bmatrix} \delta q \\ \delta p \end{bmatrix} dt \tag{9.6}$$

and $\hat{H}$ is the Hessian matrix of H evaluated on the periodic trajectory, J is the symplectic inner product matrix (8.13), and the second line is obtained by integrating by parts. In order to evaluate the path integral (9.5) we need the determinant of the operator $J\partial_t - \hat{H}$. Since det $J=1$, this is equal to det J det $(J\partial_t - \hat{H}) = -$ det $(\partial_t + J\hat{H})$. Let $\hat{O} = \partial_t + \hat{H}$, and observe that det $\hat{O}$ is the product of the eigenvalues of $\hat{O}$. Suppose $\Delta = \begin{bmatrix} \delta q \\ \delta p \end{bmatrix}$ is an eigenfunction, $\hat{O} \Delta = \lambda \Delta$, with the required periodic boundary conditions. Let $\tilde{\Delta}(t) = \Delta(t) e^{-\lambda t}$, so that

$$\hat{O}\tilde{\Delta} = e^{-\lambda t} (-\lambda + \hat{O}) \Delta = 0 , \tag{9.10}$$

$$\tilde{\Delta}(T) = e^{-\lambda T}\tilde{\Delta}(0) .$$

But (9.10) is the equation satisfied by classical trajectories in the vicinity of the "base" trajectory of (9.5), and we showed in §8 that $\tilde{\Delta}$ can only be a combination of the four linearly independent columns of the matrix $L(T)$. Thus $-\lambda T$ can be $\pm i\nu + 2\pi n$ for a stable orbit, with n running from $-\infty$ to ∞. There are two linearly independent solutions with zero stability angle which are periodic, and thus give eigenvalues of zero, and the physical reason for them is exactly the same as in §8, corresponding to time-translation and period-changing. These zero eigenvalues appear to show that det $\hat{O} = 0$; but we can ignore the period-changing variation because

we are calculating the Greens function for one particular period, and we can treat the time-translation variation by integrating it out of the path integral explicitly, rather than attempting a local (in path space) analysis; we just obtain an irrelevant multiplicative factor T. We will assume that only stable trajectories can be identified with bound states, and this will be justified later: in any case, making ν imaginary will reproduce the analysis for unstable orbits. The other two non-trivial solutions give rise to the set of eigenvalues $(\pm\nu + 2\pi n)/T$, where n runs from $-\infty$ to ∞. The semiclassical approximation to $G(T)$ is thus

$$G_{sc}(T) \propto \sum_{p.t.} e^{iS/\hbar} \prod_{-\infty}^{\infty} \left[\frac{\nu^2 - 4\pi^2 n^2}{T^2} \right]^{-\frac{1}{2}} \tag{9.11}$$

to within an infinite normalization constant, which comes from the measure of the path integral. If we were being completely rigorous, we could change the variables of the path integral (9.5) to the coefficients of the complete orthonormal set of eigenfunctions of $\hat{O}$, and the Jacobian would exactly cancel this infinite constant. Thus the product in (9.11) can be written

$$\prod_{-\infty}^{\infty} \left[1 - \frac{\nu^2}{4\pi^2 n^2} \right]^{-\frac{1}{2}} = \operatorname{cosec} \tfrac{1}{2}\nu \ . \tag{9.12}$$

In addition, there is a factor $e^{-\frac{1}{2}i\pi\alpha}$, where α is the Maslov Index of the trajectory, which we now compute.

Suppose we evaluate $G(q,q,T)$ in stationary phase, before taking the trace. We obtain the same path integral expression (9.5), except that $\delta q(0) = \delta q(T) = 0$ instead of periodic boundary conditions. The operator $J\, d/dt - \hat{H}$ is now a Sturm-Liouville operator, with real eigenvalues, a finite number of which are negative. According to the formula (7.8) the

Maslov Index is this number of negative eigenvalues modulo 4. Consider the eigenvalue spectrum $\lambda_n(t)$, where the zero boundary condition at 0 and T is replaced by zero at 0 and t, where $0 \le t \le T$. Each eigenvalue is non-increasing with t, and the number of negative eigenvalues increases by unity each time an eigenvalue passes through zero. A zero eigenvalue means that the points $q(0)$ and $q(t)$ are conjugate, that many trajectories emanating from $q(0)$ can pass through the same point $q(t)$. Thus the Maslov Index is the number of conjugate points modulo 4. For details see Milnor, Mi63, or Schulman, Sc81.

A single periodic trajectory contributes

$$G_{sc}(T) = \frac{e^{i\overline{S}/\hbar} e^{-\frac{1}{2}i\pi\alpha}}{\sin\frac{1}{2}\nu} = 2i \exp\left[i\overline{S}/\hbar - i\pi\alpha/4 - \sum_{l=0}^{\infty} i(l+\frac{1}{2})\nu\right] \quad .(9.13)$$

Since the phase of $G_{sc}(T)$ is already embodied in the Maslov Index, we can take ν between 0 and π. We now take the Fourier Transform of $G_{sc}(T)$ to obtain a quantization condition,

$$G_{sc}(E) = \int_{0}^{\infty} dT \, e^{iET/\hbar} \, G_{sc}(T) \quad . \tag{9.14}$$

Using stationary phase on this integral, we need

$$0 = \frac{d}{dT}\left(ET + \overline{S} - \frac{\pi\alpha\hbar}{2} - (l+\frac{1}{2})\hbar\nu\right)$$

$$\rightarrow \quad E = \overline{E} + (l+\frac{1}{2})\hbar\frac{d\nu}{dT} \tag{9.15}$$

where $\overline{E}$ is the classical energy, $-d\overline{S}/dT$, of the trajectory. Thus in SPA the phase of $G_{sc}(E)$ is

$$W_0(E) = \frac{ET + \overline{S}}{\hbar} - \frac{\pi\alpha}{4} - (l + \frac{1}{2})\nu \tag{9.16}$$

evaluated at the value of E given by (9.15). Now we notice that each periodic trajectory can be traversed not just once, but any number of times, so that $W(E)$ for n traverses is $nW_0(E)$. Then

$$G_{sc}(E) \propto \sum_{n=1}^{\infty} e^{inW_0(E)}$$

$$= \frac{1}{e^{-iW_0(E)} - 1} \qquad (9.17)$$

so that $G_{sc}(E)$ has poles, and hence bound states, whenever $W_0(E)$ is a multiple of 2π, which is then the quantization condition,

$$\hbar W_0(E) = 2\pi\hbar n$$

$$= ET + \overline{S} - \tfrac{1}{2}\alpha\hbar - (l + \tfrac{1}{2})\hbar\nu$$

$$= \overline{E}T + \overline{S} - \tfrac{1}{2}\alpha\hbar + (l + \tfrac{1}{2})\hbar\left[T\frac{d\nu}{dT} - \nu\right] . \qquad (9.18)$$

Using $\overline{E}T + \overline{S} = \int_0^T H + L \, dt = \int_0^T p \cdot \dot{q} \, dt = \int p \cdot dq$, the quantization condition is

$$\int p \cdot dq + (l + \tfrac{1}{2})\hbar(T\frac{d\nu}{dT} - \nu) = (n + \frac{\alpha}{4})2\pi\hbar \qquad (9.19)$$

for some integer n, and some integer $l \geq 0$.

For an unstable orbit, the same analysis goes through, but with ν replaced by $i\nu$. We can see that it is only the stable periodic trajectories which contribute to the bound-state spectrum, since the unstable ones would lead to complex energies. This is physically intuitive, since the parts of the quantization involving ν are adding harmonic variations about the original trajectory, and if those variations grow unstably, one

cannot consider them harmonic. In summary, quantization by periodic trajectories consists of finding a periodic orbit which satisfies (9.19), then computing the bound-state energy from (9.15).

§10. Discussion.

At first sight, EBK and periodic trajectory quantization are completely different. However, Berry and Tabor (Be77, Ri82) have shown that the two are, in a sense, equivalent in the regular part of the classical phase-space. They are equivalent in that a stationary phase approximation to the EBK method produces a sum over periodic trajectories, which can also be obtained from the path integral formulation. In the regular regime, the trajectory has (non-analytic) isolating constants of the motion, which are the actions obtained by integration along a circuit on the invariant torus, as in §3. These together with the corresponding angle variables are canonical, and are a good coordinate system since the Hamiltonian is a function only of the actions (Ar68). Setting these actions to $2\pi\hbar\,(n+\frac{1}{2})$ gives the semiclassical energy levels. Berry and Tabor wrote the density of states as a sum of δ-functions at these values,

$$n(E) = \sum_{\mathbf{m}} \delta(E - H((\mathbf{m} + \frac{1}{4}\alpha)\hbar)) \ , \tag{10.1}$$

where α represents the Maslov index. They then used Poisson's formula to transform each δ-function to an integral, and invoked the SPA for each integral. Since the action variables are intrinsically positive numbers, they used the *uniform* SPA, which takes into account the fact that the integral has a finite limit. Their result is a sum over periodic orbits in the classical system,

$$n(E) = n_{TF}(E) + \frac{2}{\hbar^{(N+1)/2}} \sum_{\mathbf{M}}' \frac{\cos\,(2\pi\mathbf{M}\cdot\mathbf{I}^{\mathbf{M}}/\hbar - \frac{1}{2}\pi\alpha\cdot\mathbf{M} + \frac{1}{4}\pi\beta_{\mathbf{M}})}{|\mathbf{M}|^{(N-1)/2}\,|\omega(\mathbf{I}^{\mathbf{M}})|\,|K(\mathbf{I}^{\mathbf{M}})|^{\frac{1}{2}}} \tag{10.2}$$

where the indices $\mathbf{M}$ refer to the *topology* of the periodic orbit; that is, the orbit makes M_i windings about the ith irreducible circuit of the

torus, for $1 \leq i \leq N$. The prime excludes the $\mathbf{M} = 0$, which gives $n_{TF}(E)$, the smoothly varying Thomas-Fermi density of states,

$$n_{TF}(E) = \hbar^{-n} \int\int d\mathbf{p}\, d\mathbf{q}\, \delta(E - H(\mathbf{q},\mathbf{p})) \; ; \qquad (10.3)$$

and $\omega(\mathbf{I}^{\mathbf{M}})$ is the frequency vector of the periodic trajectory, $K(\mathbf{I}^{\mathbf{M}})$ is the scalar curvature of the energy surface in action space and $\beta_{\mathbf{M}}$ is a phase associated with this. For a system of two degrees of freedom, each term is of order $\hbar^{-3/2}$. Using the Thomas-Fermi as background, Berry and Tabor showed that succeeding terms "eat away" this background to eventually give a sum of δ-functions. For computation, it is easier to calculate the smoothed density of states $n(E + i\gamma)$, which replaces the δ-functions by Lorentzians at the bound states. Semiclassically, we find that the contribution of each periodic trajectory is then weighted by a factor $e^{-\gamma T/\hbar}$, where T is the period. This is plausible, since we feel that trajectories of very long period are "less periodic" than those of short period.

The same sum over periodic trajectories can be obtained from the quantum expression Tr $\delta(E-H)$ for the density of states. Expressed as a path integral in the action-angle coordinates, the trace becomes a trivial integration over angles. Thus the correct approximation to EBK quantization shows that the density of states is a sum over all periodic trajectories. One can further approximate (10.2) to derive the Gutzwiller (Gu73) quantization condition found at the end of the last chapter (Ri82), and using the uniform SPA, derive it without the infinite contributions when the stability angle is a multiple of 2π, which can be seen from (9.12).

Although the EBK method has the drawback that it only works in the regular part of phase space, the Gutzwiller periodic trajectory method

seems to have more drawbacks. For example, it makes no distinction between long and short period trajectories; it takes no account of the integer lattice topology of the Berry and Tabor expression; under some circumstances it predicts discrete energy levels in the continuum, and a continuous level distribution in a bound system (Be72); and it fails in the limit of separability (Mi75): a pair of uncoupled harmonic oscillators with incommensurate frequencies has no periodic orbits.

§11. Birkhoff-Gustavson Quantization

The Birkhoff-Gustavson method of semiclassical quantization (Bi66, Re83) is based on an expansion about an elliptic fixed point in harmonic oscillator modes, treating cubic and higher terms in the potential as perturbations. This method yields an algebraic expression for the semiclassical eigenvalues. We shall define a sequence of canonical transformations which make the Hamiltonian a function only of the harmonic oscillator action variables $J_k / 2\pi \equiv \frac{1}{2}(q_k^2 + p_k^2)$, for $k = 1, \ldots, N$, where the system has N degrees of freedom. This form is known as the Birkhoff normal form. First we normalize the second order terms, then show the induction step which transforms a Hamiltonian H, normalized to order $s-1$, into a new Hamiltonian Γ, normalized to order s. Let the Hamiltonian be given by a power series,

$$H(\bar{q},\bar{p}) = H^{(2)}(\bar{q},\bar{p}) + H^{(3)}(\bar{q},\bar{p}) + \cdots, \tag{11.1}$$

where $H^{(s)}$ is a homogeneous polynomial of order s in $\bar{q}$ and $\bar{p}$, and we have set the zeroth and first order terms to zero by relocating the zero of energy, and assuming that the origin is an elliptic (stable) fixed point of the motion. Let

$$H^{(2)}(\bar{q},\bar{p}) = \frac{1}{2}\bar{p}^T H_{pp} \bar{p} + \frac{1}{2}\bar{q}^T H_{qq} \bar{q} \tag{11.2}$$

where H_{pp} and H_{qq} are the second derivative matrices with respect to these variables, and superscript T means transpose. There are no terms like $\bar{p}_i \bar{q}_j$, since H is assumed time-reversal invariant: $H(\bar{q},\bar{p}) = H(\bar{q},-\bar{p})$. We first need a canonical transformation to new variables q, p to diagonalize $H^{(2)}$ in the form

$$H^{(2)}(q, p) = \sum_k \frac{1}{2}\omega_k (q_k^2 + p_k^2) \tag{11.3}$$

Since the origin of $\bar{q}, \bar{p}$ is assumed to be a *stable* fixed point, H_{qq} and H_{pp} are positive definite, so $U = H_{pp}^{-\frac{1}{2}}$ exists, and $U^{-1}H_{qq}U^{-1}$ has positive eigenvalues:

$$W^{-1}U^{-1}H_{qq}U^{-1}W = \text{Diag } \omega^2 \tag{11.4}$$

where W is the eigenvector matrix of $U^{-1}H_{qq}U^{-1}$, and the numbers ω_k^2 are its eigenvalues. Let $D = \text{Diag } \omega^{\frac{1}{2}}$, so that the required transformation is

$$\bar{q} = U^{-1}WD^{-1}q \quad , \tag{11.5}$$

$$\bar{p} = U^T W^{-T} D^T p \quad .$$

Then $H^{(2)}$ is in the form (11.3). This transformation is canonical since for any matrix A the generating function $F_2(P,q) = P^T A q$ gives (Go80)

$$\begin{array}{ccc} Q = Aq & & Q = Aq \\ p = A^T P & \rightarrow & P = A^{-T}p \end{array} \quad . \tag{11.6}$$

In the above case, $A = U^{-1}WD^{-1}$.

The Birkhoff-Gustavson transformation works inductively order by order in the Hamiltonian. The induction step assumes that H is in normal form up to order $s-1$, and produces a new Hamiltonian Γ which is in normal form to order s. Let us consider a further canonical transformation given by the generating function

$$F_2(P,q) = P \cdot q + W^{(s)}(P,q)$$

$$\begin{array}{c} Q = q + \partial W^{(s)} / \partial P \\ p = P + \partial W^{(s)} / \partial q \end{array} \Bigg\} \tag{11.7a}$$

$$H\left(P + \frac{\partial W^{(s)}}{\partial q}, q\right) = \Gamma\left(P, q + \frac{\partial W^{(s)}}{\partial P}\right) \quad , \tag{11.7b}$$

where $W^{(s)}$ is a homogeneous polynomial of order s, and Γ is the new Hamiltonian for the correct choice of $W^{(s)}$. Expanding (11.7b) in a Taylor series,

For $i < s$
$$\Gamma^{(i)}(P,q) = H^{(i)}(p,Q) \tag{11.8a}$$

For $i = s$
$$\Gamma^{(s)}(P,q) = H^{(s)}(P,q) + DW^{(s)}(P,q) \tag{11.8b}$$

For $i > s$
$$\Gamma^{(i)}(P,q) + \sum_{\mathbf{j}} \frac{1}{j!} \left[\frac{\partial W^{(s)}}{\partial P} \right]^{\mathbf{j}} \left[\frac{\partial^{\mathbf{j}} H^{(l)}}{\partial q^{\mathbf{j}}} \right]$$

$$= H^{(i)}(P,q) + \sum_{\mathbf{j}} \frac{1}{j!} \left[\frac{\partial W^{(s)}}{\partial q} \right]^{\mathbf{j}} \left[\frac{\partial^{\mathbf{j}} H^{(l)}}{\partial P^{\mathbf{j}}} \right] \tag{11.8c}$$

where
$$D = - \sum_{k=1}^{n} \omega_k \left(q_k \frac{\partial}{\partial p_k} - p_k \frac{\partial}{\partial q_k} \right)$$

and $\mathbf{j}$ is a vector of integers $(j_1, \ldots, j_n)$, with $|j| = j_1 + \cdots + j_n$ and

$$l = i - |j|(s-2) \tag{11.9}$$

$$1 \le |j| \le l$$

$$l \ge 2$$

$$s \ge 3$$

and $\Gamma(P,Q) \equiv \Gamma(P,q)\big|_{q=Q}$ since we have used a Taylor series, and evaluate quantities at the point of expansion P,q. Thus we need not make any distinction between P, Q and p, q in the manipulations. To calculate the generating function $W^{(s)}$, we solve (11.8b),

$$W^{(s)} = D^{-1}(\Gamma^{(s)} - H^{(s)}) \tag{11.10}$$

$$\left. \begin{array}{l} q = i/\sqrt{2}(\eta - i\xi) \\ p = 1/\sqrt{2}(\eta + i\xi) \end{array} \right\} \tag{11.11}$$

to diagonalize D,

$$D = i \sum_k \omega_k \, (\xi_k \frac{\partial}{\partial \xi_k} - \eta_k \frac{\partial}{\partial \eta_k}) \ . \tag{11.12}$$

A typical term of $H^{(s)}$ is $\tau = \prod_k \eta_k^{l_k} \, \xi_k^{m_k}$ so that D^{-1} is given by

$$D^{-1} \tau = \frac{\tau}{i \sum_k \omega_k (m_k - l_k)} \ . \tag{11.13}$$

We now make a crucial assumption, upon which the success of the method depends, that is that the ω_k's are incommensurable, in other words, linearly independent over the rationals. Thus the sum in (11.13) is zero if and only if $l_k = m_k$ for all k. The terms of $H^{(s)}$ for which D^{-1} exists lie in the *range-space*, and terms for which it doesn't are in the *null space*. $H^{(s)}$ thus splits into two parts,

$$H^{(s)} = R^{(s)} + N^{(s)} \tag{11.14}$$

$$DN^{(s)} = 0$$

$$W^{(s)} = -D^{-1}R^{(s)}$$

$$\Gamma^{(s)} = N^{(s)}$$

The null-space terms are functions of $i\eta_k\xi_k = \frac{1}{2}(q_k^2 + p_k^2) \equiv J_k/2\pi$. After a lot of algebra, using (11.8) and (11.14), we have the new Hamiltonian $\Gamma^{(s)}$ expressed as a function of the $J_k/2\pi$ to any desired order. These J_k are action variables, with conjugate angle variables $\vartheta_k = \partial\Gamma/\partial J_k$. The system is now trivially integrable, and the quantization condition is

$$\frac{J_k}{2\pi} = n_i + \frac{1}{4} \alpha_i \tag{11.15}$$

with α_i the Maslov Index, which is 2 for each of these one-dimensional systems.

We shall illustrate the method with a simple one-dimensional example, which is a slightly perturbed harmonic oscillator,

$$H = \tfrac{1}{2}(p^2 + q^2) + \varepsilon q^4 \ . \tag{11.16}$$

The Hamiltonian is already in normal form (function only of $p^2 + q^2$) through order 3, and the first non-normal term is $H^{(4)} = \varepsilon q^4$. We first split $H^{(4)}$ into a null-space and range space, by making the transformation (11.11), so that D is diagonal,

$$H^{(4)} = \frac{\varepsilon}{4}(\eta^4 - 4i\eta^3\xi - 6\eta^2\xi^2 + 4i\eta\xi^3 + \xi^4) \ . \tag{11.17}$$

The null space is the sum of terms which are functions of $\eta\xi$, so that $N^{(4)} = -3/2 \, \varepsilon\eta^2\xi^2 = \frac{3\varepsilon}{2}[\tfrac{1}{2}(p^2 + q^2)]^2$. The generating function $W^{(4)}$ is then

$$W^{(4)} = -D^{-1}\left\{\frac{\varepsilon}{4}(\eta^4 - 4i\eta^3\xi + 4i\eta\xi^3 + \xi^4)\right.$$

$$= -\frac{\varepsilon}{4}\left[\frac{\eta^4}{-4i} - \frac{4i\eta^3\xi}{-2i} + \frac{4i\eta\xi^3}{2i} + \frac{\xi^4}{4i}\right]$$

$$= -\frac{5}{8}\varepsilon q^3 p - \frac{3}{8}\varepsilon q p^3 \ . \tag{11.18}$$

Using this generating function we can evaluate the higher order terms of the new Hamiltonian using (11.8c). We get $\Gamma^{(5)} = 0$, and

$$\Gamma^{(6)} = \frac{\varepsilon^2}{128}(295q^6 + 711q^4p^2 + 9q^2p^4 + 9p^6) \ . \tag{11.19}$$

This completes the induction step, so the new Hamiltonian is normal through order 4. With a little more work, we can get those terms which contribute to the energy in next order too, by extracting the null-space part of $\Gamma^{(6)}$, using the transformation (11.11),

$$N^{(6)} = -\frac{17\varepsilon^2}{4}[\tfrac{1}{2}(p^2 + q^2)]^3 \tag{11.20}$$

so to second order in ε, in terms of the action variable $j \equiv J/2\pi = \tfrac{1}{2}(p^2 + q^2)$, the energy is

$$\Gamma(j) = j + \frac{3\varepsilon}{2}j^2 - \frac{17\varepsilon^2}{4}j^3 + \cdots \tag{11.21}$$

and the quantum levels are then $\Gamma(1/2)$, $\Gamma(3/2)$, $\Gamma(5/2)$, $\cdots$.

The nice thing about a one-dimensional example is not only that the algebra is simpler, but also that one can check the answer. The exact answer is

$$j = J/2\pi = 2/\pi \int_0^{q_+} dq\ \sqrt{2E - q^2 - 2\varepsilon q^4} \tag{11.22}$$

where $\quad -2\varepsilon(q^2 + q_-^2)(q^2 - q_+^2) = 2E - q^2 - 2\varepsilon q^4$

so that $\pm q_+$, $\pm i q_-$ are the roots of the quartic. Changing variable to λ, with $q_+ \cos \lambda = q$,

$$j = (2/\pi)\ q_+^2\ \sqrt{2\varepsilon(q_+^2 + q_-^2)} \int_0^{\pi/2} d\lambda\ \sin^2 \lambda\ \sqrt{1 - k^2 \sin^2 \lambda} \tag{11.23}$$

where $\quad k^2 = \dfrac{q_+^2}{q_+^2 + q_-^2}$.

We can expand the square root in the integrand for small k^2, and expand

the prefactors to obtain the power series,

$$j = E\left(1 - 3\varepsilon E/2 + 35\varepsilon^2 E^2/4 + \cdots\right) \tag{11.24}$$

so that reversal of this series gives the same as the Birkhoff-Gustavson answer to this order,

$$E = j + \frac{3\varepsilon}{2}j^2 - \frac{17\varepsilon^2}{4}j^3 + \cdots \tag{11.25}$$

We are lucky that in one dimension this power series has a finite radius of convergence. However in two or more dimensions, the power series generated by the BG procedure diverges everywhere (Si41) if the Hamiltonian under consideration is not integrable. This is because there is always a resonance arbitrarily close to any set of the frequencies ω_k, so that $D^{-1}\tau$ from (11.13) can become arbitrarily large. There are however methods of summing divergent power series (Co65), the simplest of which is to take the partial sum whose final summand is a minimum. This is the method we used for the SU(3) model of §12. Another approach would be to calculate a Pade approximant for the action variables from the B-G power series (Re83), which incorporates the pole structure, not just the behavior of the function at the origin. One might even try to rederive the whole algorithm rooted in Pade approximants rather than Taylor series. There is obviously much work needed here, which may be fruitful.

§12. The SU(3) Model.

In this section and the next, we illustrate and test the quantization methods of the previous sections with two specific examples. The first, the SU(3) schematic nuclear shell model (Fl81), incorporates the many-body quantization using the EBK and Birkhoff-Gustavson methods, and we expand on a previous paper, Wi82. That work stimulated an investigation of the method of quantization using periodic trajectories, but since the classical Hamiltonian for the SU(3) model is complicated by being quartic in both momentum and coordinate, we settled for the simpler Henon-Heiles system. The SU(3) model results are presented in §12, and the Henon-Heiles results in §13. The EBK quantization seems to be successful only when the system is close to a pair of harmonic oscillators, and the quantization by periodic trajectories fails completely.

This schematic shell model system is a nice example of how coherent states might be applied to the many-body problem. Our goal is to find the energies of the stationary states.

The SU(3) model is a member of a class of exactly soluble schematic nuclear shell models. These SU(K) models are defined by a large number N of distinguishable particles labelled by an index n, which can occupy K single particle levels $k = 0, \ldots, K-1$, with energies ε_k. Furthermore there is a two-body interaction of strength $-V$ which can move pairs of particles between these levels. The Hamiltonian is

$$H = \sum_{k=0}^{K-1} \varepsilon_k \left(\sum_n a_{nk}^+ a_{nk} \right) + \tfrac{1}{2} \sum_{k,l=0}^{K-1} V_{kl} \left(\sum_n a_{nk}^+ a_{nl} \right)^2 , \qquad (12.1)$$

where $V_{ij} = V(1 - \delta_{ij})$ and $V > 0$. We shall restrict ourselves to the band of states which are totally symmetric under interchange of any two

particles, since this is a natural realization of collectivity: all the particles are "doing the same thing." We can use the coherent states of §5; there is one hole level, the $k = 0$ level, and $K-1$ particle states, $k = 1, \ldots, K-1$. The matrix z_{ph} is thus a $1\times(K-1)$ matrix, and the many-body state can be defined in terms of a wave function,

$$|\Psi> = \int Dz_1 \cdots Dz_{K-1} \exp \sum_{k=1}^{K-1} (z_k \sum_n a_{nk}^+ a_{n0}) |0> \varphi(z_1, \ldots, z_{K-1}) \quad (12.2)$$

where the vacuum $|0>$ is the state with all particles in the lower orbital, and with Dz the same measure as in (5.9). The z's are independent of n because we consider only totally symmetric states. We now change variables to the β_k's, using the transformation (5.17). The classical Hamiltonian is then expressed in terms of the density matrix elements (5.18),

$$\frac{H}{N} = \varepsilon_0 + \sum_k (\varepsilon_k - \varepsilon_0)|\beta_k|^2 + \tfrac{1}{2}V(N-1)\left[\sum_k(1 - \sum_{k'}|\beta_{k'}|^2)(\beta_k^2 + \beta_k^{*2})\right.$$

$$\left. + \sum_{k>l} \beta_k^2\beta_l^{*2} + \beta_l^2\beta_k^{*2}\right] , \quad (12.3)$$

where the sums on k and l are from 1 to $K-1$.

The simplest SU(K) model is the SU(2) model, also known as the Lipkin-Meshkov-Glick model (Li65, Ka79, Le80, Sh80, Ko81), in which there are just two levels, and one complex classical coherent-state parameter β, so that the classical system has one degree of freedom. Putting $\varepsilon_0 = -\tfrac{1}{2}\varepsilon$, $\varepsilon_1 = \tfrac{1}{2}\varepsilon$, we obtain the Hamiltonian,

$$\frac{H}{N} = -\tfrac{1}{2}\varepsilon + \varepsilon|\beta|^2 + \tfrac{1}{2}(N-1)V(1 - |\beta|^2)(\beta^2 + \beta^{*2}) . \quad (12.4)$$

We let $\chi = (N-1)V$ and make the canonical transformation from β,β^* to $q = \arg \beta + \pi/4$, $p = |\beta|^2 - \tfrac{1}{2}$, so that the new Hamiltonian is

$$\frac{H}{N} = \varepsilon p - \chi \left(\frac{1}{4} - p^2 \right) \sin 2q \quad . \tag{12.5}$$

The quantization is straightforward, and well documented. There is a phase transition at $\chi = \frac{1}{2}$; for $\chi < \frac{1}{2}$, all the orbits are rotational, that is, the angular variable q increases by 2π each period of the motion, and for $\chi > \frac{1}{2}$, orbits appear in which q librates about some fixed value. This is the same phase transition that occurs in the simple pendulum when the bob gets enough energy to rotate around the fixed point rather than just oscillate about equilibrium. The exact energies of the LMG model can easily be calculated in a representation of SU(2), with ordinary angular momentum states.

In order to test many-dimensional quantization methods, we need a larger phase space, with two or more degrees of freedom. Such a system is the SU(3) model. We have chosen the parameters $\varepsilon_0 = -\varepsilon$, $\varepsilon_1 = 0$, $\varepsilon_2 = \varepsilon$. First we shall deal with the calculation of the exact eigenstates, then with the semiclassical quantization.

The exact eigenstates of the model can be obtained by diagonalization of H in a basis which has definite occupation numbers in each level. The number of such states (partitions of N into three integers) is of order $\frac{1}{2}N^2$, so the matrix size soon becomes quite large. Since H only connects states with even differences in occupation numbers, the calculation can be reduced to four diagonalizations, each of dimensionality $\approx N^2 / 8$.

The coherent state representation of a totally symmetric wavefunction for the SU(3) system is as in (12.2), and the classical limit is from (12.3),

$$H(\beta, \beta^*) = N\varepsilon(-1 + |\beta_1|^2 + 2|\beta_2|^2)$$

$$+ \tfrac{1}{2}VN(N-1)[(1-|\beta_1|^2 - |\beta_2|^2)(\beta_1^2 + \beta_1^{*2} + \beta_2^2 + \beta_2^{*2}) \tag{12.6}$$

$$+ \beta_1^{*2}\beta_2 + \beta_1^2\beta_2^{*2})] \ .$$

A more convenient set of variables can be obtained from the real and imaginary parts of β

$$\beta\sqrt{2} = \mathbf{q} + i\mathbf{p} \ ;$$

$$\beta^*\sqrt{2} = \mathbf{q} - i\mathbf{p} \ ;$$

so that

$$\frac{H(\mathbf{q},\mathbf{p})}{N\varepsilon} = -1 + \tfrac{1}{2}q_1^2(1-\chi) + \tfrac{1}{2}q_2^2(2-\chi) + \tfrac{1}{2}p_1^2(1+\chi) + \tfrac{1}{2}p_2^2(2+\chi)$$

$$+ \frac{1}{4}\chi[(q_1^2 + q_2^2)^2 - (p_1^2 + p_2^2)^2 - (q_1^2 - p_1^2)(q_2^2 - p_2^2) \tag{12.7}$$

$$- 4q_1q_2p_1p_2] \ ,$$

where $\chi=(N-1)V/\varepsilon$ is the dimensionless strength of the interaction. In the classical limit, the time evolution of the system is independent of the particle number N at fixed χ, so that N appears only in the quantization condition

$$\int_{\gamma_i} \mathbf{p} \cdot d\mathbf{q} = \frac{2\pi\hbar}{N}(n_i + \alpha_i/4) \ . \tag{12.8}$$

We identify $\mathbf{q}$ as the coordinate and $\mathbf{p}$ as the momentum because of the behavior of the coherent-state wave-function under time-reversal, viz, $\beta \rightarrow -\beta$, $\mathbf{q} \rightarrow \mathbf{q}$, $\mathbf{p} \rightarrow -\mathbf{p}$. Further support for this identification is the fact that $p_1=p_2=0$ implies $\dot{q}_1=\dot{q}_2=0$. Notice that this Hamiltonian is certainly not simply a particle in this potential: it is quartic in the momenta. This

is why we elected to use the Henon-Heiles system, §13, to calculate periodic orbits, because of the difficulties cited at the end of §8.

In Figures 7-9 are contour plots of the "static" Hamiltonian $H(\mathbf{q}, \mathbf{p}=0)/N\varepsilon$ for $\chi=0.75$, 2, and 10 respectively. This "potential energy" exhibits one minimum for $0 \le \chi < 1$, two minima for $1 < \chi < 3$, and four minima for $\chi > 3$. The minimum value of this potential is the Hartree-Fock ground-state energy of the system. The locations of the minima and the HF energies are

$$
\begin{aligned}
&q_1 = 0, && q_2 = 0, && E = -1, && \chi < 1 ; \\
&q_1 = 1 - \frac{1}{\chi}, && q_2 = 0, && E = -1 - \frac{(\chi-1)^2}{4\chi}, && 1 < \chi < 3 ; \\
&q_1^2 = \frac{2}{3}, && q_2^2 = \frac{2\chi - 6}{3\chi}, && E = -\frac{\chi}{3} - \frac{1}{\chi}, && 3 < \chi .
\end{aligned}
\tag{12.9}
$$

The frequencies ω_1, ω_2 of small oscillations about the minimum are N times the RPA frequencies. The low-lying energy levels are then given by the RPA as

$$
E = E_{HF} + \sum_{i=1}^{2} \frac{\hbar \omega_i}{N} (n_i + \tfrac{1}{2}), \quad n_i = 0, 1, 2, \cdots .
\tag{12.10}
$$

These frequencies are,

$$
\begin{aligned}
&\omega = \sqrt{1 - \chi^2}, \sqrt{4 - \chi^2}, && \chi < 1 ; \\
&\omega = \sqrt{2(\chi^2 - 1)}, \tfrac{1}{2}\sqrt{3(\chi+1)(\chi-3)}, && 1 < \chi < 3 ; \\
&\omega = \left[\frac{4}{3}(\chi^2 - 3 \pm \sqrt{3\chi^2 + 9}) \right]^{\frac{1}{2}} && 3 < \chi .
\end{aligned}
\tag{12.11}
$$

For $1 < \chi < 3$ and $\chi > 3$ at sufficiently low energies, the classically allowed region is split into two or four identical separate regions, respectively. The energies at which these regions coalesce are the energies of the saddle points of the "potential energy"

$$E = -1 \; , \qquad\qquad\qquad\qquad 1 < \chi < 3 \; ;$$
$$E = -1 - \frac{(\chi-1)^2}{4\chi} \; , \quad E = -1 - \frac{(\chi-2)^2}{4\chi} \; , \qquad 3 < \chi \; . \qquad (12.12)$$

The quantum Hamiltonian only connects states with even differences in occupation numbers, which is reflected in the classical hamiltonian by symmetry about the q_1 and q_2 axes. Thus the states of the classical system are labelled by a positive or negative "parity" for each of the q_1, q_2 directions. When the classically allowed region is in four separate pieces, one expects the quantum energy levels to be approximately four-fold degenerate, similar to the parity doublet of a one-dimensional double well. However, since the classical approximation cannot reproduce this purely quantum mechanical effect, the splittings of the exact quantum levels are an indication of the validity of the classical approximation. For the levels we calculated in this regime ($\chi = 10$ and 100) these splittings were in the third significant figure. It may be possible to calculate these splittings semiclassically by instanton techniques, letting the action and momentum be imaginary (Ke81) or complex (Pa81), and calculating trajectories on the "inverted" energy surface. This has been done in the much simpler SU(2) model, where a similar such large-χ degeneracy occurs (Gu78).

We quantized the SU(3) model for three values of χ (0.75, 10, and 100) using both the surfaces of section and the BG method. For the former, Hamilton's equations require four initial conditions. We chose $p_1 = p_2 = 0$, and two "RPA actions" such that in the RPA limit these numbers are the exact actions. These initial conditions make the true actions a smooth single-valued function of the RPA actions. Hamilton's equations were integrated by a fifth order Runge-Kutta procedure in double precision and the trajectory was plotted in (q_1, q_2) space until it was clear whether

or not it was quasiperiodic. A line was then chosen such that the line and its normal defined independent surfaces of section, as in §4. Quadratic inverse interpolation was used to calculate the points where the trajectory cut the section plane. Since the differential equations of motion were complicated, we chose to calculate every intersection, instead of just those with some $p > 0$, halving the computation time, but obtaining the reflected section as well as the section. The area of the section was then measured by reducing the figure to a single circuit by reflecting half of the points, ordering them, and using a Simpson's rule for unequally spaced points. Our procedure is self-checking for rounding error since points on a section may be very close in the plane but widely separated in time. Thus if a section is a smooth curve, even when highly magnified, the rounding error must be small. Figure 10 illustrates a progression of the surfaces of section with increasing energy for $\chi=10$. At low excitation, the system behaves like a pair of oscillators; as the energy increases, the torus becomes highly convoluted; at still higher energy, the system is stochastic.

From the above procedure we calculated the two actions, I_1 and I_2. There were two reasons for not being able to measure the actions: either the system was stochastic, or the torus so convoluted that the planar surfaces of section were unable to define two topologically distinct paths. We illustrate the "action space" (Be77) in Figure 11 for $\chi=10$, showing where the trajectories were ergodic or unreachable, and the integer lattice at which the EBK quantization method predicts an energy level for $N=60$. The figure also shows the Birkhoff-Gustavson energy as a function of action variables (see below). The quantization grid is defined by

$$I_i = \frac{1}{2\pi} \int \mathbf{p} \cdot d\mathbf{q} = \frac{1}{N}(n_i + 1/2) \ . \qquad (12.13)$$

For both the $\chi=10$ and $\chi=100$ cases we could find few energy levels, with difficulty, due to the convolution of the surfaces of section and the rapid transition to stochasticity. The trajectories can be stochastic even when confined to a single minimum and were always stochastic when the energy was above the saddle energy. For $\chi=0.75$, however the surfaces of section were almost circles even for relatively high energies, enabling us to find many energy levels. For all three values of χ, the upper limit of energy at which we could quantize was often fixed by the insufficiency of planar surfaces of section; polyhedral surfaces could have been used to extend the procedure to higher energy, although at the cost of a greater computational complexity.

The BG procedure to quantize the system for all three values of χ was used to generate a Taylor series for the energy to fourth order in the actions. For $\chi=10$ and $\chi=100$, we show the terms of the power series generated by the method for $\chi=10$ and 100. The same problems as before are evident, which the power series exhibits by being quickly and strongly divergent. The asterisk by some of the terms indicates that they were so large that the series diverges even faster. Since the method of summing a divergent series eliminates terms somewhat arbitrarily, we eliminated these terms too. For $\chi=0.75$, however, the BG procedure provided almost as many levels as did the surface of section approach, though with less accuracy.

The calculated energy levels are illustrated in Figures 12 and 13. All exact quantal energies and the Hartree-Fock energy have been shifted up by their 'zero-point energy' (approximately one-half the sum of the RPA frequencies) such that the energy of the exact ground state is exactly equal to the RPA value. For $\chi=0.75$, the exact levels can be easily

classified by the two oscillator quantum numbers shown. For $\chi=10$, and $\chi=100$, though, the system is harmonic only for low excitation energy. We thus display the 'raw' levels in these cases. Table 1 shows the comparison in numerical form for a few levels.

§ 13. The Henon-Heiles System.

This system was originally suggested by Henon and Heiles (He64) as a model of the motion of a star in the gravitational field of a disk-shaped galaxy, and has been extensively analysed as a convenient non-linear system. The EBK quantization has been carried out by Noid and Marcus (No77) for a particular value of the coupling parameter $\varepsilon = 1/\sqrt{80}$ (see below for the definition of ε) with reasonable results. The exact levels of this potential have been calculated by Nordholm and Rice (No74), though with no explanation of the fact that the potential has no bound states.

In order to test quantization by periodic trajectories, we chose the Henon-Heiles system,

$$H = \frac{1}{2m}(\tilde{p}_x^2 + \tilde{p}_y^2) + \frac{m\Omega^2}{2}(\tilde{x}^2 + \tilde{y}^2) + \lambda(\tilde{x}^2\tilde{y} - \tilde{y}^3/3) \ . \qquad (13.1)$$

We can scale the coordinates $\tilde{x},\tilde{y}$ to $x = \lambda\tilde{x}/m\Omega^2$, $y = \lambda\tilde{y}/m\Omega^2$, and introduce the dimensionless parameter $\varepsilon = \lambda^2\hbar/m^3\Omega^5$, so that the quantum-mechanical Hamiltonian is

$$\frac{H}{\hbar\Omega} = \frac{\varepsilon}{2}\nabla^2 + \frac{1}{\varepsilon}V(x,y) \ , \qquad (13.2)$$

where $\qquad V(x,y) = \frac{1}{2}(x^2 + y^2) + x^2y - y^3/3 \ .$

If in addition we rescale the natural time parameter to the dimensionless $\tau = \Omega t$, we can obtain the equivalent classical Lagrangian,

$$\tilde{L} \equiv \frac{L\varepsilon}{\hbar\Omega} = \frac{1}{2}(\dot{x}^2 + \dot{y}^2) - V(x,y) \ . \qquad (13.3)$$

When the classical mechanics is based on the Lagrangian $\tilde{L}$, the quantization condition (9.12) becomes

$$\frac{Q}{\omega} - \frac{(l + \frac{1}{2})}{2\pi} \frac{d}{d\omega}(\omega\nu) = (n + \frac{1}{4}\alpha)\varepsilon \ , \qquad (13.4)$$

$$\text{where} \qquad Q \equiv \frac{\omega}{2\pi} \int_0^{2\pi/\omega} (\dot{x}^2 + \dot{y}^2) \, dt \ ,$$

and the bound-state energy (9.10) is

$$\frac{E}{\hbar\Omega} = \frac{\bar{E}}{\varepsilon} - \frac{(l + \frac{1}{2})}{2\pi} \omega^2 \frac{d\nu}{d\omega} \ . \qquad (13.5)$$

Thus ε plays the role of $\hbar$. When ε is very small, the cubic terms in the Hamiltonian (13.2) become negligible, and the ground-state wave function and energy are

$$\varphi_0(x,y) = \left[\frac{2}{\pi\varepsilon^3}\right]^{\frac{1}{4}} e^{-(x^2 + y^2)/2\varepsilon} \ , \quad \frac{E_0}{\hbar\Omega} = 1 \ , \qquad (13.6)$$

as expected. Under the same circumstances in the classical case, the motion is harmonic with some small amplitude,

$$x = A \cos t$$

$$y = A \sin t$$

$$\rightarrow \quad \bar{E} = A^2 \ . \qquad (13.7)$$

The Maslov index is 4, and the stability angle zero, so the quantization condition gives for the ground state $Q/\omega = A^2 = \bar{E} = \varepsilon$, so that $E/\hbar\Omega = 1$ as expected. We have thus established that quantization by periodic trajectories works for the two-dimensional harmonic oscillator.

In order to test the procedure more rigorously, we need both the exact quantum levels as a function of ε, and some periodic trajectories. Unfortunately, the Henon-Heiles potential has a dissociation energy of

$V = 1/6$, above which the (classical) trajectory can escape to infinity with infinitely negative potential energy, and infinitely positive kinetic energy. Classically, we need not worry about this for $E < 1/6$, so long as the particle is confined to the equilateral triangle of vertices $(0, 1)$, $(\pm\sqrt{3}/2, 1/2)$, where the phase space is compact; see Figure 2. Quantum-mechanically, though, there are only metastable states, which will eventually decay by tunnelling. We therefore calculated the energies of a modified Henon-Heiles potential which is identical to (13.2) inside the triangle, but has hard walls (i.e., $V \to \infty$) at the edges of the triangle. If in the quantization we consider only periodic trajectories wholly inside the triangle, we can presumably get the bound states of the walled potential.

For these quantum states of the walled potential, we used perturbation theory both in the $\varepsilon \to 0$ and $\varepsilon \to \infty$ limits. For the small ε case, the unperturbed states are the two-dimensional harmonic oscillator states, and the perturbation is the cubic part of V. There should also be a perturbation corresponding to the hard wall, but since the oscillator wave functions have $e^{-(x^2 + y^2)/\varepsilon}$ as a factor, the overlap with the area outside the triangle is of order $e^{-1/\varepsilon}$, which has an identically zero Taylor series about $\varepsilon = 0$. Thus to all orders of perturbation theory, the wall is negligible. This is not surprising, since $\varepsilon \to 0$ is exactly the classical limit, and we know that classically the wall is negligible. The length scale for the unperturbed states is $\varepsilon^{\frac{1}{2}}$, and the perturbation is a length cubed multiplied by ε^{-1}, from (13.6) and (13.2), so the perturbation series is in powers of $\varepsilon^{\frac{1}{2}}$. The matrix elements of the cubic part of V between standard ($\varepsilon = 1$) oscillator states $|nm>$ are shown in Table 1. The first order terms are identically zero, and second order degenerate perturbation theory gives the bound-state energies shown in the second column of Table 2. For the

$\varepsilon \rightarrow \infty$ limit, we used unperturbed states which are those of a free particle confined within an equilateral triangle (Pi80). These eigenfunctions are combinations of six plane waves, and ε does not appear in the functions. Thus the energies are proportional to ε, and the corrections from first order perturbation theory are proportional to ε^{-1}. These matrix elements were computed numerically by integration on a triangular mesh with some 2000 points. The $\varepsilon \rightarrow \infty$ energy levels are shown in Table 2, together with the degeneracies of each level. Note that the degeneracy can only be 1 or 2, since the irreducible representations of the symmetry group D_3 of the system have dimensionality 1 or 2. The two limits and a freehand interpolation are shown in Figure 14. It would be better for comparison to have exact energy levels for all ε, but in view of the complete failure of the method of quantization by periodic trajectories (see below) this would seem unnecessary. Nordholm and Rice calculated their energy levels for only one value of ε, $1/\sqrt{80}$, and the energy levels are slightly lower than ours, because their system is not constrained by the wall.

The quantization prescription of §9, requires stable periodic trajectories. For the Berry & Tabor calculation of the density of states (Be77), we would need *all* stable periodic trajectories, but the algorithm of §8 does not guarantee to find all periodic trajectories, nor even for those trajectories of period less than some limit.

We shall now restate the method of §8 for the particular case of the Henon-Heiles potential, and explain the numerical technique and convergence criterion, as well a how to find an approximate periodic trajectory as input to the Newton iteration.

The algorithm consists of a Newton iteration scheme for finding the Fourier coefficients for the coordinates, given an approximate set of

coefficients. As explained in §8, we can treat only trajectories with real Fourier coefficients, or equivalently with zero velocity at time zero, or equivalently trajectories with $x,y(t) = x,y(T-t)$ for period T. If A_k, B_k are the coefficients as in (8.2) with $A_k = A_{-k}, B_k = B_{-k}$, then we need only retain $A_0, A_1, \cdots$ and $B_0, B_1, \cdots$. A periodic trajectory $x(t), y(t)$ is a classical trajectory of the Henon-Heiles Lagrangian $\tilde{L}$ of frequency ω if and only if

$$\frac{\omega}{\pi}\frac{\partial S}{\partial A_{-k}} \equiv F_k = (k^2\omega^2 - 1)A_k - \sum_{m=-\infty}^{\infty} 2A_{|m|}B_{|k-m|} = 0 \qquad (13.8)$$

$$\frac{\omega}{\pi}\frac{\partial S}{\partial B_{-k}} \equiv G_k = (k^2\omega^2 - 1)B_k - \sum_{m=-\infty}^{\infty} (A_{|m|}A_{|k-m|} - B_{|m|}B_{|k-m|}) = 0$$

where $k = 0,1,2,\cdots$. The second derivative matrix of S can be written in terms of 2×2 sub-matrices, so the Newton iteration becomes

$$\sum_{k=-\infty}^{\infty} \begin{bmatrix} \lambda^{(k)}\delta_{lk} - 2B_{|k-l|} & -2A_{|k-l|} \\ -2A_{|k-l|} & \lambda^{(k)}\delta_{lk} + 2B_{|k-l|} \end{bmatrix} \begin{bmatrix} \delta A_k \\ \delta B_k \end{bmatrix} = - \begin{bmatrix} F_l \\ G_l \end{bmatrix} \qquad (13.9)$$

where $\lambda^{(k)} = k^2\omega^2 - 1$, or equivalently,

$$\begin{bmatrix} \lambda^{(0)} - 2B_0 & -2A_0 & \cdots & -2\sqrt{2}B_l & -2\sqrt{2}A_l & \cdots \\ -2A_0 & \lambda^{(0)} + 2B_0 & & -2\sqrt{2}A_l & 2\sqrt{2}B_l & \\ \cdots & & & \cdots & & \\ -2\sqrt{2}B_k & -2\sqrt{2}A_k & \cdots & \begin{matrix}\lambda^{(k)}\delta_{lk} \\ -2B_{k+l} \\ -2B_{|k-l|}\end{matrix} & \begin{matrix}-2A_{|k-l|} \\ -2A_{k+l}\end{matrix} & \cdots \\ -2\sqrt{2}A_k & 2\sqrt{2}B_k & & \begin{matrix}-2A_{|k-l|} \\ -2A_{k+l}\end{matrix} & \begin{matrix}\lambda^{(k)}\delta_{lk} \\ +2B_{k+l} \\ +2B_{|k-l|}\end{matrix} & \\ \cdots & & & \cdots & & \end{bmatrix} \begin{bmatrix} \delta A_0/\sqrt{2} \\ \delta B_0/\sqrt{2} \\ \cdots \\ \delta A_l \\ \delta B_l \\ \cdots \end{bmatrix} = - \begin{bmatrix} F_0/\sqrt{2} \\ G_0/\sqrt{2} \\ \cdots \\ F_k \\ G_k \\ \cdots \end{bmatrix}$$

$$... (13.10)$$

which puts the second-derivative matrix in symmetric form.

Following Helleman and Bountis, we tried analytically to find approximate solutions for the Fourier coefficients, which might be close enough for the Newton method to converge. They assumed that the x and y motions were each dominated by one coefficient, so that

$$x(t) \approx A_0 + 2A_\alpha \cos \alpha\omega t$$

$$y(t) \approx B_0 + 2B_\beta \cos \beta\omega t \ , \qquad (13.11)$$

and by much juggling with the equations for $\partial S/\partial A_0$, $\partial S/\partial B_0$, $\partial S/\partial A_\alpha$, $\partial S/\partial B_\beta$ they obtain a set of equations that converge. We found that with our (different) Newton iteration, this approximation either converges to the trivial solution $x(t) = y(t) = 0$, or $x(t)$, $y(t) \to \infty$, or that it converges to a periodic trajectory with no resemblance to the so-called approximation. One can include more coefficients by the hypothesis

$$1 \gg |A_\alpha|, \ |B_\beta| \gg |A, B_{|\alpha-\beta|}|, \ |A, B_{\alpha+\beta}|, \ |A_{2\alpha}|, \ |B_{2\beta}| \qquad (13.12)$$

and still solve the equations (13.9) analytically, but we encountered the same problems as before. It seems artificial to separate the x and y motions for the Henon-Heiles potential, since this completely destroys its D_3 symmetry. This approach only works for the trajectories which stay close to the origin, because there the potential is essentially a harmonic oscillator, and the motion separates into x and y components anyway.

A more successful strategy for obtaining an approximate Fourier series is as follows. Choose some maximum period T_1 much bigger than the fundamental oscillator period, which is 2π in our dimensionless units.

Choose a fine mesh in the xy-plane, and for each point in this mesh integrate the differential equations of motion for a time T_1, with zero-velocity initial conditions. Find the time $t_1 \in (1, T_1)$ at which the speed $(\dot{x}^2 + \dot{y}^2)^{1/2}$ is minimized. If this speed is greater than some tolerance, go to the next mesh point, and otherwise assume that a periodic trajectory of period $2t_1$ is close, in the sense of having nearby initial conditions. We then calculate the stability matrix $L(t_1)$ by solving the 16 differential equations (8.11), then use Newton's method to find better initial conditions, which hopefully make the speed smaller than a second, smaller, tolerance. If this process converges, we can calculate the Fourier series for the trajectory (keeping only 10 coefficients for each coordinate) and use this as input to the Fourier-space Newton iteration. Clearly the method will only find periodic trajectories which are stable, or nearly so. However, the methods of §8 extend this single trajectory to a continuous family of periodic trajectories, so by calculating the coefficient vector (u_ω, v_ω) of (8.9) we can change the frequency slightly and then converge exactly to the trajectory with the new frequency using the Newton iteration. Having found one trajectory, it is easy to move far from it in small steps, and of course back again, by this means. The stability index can be > 1000 for the most unstable trajectories; in other words, if the initial conditions have an error δ, then after one period the error is $e^{1000}\delta$.

The equations (13.9) call for inverting an infinite matrix, which is obviously not possible numerically. Instead we used a basis $A_0, A_1, \ldots, A_K, B_0, B_1, \ldots, B_K$, and used the following convergence criterion. If the sum of the absolute values of the right hand sides of equations (13.8), $\sum_0^K |F_k| + |G_k|$, was not less than 10^{-6}, apply the Newton iteration again until it is, but quit after 15 steps. When this is achieved,

demand that the sum of the absolute values of the last few coefficients,

$\sum\limits_{K-10}^{K} |A_k| + |B_k|$, be less than 10^{-6}, otherwise increase K by 10 and start

with the Newton iteration again. When these criteria are both satisfied, we

have a Fourier series with the last ten coefficients essentially zero, which

satisfies (13.8). In a few cases, we tried doubling the size of the basis at

this stage, and converging again, and found that no Fourier coefficient

changed by more than 5×10^{-6}.

Given the trajectory, we calculated the initial conditions $x_\omega(0)$, $y_\omega(0)$;

since the potential has six-fold symmetry, these can be reflected about

the symmetry axes and rotated by 120° until they lie in the sextant

$x_\omega > 0$, $y_\omega > x_\omega/\sqrt{3}$. In addition, the "other end" of the trajectory

$x_\omega(\pi/\omega)$, $y_\omega(\pi/\omega)$ furnishes another initial condition for a periodic tra-

jectory without further work, which has the same characteristics as the

first. We also computed the energy,

$$\overline{E} = \frac{1}{2}(x_\omega^2 + y_\omega^2) + x_\omega^2 y_\omega - y_\omega^3/3 \ , \tag{13.13}$$

and the quantization integral,

$$Q \equiv \frac{\omega}{2\pi} \int\limits_0^{2\pi/\omega} (\dot{x}^2 + \dot{y}^2) \, dt = \sum\limits_{k=1}^{K} 2k^2\omega^2(A_k^2 + B_k^2) \ . \tag{13.14}$$

By the methods of §8 we calculated the stability angle ν, and the rates of

change of ν, $x_\omega(0)$, and $y_\omega(0)$ with frequency.

The results are shown in Figure 15. Each point of each solid line

(except the x-axis) represents the initial condition for a periodic trajec-

tory, with the frequency varying continuously along each line. The thin

lines represent unstable trajectories, and the thick lines stable trajec-

tories. Where the length of the stable part is smaller than the thickness

of the line, there is just a blob. The area shown is only one sixth of the plane; the full plane can be obtained by applying the D_3 symmetry operations. The contour $E = 1/6$ is marked with a dashed line; this is the position of the hard wall. In some cases the lines (families of trajectories) appear to be unbounded in the xy-plane, and we have followed some out to $x \gtrsim 10$, where the stability index is large and positive. Others seem to just end, and are marked with a short perpendicular line; the stability index is arbitrarily large and positive close enough to this end-point. We have checked that at these end-points the determinant of the second derivative matrix of S goes to zero, so probably there is some kind of bifurcation there.

A bifurcation in this context is a point of frequency ω on a continuous family of periodic trajectories (the "mother") where another family of frequency ω/n is formed (the "daughter"). The locus of the initial conditions looks like a pitchfork (see Figure 15 for examples), and hence these are sometimes referred to as "pitchfork bifurcations" (Li83). Following the daughter family toward the bifurcation, we found that the initial point $x(0), y(0)$ and the "other end" point $x(\pi/\omega), y(\pi/\omega)$ were on opposite tines of the pitchfork, and both approach the junction as the frequency approaches ω/n. From that point on, the algorithm follows the mother, but the Fourier series is "stretched," with the only non-zero harmonics being multiples of n, and the frequency reduced by a factor n from the primitive frequency ω.

There are also bifurcations within the stable regions. As explained in §8, this is where the stability index is some rational multiple of 2π, so that $\nu = 2\pi m/n$. Since only $\cos \nu$ is actually computed, without loss of generality we can take $2m < n$. The fraction m/n is written beside some

of the bifurcations shown, and those and many others are listed in Table 5, together with the coordinates, energy, quantization integral, and the larger of the two frequencies at the bifurcation. As explained above, there is another periodic trajectory with initial conditions $x_\omega(\pi/\omega)$, $y_\omega(\pi/\omega)$, and if this is different from the original initial conditions, this is shown immediately below. In both Figure 15 and Table 5, we restricted ourselves to frequencies greater than 0.1.

Figure 16 shows a sequence of bifurcations, from the origin, marked A, to the point marked B, to C, to D, to E, which is a copy of part of Figure 15. The side panels show $\frac{1}{2}\mathrm{Tr}\, L - 1 = \cos \nu$ or $\pm\cosh \nu$ (cf. §8) and the frequency against either a normalized x or y coordinate, depending on how the initial condition point is moving. The behavior of $\cos \nu$ between B and C is distinctly different from that between AB, CD, and DE, in that $\cos \nu$ is not only equal to, but also tangent to the line at -1. This is in some sense a higher order bifurcation than the usual one, and this and three similar ones are marked "Double" in Table 5.

It is now easy to show that quantization by periodic trajectories does not yield sensible results. First we rewrite (13.4),

$$Q - \frac{l + \frac{1}{2}}{2\pi}\omega\nu - \frac{l + \frac{1}{2}}{2\pi}\omega^2 \frac{d\nu}{d\omega} = (n + \frac{1}{4} \alpha)\omega\varepsilon \;. \qquad (13.15)$$

For a harmonic oscillator, the quantization integral Q is exactly equal to the classical energy $\bar{E}$, and we find that this remains approximately true for the Henon-Heiles potential: within 50% even near the edge of the triangle. Hence $Q \lesssim 0.2$. The second term has magnitude less than $l + \frac{1}{2}$ because $\omega \le 1$ and $0 \le \nu \le 2\pi$. The third term is much larger than $l + \frac{1}{2}$, and easily dominates the left side of (13.15), as can be seen from Figure 17, which shows $e = |\frac{\omega^2}{2\pi} \frac{d\nu}{d\omega}|$ against $\cos \nu$ for all the stable orbits we

found. In fact, e is greater than 5, and thus off the scale, for all orbits except those restricted to the y-axis. It is clear from the exact energy spectrum (Figure 14) that for $\varepsilon \gtrsim 0.1$, the spectrum is that of a free particle in a hard-walled triangle, and here we are interested in the Henon-Heiles spectrum, so we want $\varepsilon \lesssim 0.1$, and consequently are forced to look only at the tail of Figure 17, lower right, where e is small enough to give a reasonable ε. In this case the trajectory is extremely close to the origin, and we can take the Maslov Index to be the harmonic oscillator value, 4. Furthermore, $Q \approx \overline{E} \approx 0$ and $\nu \approx 0$ to a good approximation, so (13.15) becomes

$$- \frac{l + \frac{1}{2}}{2\pi} \omega^2 \frac{d\nu}{d\omega} = (n + 1)\varepsilon \ . \tag{13.16}$$

Substituting in the energy equation (13.5), we obtain

$$\frac{E}{\hbar\Omega} = (n + 1)\varepsilon \ . \tag{13.17}$$

This spectrum is a set of lines radiating the origin, and is obviously completely unlike the true levels in Figure 14.

§14. Summary and Conclusions

The first part of this work has been an attempt to apply semiclassical methods to a nuclear shell model Hamiltonian. We used two equivalent ways to derive the classical Hamiltonian system representing a given shell model: the TDHF variational principle using a Thouless state trial wavefunction and the WKB approximation to the Schrödinger equation for the coherent state wavefunction. Both of these methods result in a generally multi-dimensional classical problem which must then be requantized to find the quantum eigenenergies of the system. This latter is a non-trivial and largely unsettled problem of high current interest, particularly in regard to intramolecular energy transfer. For a schematic three-level shell model, we found that the classical trajectories evolved from harmonic through quasi-periodic to stochastic as the excitation energy increased above the Hartree-Fock minimum. Among the methods we investigated to quantize these trajectories were EBK quantization using surfaces of section, the Birkhoff-Gustavson transformation to action-angle variables, and the ordinary harmonic (RPA) approximation. When the exact quantum level structure was harmonic (or nearly so) we found that all of these semiclassical methods predicted the excitation energies reasonably accurately. However, in more complicated situations all of these methods gave poor results and could, in fact, only find the few lowest energy levels.

In the second part of this work, we used the path-integral representation of the quantum propagator and the stationary phase approximation to derive a quantization prescription relating a particular stable periodic trajectory to a bound state of the quantum system. The energy of the bound state was the sum of the classical energy of the path and the

energy of a harmonic oscillator representing small variations of the classical path transverse to the periodic trajectory. We devised a new algorithm for calculating periodic solutions of a Lagrangian system with polynomial potential, and applied it to the Henon-Heiles potential, with good results. The quantization condition failed to give reasonable results because the zero-point energy of the transverse oscillations was much larger than the energy scale of the system. The problem seems to be that a wave-packet spreads with time, and these zero-point fluctuations are an expression of this, so that even though the classical mechanics predicts stable periodic motion, the quantum motion is dominated by diffusion of the packet.

As a practical tool, semiclassical quantization leaves much to be desired. It is far more laborious than the harmonic approximation, yet produces results only when this is already fairly accurate. Realistic physical systems involving many variables will certainly correspond to more complicated classical systems than the two-dimensional ones we have used as our examples, and here the situation can only be worse: the surface of section method is a very arduous proposition even in three dimensions and the computer implementation of the algebra for the Birkhoff-Gustavson procedure uses prodigious amounts of time for more than three or four dimensions. Periodic trajectory quantization does not work as derived above, and the only hope seems to be the methods of Berry and Tabor, but these methods require all the periodic orbits of the system, which is not possible at present for a dynamical system, and is very difficult even for a simple two-dimensional map (Ta83).

Of more basic interest, we have shown that these semiclassical methods, while derived from quantum mechanics, appear to have

structure not present therein, such as stochasticity and entropy. Their connection with the properties of the exact quantum system and the insight that they might offer into physical problems seems a particularly intriguing area for future study.

EBK quantization is by now a fairly well-known procedure, but limited to the regular part of the classical phase space. The real challenge is to achieve a statement about a quantum system based on the stochastic phase space, which may be possible using periodic orbits. Some possible approaches might be motivated by catastrophe theory: the path-integral for the propagator can be restated as an integral over Fourier coefficients, and one might be able to relate the elementary catastrophes (Be76, Gu78) in this space to the bifurcations of various types, and thence to quantum mechanics. Alternatively, one might calculate the evolution of a Wigner transformed wave-packet (Oz82), in which case the motion can be directly expressed as a classical trajectory, with systematic quantum corrections. Since the level structure is well-described by random matrix theory, one might accept that the wave-functions in the stochastic regime are in some sense random, and therefore study properties of waves in random Hamiltonians (Gu78). Yet another approach is that the hierarchy of daughter periodic trajectories due to bifurcation from a mother suggests the use of renormalization techniques to calculate a better stationary phase approximation.

References

Ab64   M. Abramowitz and I. A. Stegun, <u>Handbook of Mathematical Functions</u>, (New York, Dover, 1964).

Ai38   G. B. Airy, Trans. Camb. Phil. Soc., **6** (1838) 379.

Al81   Y. Alhassid and S. E. Koonin, Phys. Rev., **C23** (1981) 1590; Y. Alhassid, B. Muller and S. E. Koonin, Phys. Rev., **C23** (1981) 487; K. R. S. Devi and S. E. Koonin, Phys. Rev. Lett., **47** (1981) 27.

Ar68   V. I. Arnold and A. Avez, <u>Ergodic Problems of Classical Mechanics</u>, (New York, W. A. Benjamin Inc., 1968) Appendix 26.

Ar78   V. I. Arnold, <u>Mathematical Methods of Classical Mechanics</u>, (New York, Springer- Verlag, 1978).

Ba77   R. Balian and C. Bloch, Ann. Phys., **69** (1977) 76.

Ba79   R. Balian, G. Parisi, and A. Voros, in <u>Feynman Path Integrals</u>, ed. S. Albeverio et. al., (New York, Springer-Verlag, 1979), p. 337.

Be72   M. V. Berry and K. E. Mount, Reps. Prog. Phys., **35** (1972) 315.

Be76   M. V. Berry, J. F. Nye, and F. J. Wright, Proc. Roy. Soc. London, **A291** (1976) 453; T. Postern and I. Stewart, <u>Catastrophe Theory and its Applications</u>, (London, Pitman, 1978).

Be77   M. V. Berry and M. Tabor, Proc. Roy. Soc. London, **A349** (1976) 101; J. Phys., **A10** (1977) 371; M. Tabor, Ref. Ca77, p. 293.

Be80   F. A. Berezin, Usp. Fiz. Nauk., **132** (1980) 497.

Be81   M. V. Berry, Ann. Phys., **131** (1981) 163.

Bi66   G. D. Birkhoff, <u>Dynamical Systems</u>, (New York, Am. Math. Soc., 1966), Vol IX; G. F. Gustavson, Astron. J., **71** (1966) 670; R. T. Swimm and J. B. Delos, J. Chem. Phys., **71** (1979) 1706; M. Robnik, J. Phys. A, to be published.

Bl81   J. P. Blaizot and H. Orland, Phys. Rev., **C24** (1981) 1740.

Ca77   Stochastic Behavior in Classical and Quantum Hamiltonian Systems, G. Casati and J. Ford, eds., Proceedings of the Volta Memorial Conference, Como, Italy, 1977, (New York, Springer-Verlag, 1979).

Ce79   D. M. Ceperly and M. H. Kalos, in Monte-Carlo Methods in Statistical Physics, ed. K. Binder, (New York, Springer-Verlag, 1979) p. 145; G. Maddison, Y. Alhassid, and S. E. Koonin, unpublished; J. G. Zabolitsky and M. H. Kalos, Nucl. Phys., **A356** (1981) 114.

Ch76   S. Chapman, B. C. Garrett, and W. H. Miller, J. Chem. Phys., **64** (1976) 502.

Ch77   R. C. Churchill, G. Pecelli, and D. L. Rod, in Ref. Ca77, p. 76.

Ch80   R. C. Churchill, G. Pecelli, and D. L. Rod, Arch. Rat. Math. Anal., **73** (1980) 313.

Co65   E. T. Copson, Asymptotic Expansions, (Cambridge University Press, 1965).

Co80   G. Contopoulos, Celestial Mech., **22** (1980) 403.

Da74   R. F. Dashen, B. Hasslacher and A. Neveu, Phys. Rev., **D10** (1974) 4114.

De79   C. DeWitt-Morette, A. Maheshwari, and B. Nelson, Phys. Repts., **50** (1979) 255.

Di58   P. A. M. Dirac, The Principles of Quantum Mechanics, (Oxford University Press, 1958).

Di80   A. E. L. Dieperink and O. Scholten, Nucl. Phys., **A346** (1980) 125; D. H. Feng, R. Gilmore and S. R. Deans, Phys. Rev., **C23** (1981) 1254; O. S. van Roosmalen and A. E. L. Dieperink, Phys. Lett., **100B** (1981) 299; O. S. van Roosmalen and A. E. L. Dieperink, Ann. Phys., **139** (1982) 198; O. S. van Roosmalen, PhD Thesis, University of Groningen 1982.

Do81   J. Dobaczewski, Nucl. Phys., **A369** (1981) 213.

Ea74   W. Eastes and R. A. Marcus, J. Chem Phys., **61** (1974) 4301. D. W. Noid and R. A. Marcus, J. Chem. Phys., **62** (1975) 2119.

Ei17   A. Einstein, Verhand Deut. Phys. Ges., **19** (1917) 82; M. L. Brillouin, J. de Physique (Ser. 6), **7** (1926) 353; K. S. Sorbie and N. C. Handy, Mol. Phys., **32** (1976) 1327.

Fe65   R. P. Feynman and A. R. Hibbs, <u>Quantum Mechanics and Path Integrals</u>, (New York, McGraw-Hill, 1965).

Fl81   B. A. Flanders, PhD Thesis, California Institute of Technology, 1981; S. Y. Li, A. Klein and R. M. Dreizler, J. Math. Phys., **11** (1970) 975; G. Holzworth and T. Yukawa, Nucl. Phys., **A219** (1974) 125.

Fr65   N. Froman and P. O. Froman, <u>The JWKB Approximation</u>, (Amsterdam, North-Holland, 1965).

Go80   H. Goldstein, <u>Classical Mechanics</u>, (Reading, Mass., Addison-Wesley, 1980).

Gu73   M. C. Gutzwiller, J. Math. Phys., **8** (1967) 1979; **10** (1969) 1004; **11** (1970) 1791; **12** (1971) 343; **14** (1973) 139.

Gu77   M. C. Gutzwiller, J. Math. Phys., **18** (1977) 806; Ref Ca77, p. 316; Physica **5D** (1982) 183; Phys. Rev. Lett. **45** (1980) 150.

Gu78   M. C. Gutzwiller, p. 163 in Ref. Kl78.

Gu79   Parts II and III in <u>Structural Stability in Physics</u>, eds. W. Guttinger and H. Eikemeier, (New York, Springer-Verlag, 1979).

He64   M. Henon and C. Heiles, Astron. J., **69** (1964) 73.

He78   R. H. G. Helleman and T. Bountis, Ref Ca77, p. 353. R. H. G. Helleman in <u>Topics in Nonlinear Dynamics</u>, S. Jorna, ed., American Institute of Physics Conference Proceedings **46**, (New York, A. I. P., 1978)

He80   R. H. G. Helleman, in <u>Fundamental Problems in Statistical Mechanics</u>, vol. 5, ed E. G. D. Cohen, (Amsterdam, North Holland, 1980).

He82   M. Henon, Physica **5D** (1982) 412.

Ka59   M. Kac, <u>Probability and Related Topics in the Physical Sciences</u>, (New York, Interscience, 1959).

Ka79   K.-K. Kan, J. J. Griffin, P. C. Lichtner and M. Dworzecka, Nucl. Phys., **A332** (1979) 109.

Ke58   J. B. Keller, Ann. Phys., **4** (1958) 180.

Ke81   A. K. Kerman and S. Levit, Phys. Rev., **C24** (1981) 1029. S. Levit, J. W. Negele, Z. Paltiel, Phys. Rev., **C22** (1980) 1979.

Kl77   H. Kleinert, Phys. Lett., **69B** (1977) 9; H. Reinhardt, Nucl. Phys., **A331** (1979) 353; **A346** (1980) 1.

Kl78   J. Klauder in <u>Path Integrals and their Applications in Quantum,</u> <u>Statistical, and Solid-State Physics</u>, ed. G. Papadopoulos and J. DeVreese, (New York, Plenum, 1978).

Ko53   A. N. Kolmogorov, Doklady Akad. Nauk., **93** (1953) 763, (English translation in Ref. Ca77, p. 51); V. I. Arnol'd, Izv. Akad. Nauk., SSSR Ser. Mat. **25** (1961) 21; Usp. Mat. Nauk. **18** (1963) 81; **18** (1963) 13; J. Moser, <u>Stable and Random Motions in Dynamical</u> <u>Systems</u>, (Princeton University Press, Princeton, 1973); Am. Math Soc. Mem., **81** (1968) 1; SIAM Review, **8** (1966) 145.

Ko81   S. E. Koonin, in <u>Nuclear Theory 1981</u>, ed. G. Bertsch, Proceedings of the Nuclear Theory Summer Workshop, Santa Barbara, California, 1981 (Singapore, World Scientific, 1982).

Ku82   H. Kuratsuji, Phys. Lett., **108B** (1982) 367, and references therein.

Le80   S. Levit, Phys. Rev., **C21** (1980) 1594; S. Levit, J. W. Negele, Z. Paltiel, Phys. Rev., **C21** (1980) 1603.

Li65   H. Lipkin, N. Meshkov, and A. J. Glick, Nucl. Phys., **62** (1965) 188.

Li83   A. J. Lichtenberg and M. A. Lieberman, <u>Regular and Stochastic</u> <u>Motion</u>, (New York, Springer-Verlag, 1983).

Ma81   V. Maslov and M. V. Fedoriuk, <u>Semiclassical Approximations in</u> <u>Quantum Mechanics</u>, (New York, Reidel, 1981).

Ma80   M. S. Marinov, Phys. Repts., **60** (1980) 1.

Mi63   J. Milnor, <u>Morse Theory,</u> (Princeton University Press, 1963).

Mi75   W. H. Miller, J. Chem. Phys., **63** (1975) 996.

Ne82   J. W. Negele, Rev. Mod. Phys., **54** (1982) 913.

No74   K. S. J. Nordholm and S. A. Rice, J. Chem. Phys., **61** (1974) 203.

No77   D. W. Noid and R. A. Marcus, J. Chem. Phys., **67** (1977) 559.

No80   D. W. Noid, M. L. Koszykowski and R. A. Marcus, J. Chem. Phys.,
        73 (1980) 391.

Oz82   A. M. Ozorio de Almeida and J. H. Hannay, Ann. Phys., **138** (1982)
        115; M. V. Berry, Phil. Trans. Roy. Soc.,**287** (1977) 237.

Pa81   A. Patrascioiu, Phys. Rev., **D24** (1981) 496.

Pi80   M. A. Pinsky, SIAM J. Math. Anal., **11** (1980) 819.

Po92   H. Poincaré, Les Methodes Nouvelles de Mechanique Celeste,
        (Paris, Gauthier-Villars, 1892).

Ra74   P. Rannou, Astron. Astrophys., **31** (1974) 289.

Ra75   R. Rajaraman, Phys. Repts., **21C** (1975) 228;

Re83   W. Reinhardt and C. Jaffe, J. Chem. Phys., to be published.

Ri80   S. A. Rice in Quantum Dynamics of Molecules, ed. R. G. Wooley,
        (New York, Plenum 1980).

Ri82   P. J. Richens, J. Phys., **A15** (1982) 2101.

Sc80   G. Scher, M. Smith, and M. Baranger, Ann. Phys., **130** (1980) 290.

Sc81   L. S. Schulman, Techniques and Applications of Path Integration,
        (New York, Wiley, 1981).

Sh80   R. Shankar, Phys. Rev. Lett., **45** (1980) 1088.

Si41   C. L. Siegel, Ann. Math., **42** (1941) 806; <u>Vorlesungen uber Him-
meshmechanik,</u> (Berlin, Springer, 1957).

Si80   Ja. G. Sinai and E. B. Vul, J. Stat. Phys., **23** (1980) 27.

Ta83   M. Tabor, Physica, **6D** (1983) 195; M. V. Berry, N. L. Balazs, M.
Tabor, and A. Voros, Ann. Phys., **122** (1979) 26.

Wi82   R. D. Williams and S. E. Koonin, Nucl. Phys., **A391**, (1982) 72.

Ya82   L. G. Yaffe, Rev. Mod. Phys., **54** (1982) 407.

Table 1.

Matrix elements of $x^2y - y^3/3$ between standard two-dimensional harmonic oscillator states $<nm|$, $|n'm'>$ with n,n' quanta in the x-direction, m,m' quanta in the y-direction.

n'	m'	$<nm\,|\,x^2y - y^3/3\,|\,n'm'>$
n	$m + 3$	$-(8\,(m + 1)\,(m + 2)\,(m + 3))^{\frac{1}{2}}/\,24$
n	$m + 1$	$(-m + 2n)\,(2\,(m + 1))^{\frac{1}{2}}/\,4$
n	$m - 1$	$(-m + 2n + 1)\,(2m)^{\frac{1}{2}}/\,4$
n	$m - 3$	$-(8m\,(m - 1)\,(m - 2))^{\frac{1}{2}}/\,24$
$n + 2$	$m + 1$	$((n + 1)\,(n + 2)\,(m + 1)/\,8)^{\frac{1}{2}}$
$n + 2$	$m - 1$	$((n + 1)\,(n + 2)\,m/\,8)^{\frac{1}{2}}$
$n - 2$	$m + 1$	$(n\,(n - 1)\,(m + 1)/\,8)^{\frac{1}{2}}$
$n - 2$	$m - 1$	$(n\,(n - 1)\,m/\,8)^{\frac{1}{2}}$

Table 2.

Energy levels of the walled Henon-Heiles system in the classical ($\varepsilon \to 0$) and the quantum ($\varepsilon \to \infty$) limits. The constant α is $8\pi^2/27 = 2.92433$.

Degeneracy	$E/\hbar\Omega$	
	$\varepsilon \to 0$	$\varepsilon \to \infty$
1	$1 - \varepsilon/9$	$3\alpha\varepsilon + 0.036493/\varepsilon$
2	$2 - 7\varepsilon/9$	$7\alpha\varepsilon + 0.060287/\varepsilon$
1	$3 - 31\varepsilon/9$	$12\alpha\varepsilon + 0.072189/\varepsilon$
1	$3 - 10\varepsilon/9$	$13\alpha\varepsilon + 0.068463/\varepsilon$
1	$3 - \varepsilon/9$	$13\alpha\varepsilon + 0.068463/\varepsilon$
2	$4 - 52\varepsilon/9$	$19\alpha\varepsilon + 0.077704/\varepsilon$
2	$4 - 10\varepsilon/9$	$21\alpha\varepsilon + 0.071789/\varepsilon$

Table 3.

Lowest energy levels for the SU(3) model. States are labelled by the number of oscillator quanta, (n_1, n_2). Missing entries for $\chi = 10, 100$ are states where corresponding classical trajectory could not be found.

χ	State	Shifted Exact	Surface of Section	Birkhoff-Gustavson	RPA (harmonic)
0.75	(0,0)	-.97904	-.97879	-.97881	-.97904
	(0,1)	-.96747	-.96672	-.96672	-.96802
	(0,2)	-.95504	-.95388	-.95375	-.95699
	(1,0)	-.94794	-.94681	-.94751	-.94814
	(1,1)	-.93611	-.93519	-.93518	-.93712
	(1,2)	-.92347	-.92216	-.92197	-.92609
10	(0,0)	-3.2446	-3.2407	-3.2407	-3.2446
	(0,1)	-3.0807	-	-3.0883	-3.0731
	(1,0)	-3.0410	-3.0484	-3.0488	-3.0386
100	(0,0)	-31.419	-31.364	-31.376	-31.419
	(0,1)	-29.549	-29.659	-29.652	-29.512
	(1,0)	-29.511	-	-29.514	-29.478

Table 4.

Birkhoff-Gustavson power series for energy as a function of the two action variables for the SU(3) model. n_1 and n_2 are the exponents of the actions. The third and fourth columns show the coefficients for $\chi = 10$ and $\chi = 100$, respectively. Note that the linear terms are the frequencies from (12.11). An asterisk indicates that the term was omitted in the quantization.

n_1	n_2	$\chi = 10$	$\chi = 100$
1	0	10.2905	114.45
0	1	12.3601	116.45
2	0	-23.8587	-178.283
1	1	-7.91484	-99.7851
0	2	-16.3961	-172.208
3	0	-90.0850	-149.959
2	1	-14.0243	-15711.5
1	2	6.53835	15228.72
0	3	7.54966	-72.9650
4	0	-1124.95	-3086.82
3	1	7457.26	2031811.*
2	2	-14510.8*	-5963665.*
1	3	-2.16765	1954006.*
0	4	3209.41	-2274.47

Table 5. (5 pages)

Bifurcations of periodic orbits of the Henon-Heiles system, sorted by energy $\overline{E}$. First column is the value of $\nu/2\pi$ for the mother trajectory; second and third columns are the initial conditions $x(0)$, $y(0)$, with $x(\pi/\omega)$, $y(\pi/\omega)$ shown below if different; fourth column is the classical energy; fifth column is the quantization integral

$$\frac{\omega}{2\pi} \int_0^{2\pi/\omega} \dot{x}^2 + \dot{y}^2 \, dt;$$

sixth column is the frequency of the mother trajectory at bifurcation; and the seventh column is comments (see §13).

Mode	x	y	$\overline{E}$	Q	ω	
1/8	0.	0.48690	0.08006	0.07627	0.91504	
	0.31125	0.17970				
1/7	0.	0.50969	0.08575	0.08125	0.90686	
	0.32115	0.18541				
1/6	0.	0.53704	0.09258	0.08710	0.89644	
	0.33251	0.19198				
1/5	0.	0.57074	0.10090	0.09402	0.88266	
	0.34574	0.19961				
1/2	0.24226	0.38676	0.10755	0.10233	0.11247	Double
1/4	0.	0.61353	0.11123	0.10219	0.86349	
	0.36130	0.20860				
1	0.24099	0.40196	0.11152	0.10605	0.11219	
1/2	0.23295	0.42247	0.11416	0.10841	0.11192	
	0.25095	0.39592				
1	0.23217	0.42643	0.11501	0.10917	0.11183	
	0.25231	0.39665				
1/2	0.14520	0.54332	0.11611	0.10945	0.14761	Double
2/7	0.	0.63953	0.11731	0.10673	0.85084	
	0.37007	0.21366				

Mode	x	y	$\bar{E}$	Q	ω	
1	0.15849	0.54542	0.12092	0.11400	0.14727	
1/3	0. 0.37942	0.66915 0.21906	0.12401	0.11143	0.83540	
1/2	0.30604	0.35574	0.12842	0.11897	0.21506	Double
2/5	0. 0.38878	0.70122 0.22446	0.13092	0.11585	0.81730	
3/7	0. 0.39151	0.71116 0.22604	0.13299	0.11707	0.81137	
1	0.30158	0.38287	0.13488	0.12526	0.21476	
1/2	0. 0.39453	0.72250 0.22778	0.13529	0.11835	0.80440	B
1/2	0.31662 0.38894	0.36305 0.40806	0.13642	0.12645	0.21417	
1/4	0.04969	0.72464	0.13874	0.12187	0.40240	
1/2	0.33216 0.27953	0.35076 0.43737	0.14100	0.12994	0.21236	
1/3	0.06459	0.72611	0.14112	0.12429	0.40254	
1	0.33503 0.27814	0.34957 0.44339	0.14222	0.13087	0.21187	

Mode	x	y	$\overline{E}$	Q	ω	
1/2	0.09019	0.72951	0.14668	0.12996	0.40287	Double
1/2	0.13429 0.05458	0.68390 0.77296	0.14859	0.13049	0.19932	
1/3	0.10935	0.73277	0.15206	0.13544	0.40318	
1/2	0. 0.41627	0.82085 0.24033	0.15254	0.12416	0.73256	
2/5	0. 0.41825	0.83228 0.24148	0.15417	0.12408	0.72248	
1/4	0.11614	0.73406	0.15422	0.13764	0.40331	
1/3	0. 0.84623 0.42052	0.15606 0.24279	0.12372	0.70951		
1	0.12496	0.73585	0.15722	0.14070	0.40348	C
1/4	0. 0.42313	0.86382 0.24429	0.15824	0.12281	0.69196	
1/4	0.10497 0.14742	0.77150 0.70784	0.15855	0.14129	0.40138	
1/3	0.10061 0.15325	0.78171 0.70186	0.15928	0.14160	0.40018	
1/5	0.	0.87337	0.15933	0.12208	0.68177	

Mode	x	y	$\overline{E}$	Q	ω	
	0.42442	0.24504				
1/6	0.	0.87912	0.15995	0.12156	0.67539	
	0.42516	0.24547				
1/2	0.09689	0.79160	0.16009	0.14193	0.39881	D
	0.15870	0.69663				
1/2	0.10511	0.78201	0.16052	0.14223	0.19923	
	0.08954	0.80460				
1/2	0.10511	0.78201	0.16052	0.14223	0.19923	E
	0.08954	0.80460				
1	0.	0.89512	0.16155	0.11973	0.65648	
	0.42705	0.24656				
1	0.	0.93187	0.16445	0.11297	0.60422	
	0.43044	0.24852				
1/5	0.	0.94321	0.16512	0.10991	0.58435	
	0.43122	0.24852				
1/4	0.	0.94700	0.16531	0.10874	0.57713	
	0.43144	0.24909				
1/3	0.	0.95266	0.16558	0.10685	0.56565	
	0.43176	0.24928				
2/5	0.	0.95622	0.16574	0.10555	0.55794	

Mode	x	y	$\overline{E}$	Q	ω
	0.43194	0.24938			
1/2	0. 0.43205	0.95865 0.24945	0.16584	0.10460	0.55243
1/2	0.08547 0.19329	0.85918 0.66886	0.16761	0.14438	0.38495
1	0.08683 0.19950	0.87057 0.66460	0.16935	0.14495	0.38186

Figure 1.

Schematic illustration of a four-dimensional invariant torus when projected in three-dimensional space. One dimension can be omitted because of energy conservation. Two of the four possible coordinate triplets are shown, with surfaces of section.
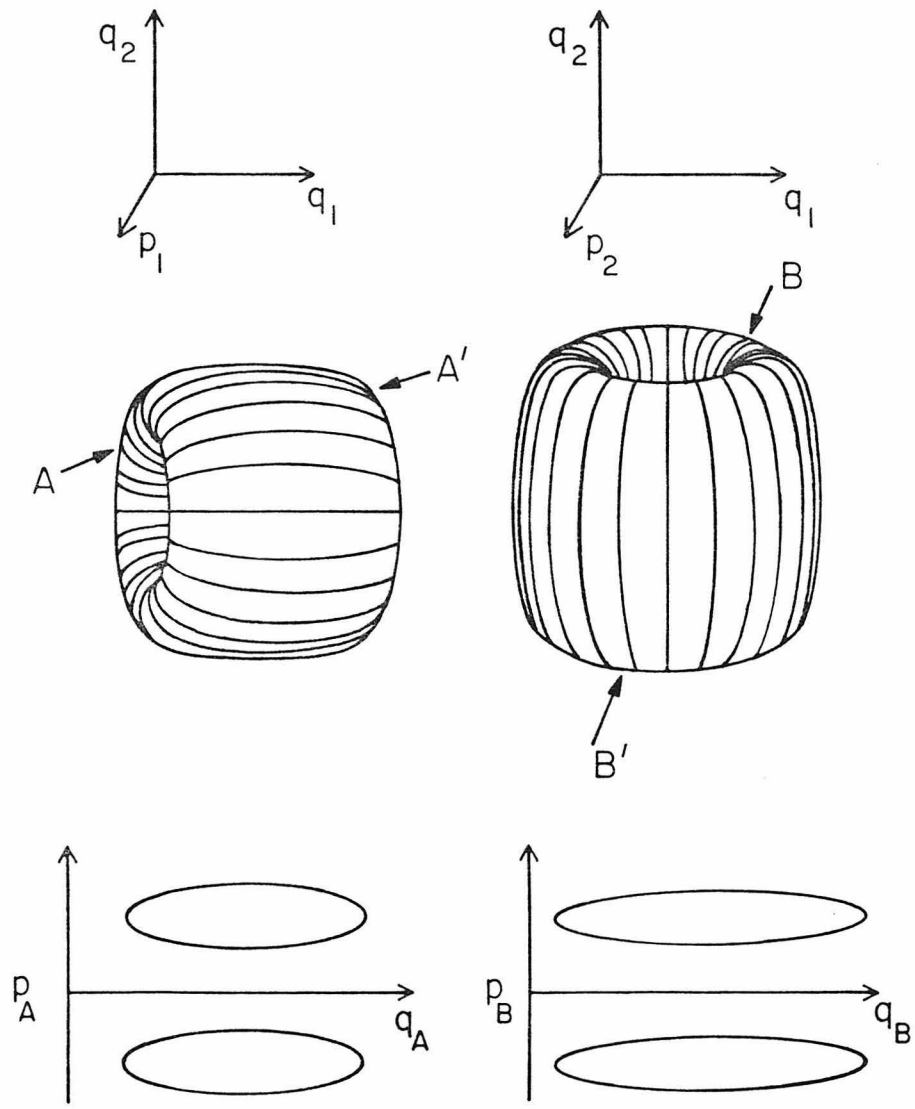
Figure 1

Figure 2.

Contour plot of the Henon-Heiles potential $V(x,y) = \frac{1}{2}(x^2 + y^2) + x^2y - y^3/3$. Phase space is compact inside the triangle, and non-compact outside. Dashed lines mark boundaries of the irreducible sextant.
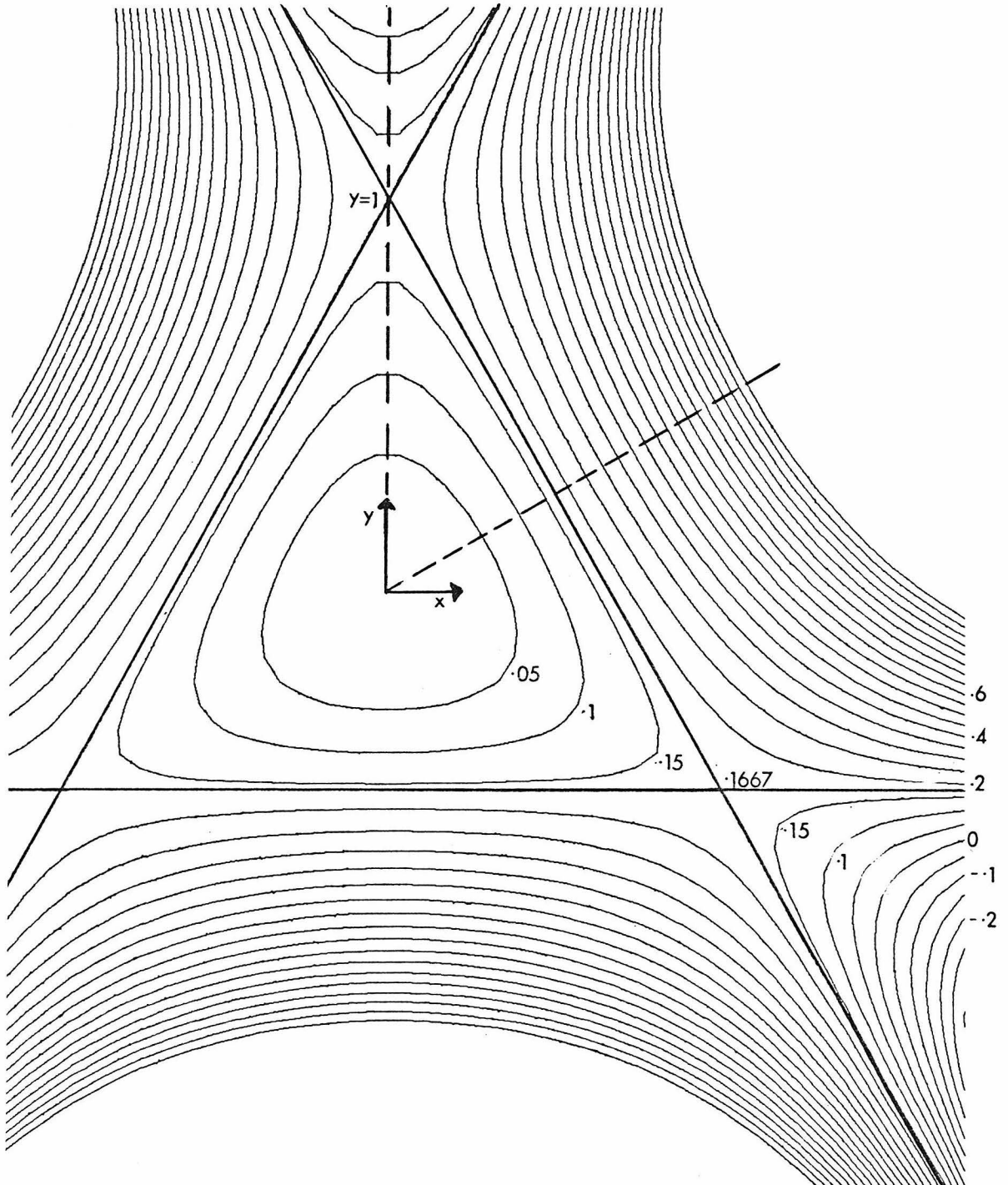
Figure 2

Figure 3. (2 pages)

Surfaces of section for the Henon-Heiles system, energy 0.02. (a) q_1, p_1 section, with $q_2 = 0$. (b) q_2, p_2 section, with $q_1 = 0$.
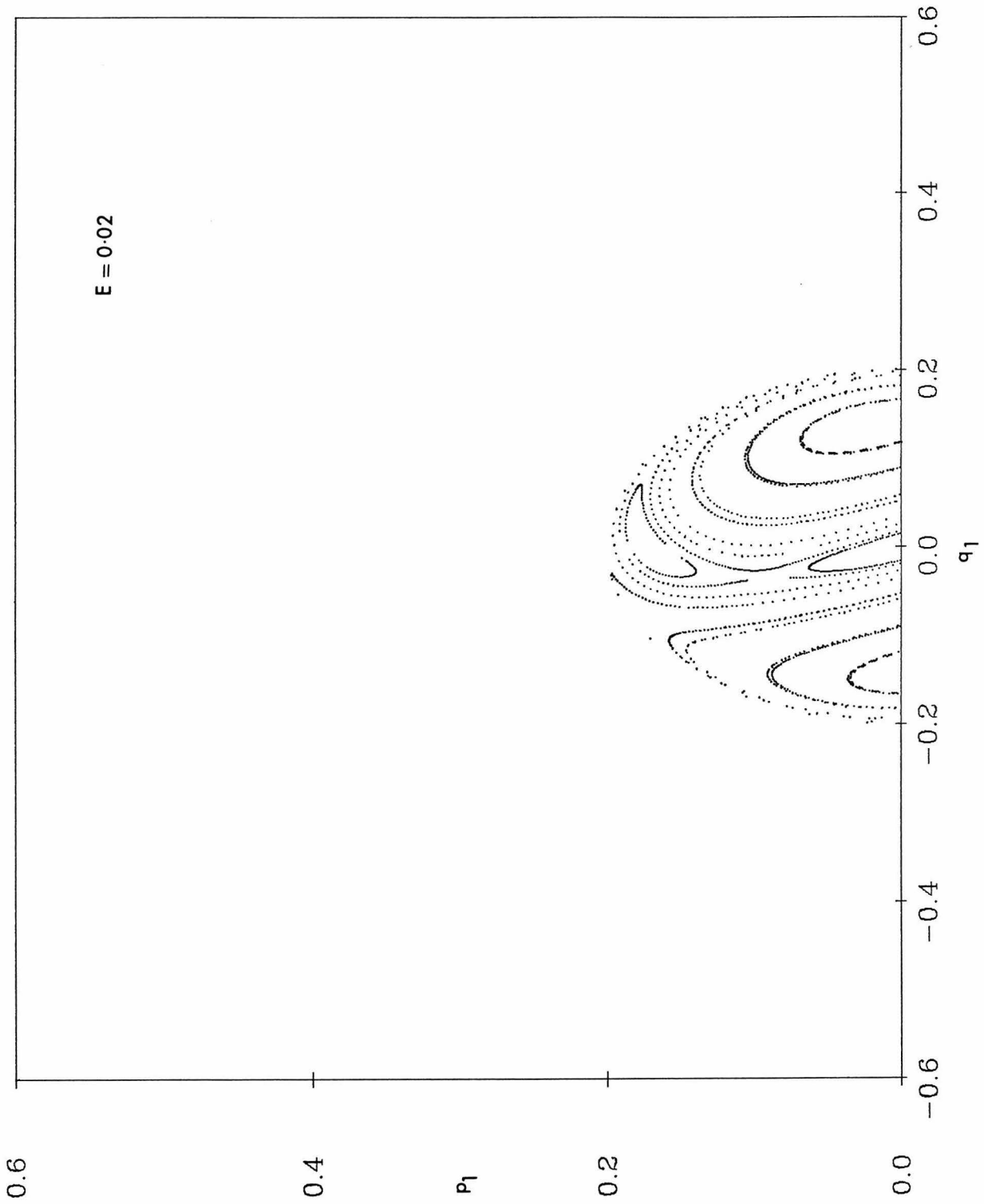
Figure 3a
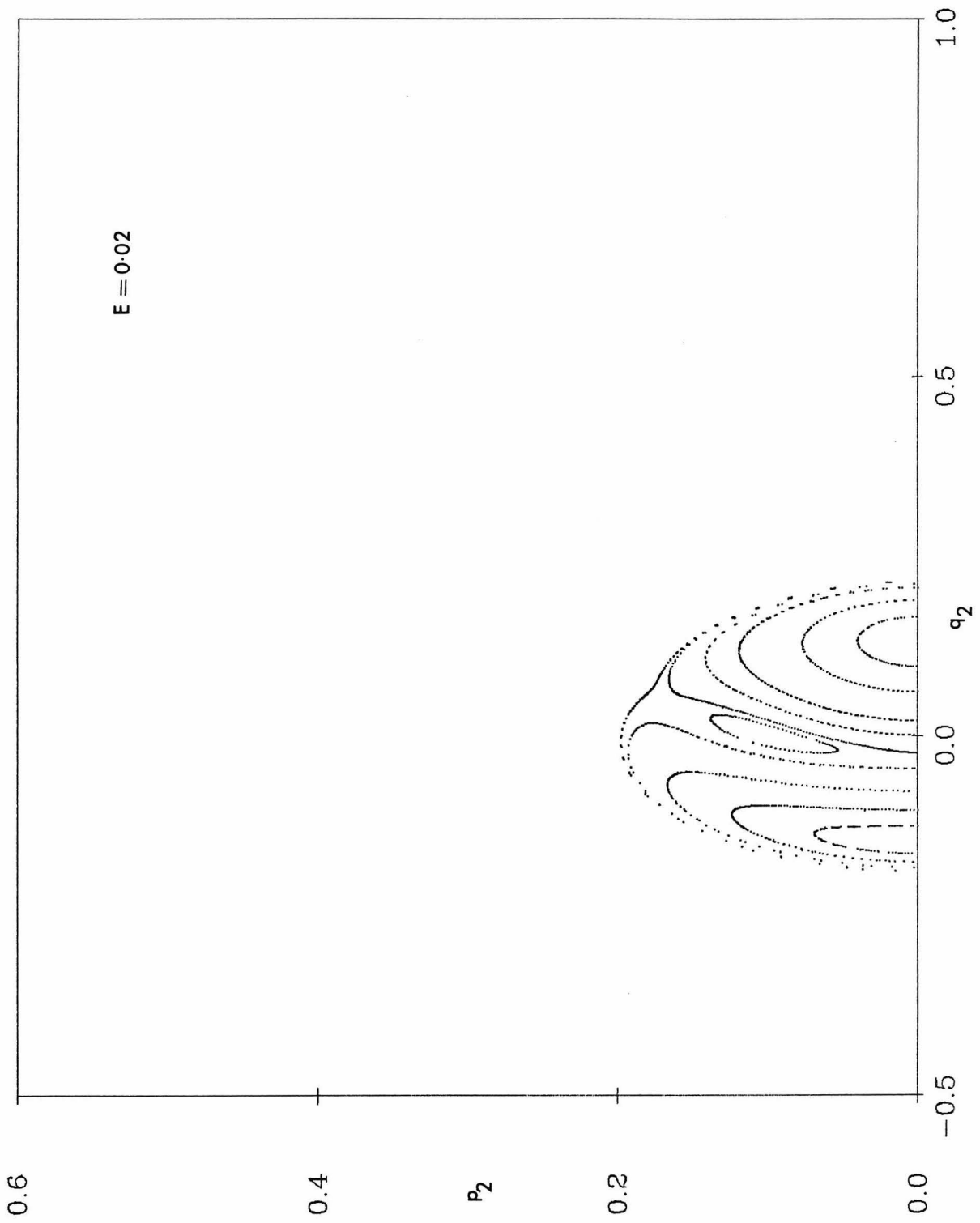
Figure 3b

Figure 4. (2 pages)

Surfaces of section for the Henon-Heiles system, energy 0.08. (a) q_1, p_1 section, with $q_2 = 0$. (b) q_2, p_2 section, with $q_1 = 0$.

E = 0·08

Figure 4a

E = 0·08

q_2

P_2
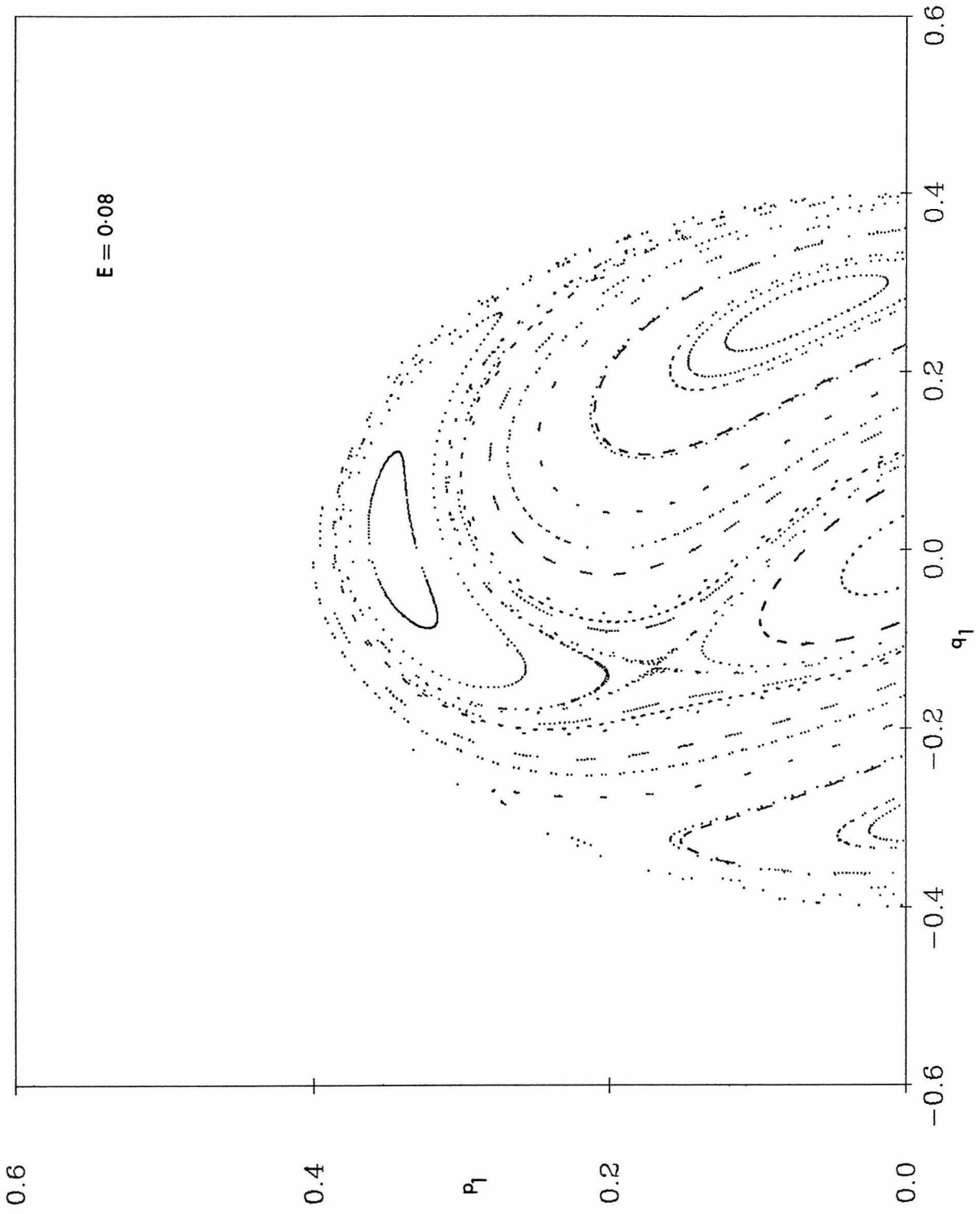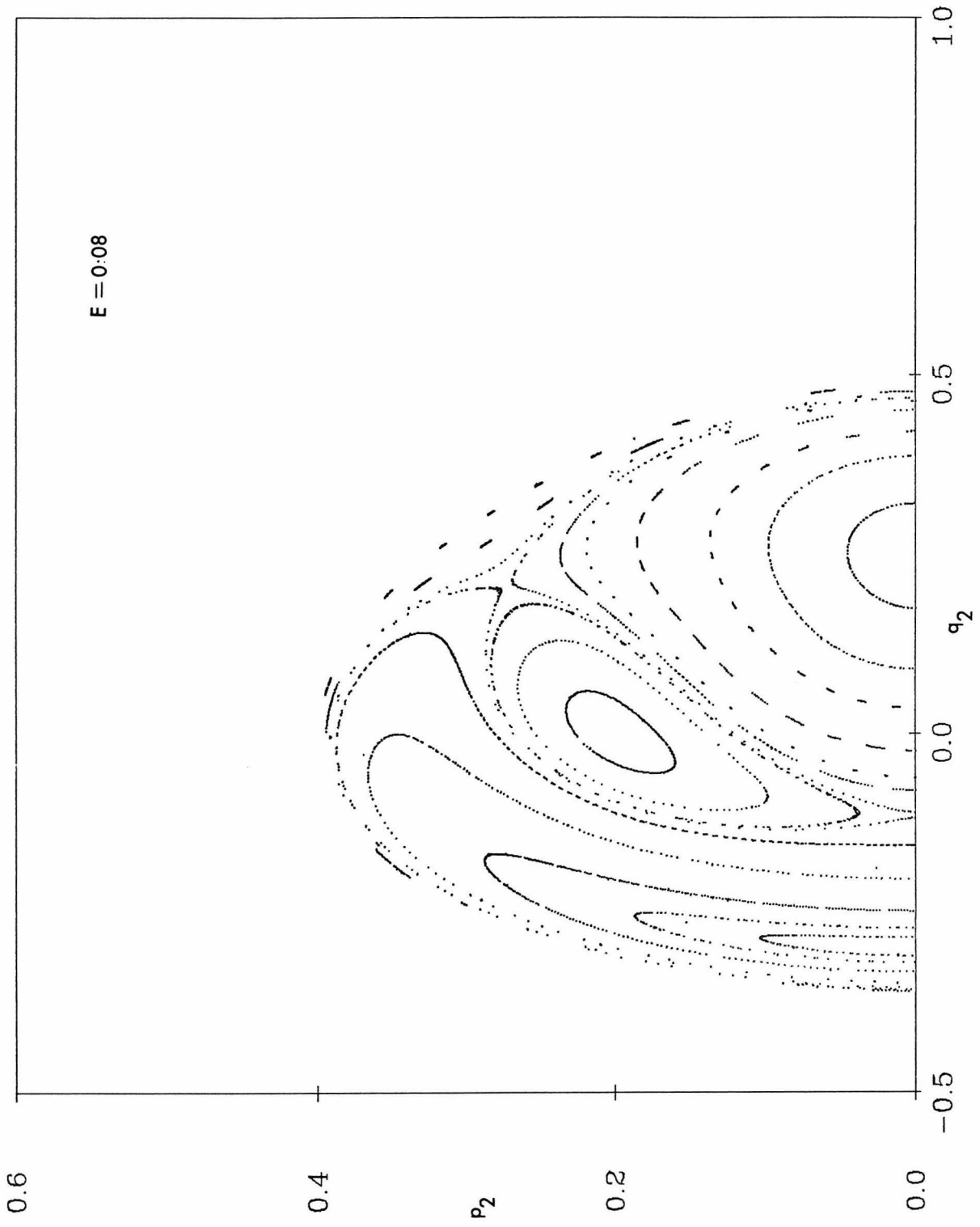
Figure   4b

Figure 5. (2 pages)

Surfaces of section for the Henon-Heiles system, energy 0.1. (a) q_1, p_1 section, with $q_2 = 0$. (b) q_2, p_2 section, with $q_1 = 0$.

Figure 5a

E = 0·1
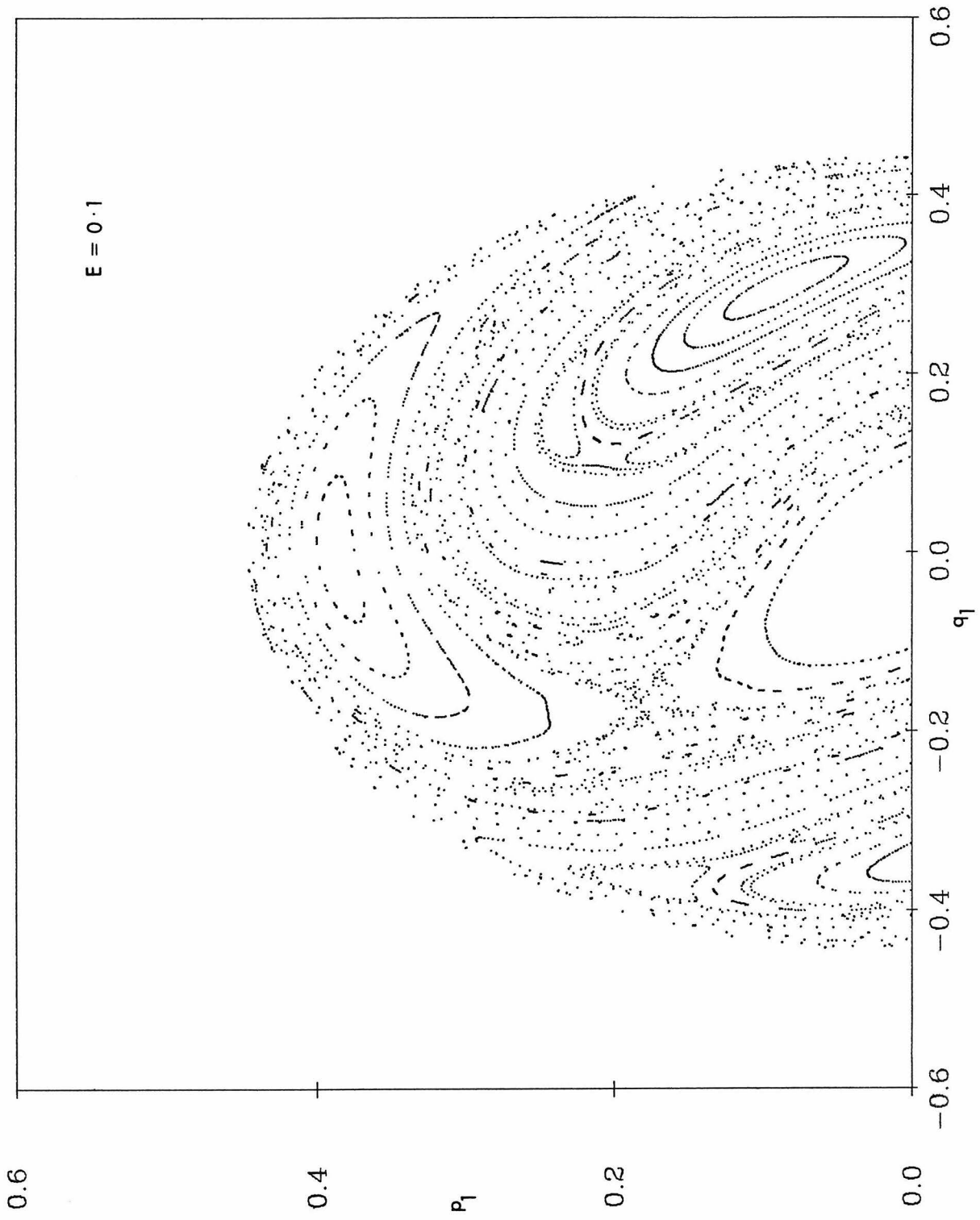
Figure   5b

Figure 6. (2 pages)

Surfaces of section for the Henon-Heiles system, energy 0.166. (a) q_1, p_1 section, with $q_2 = 0$. (b) q_2, p_2 section, with $q_1 = 0$.

Figure 6a

E = 0·166
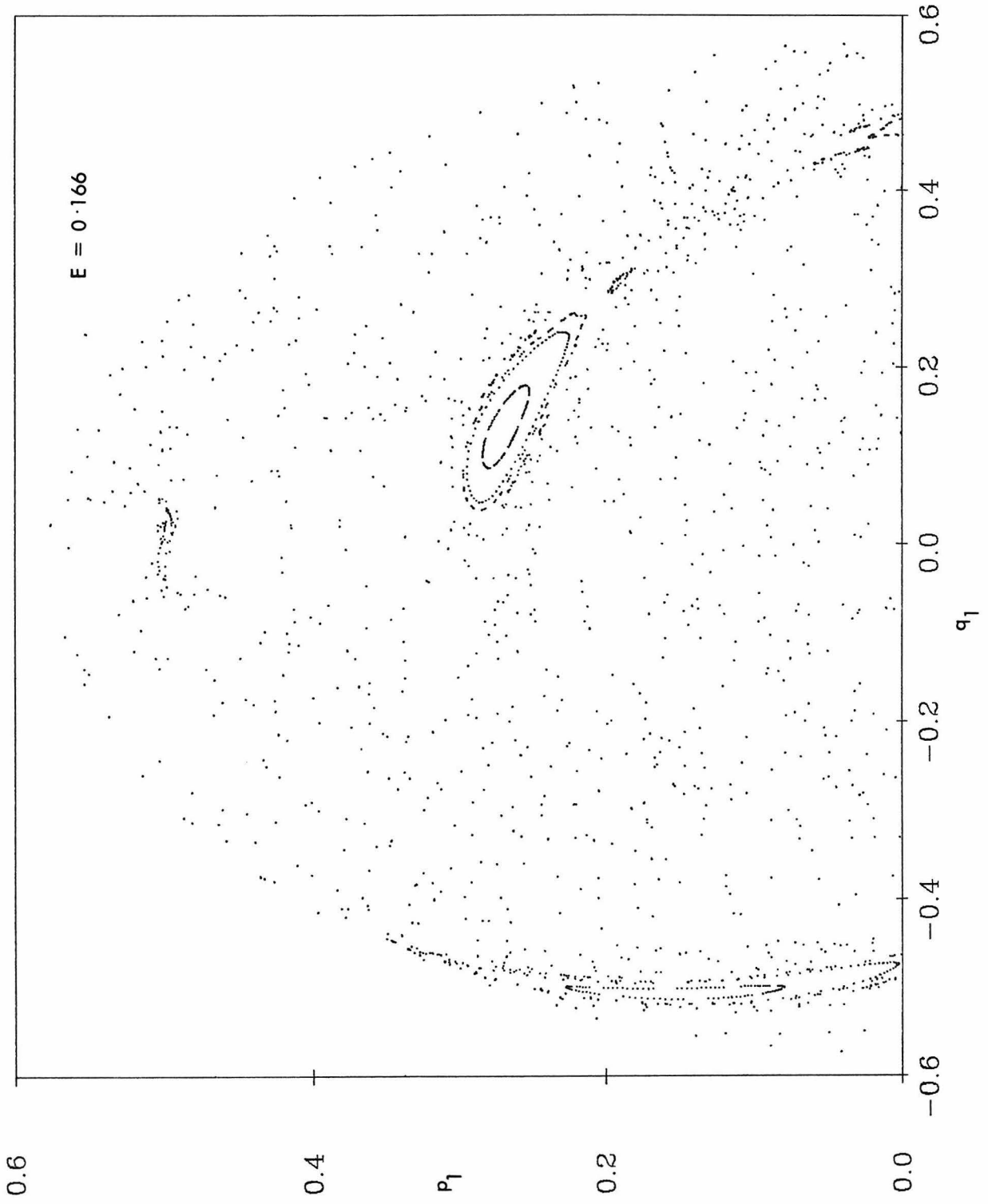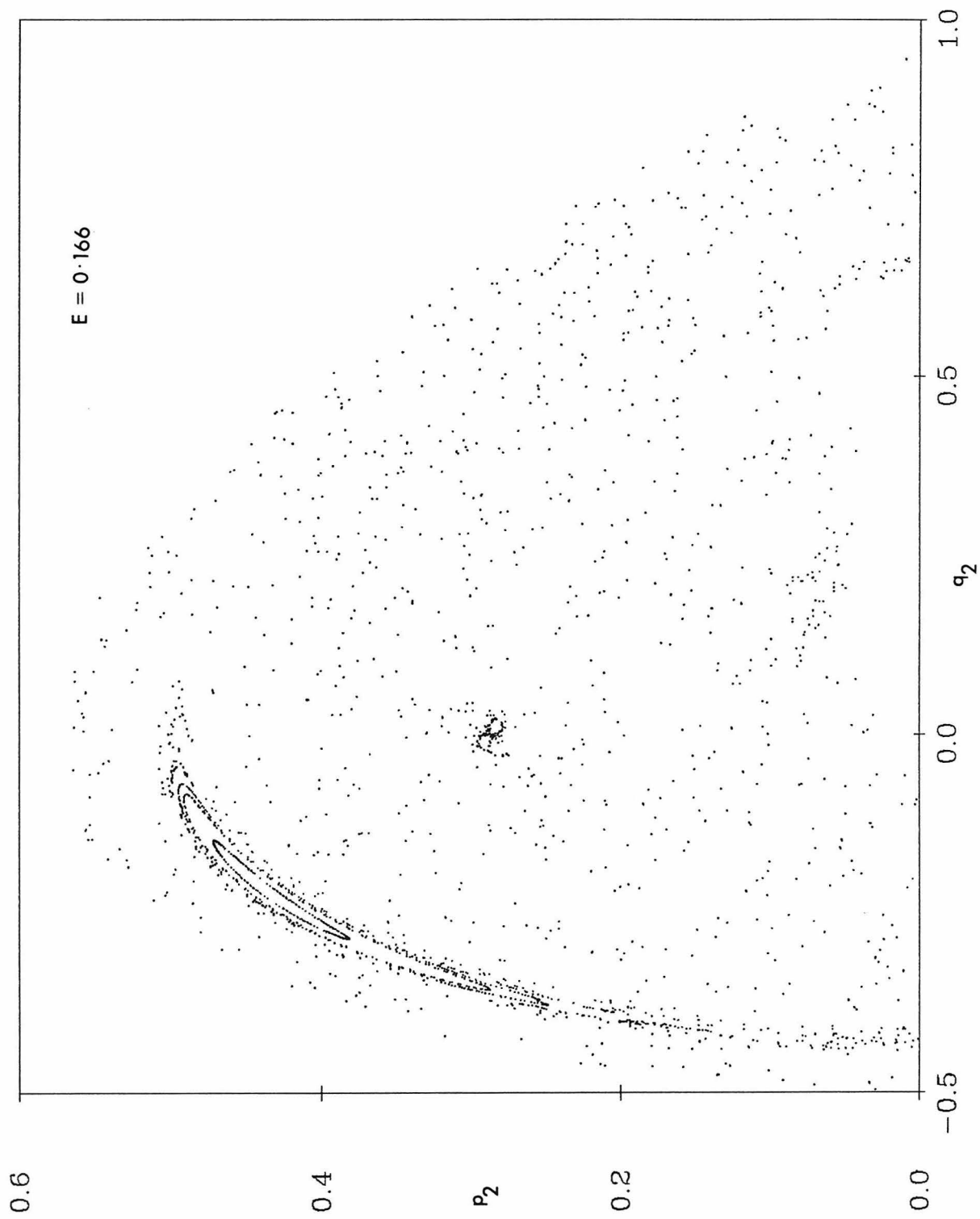
Figure 6b

Figure 7.

Contour plot of the static Hamiltonian H($\mathbf{q}, \mathbf{p} = 0$), for the SU(3) model. $\chi = 0.75$, with one minimum.
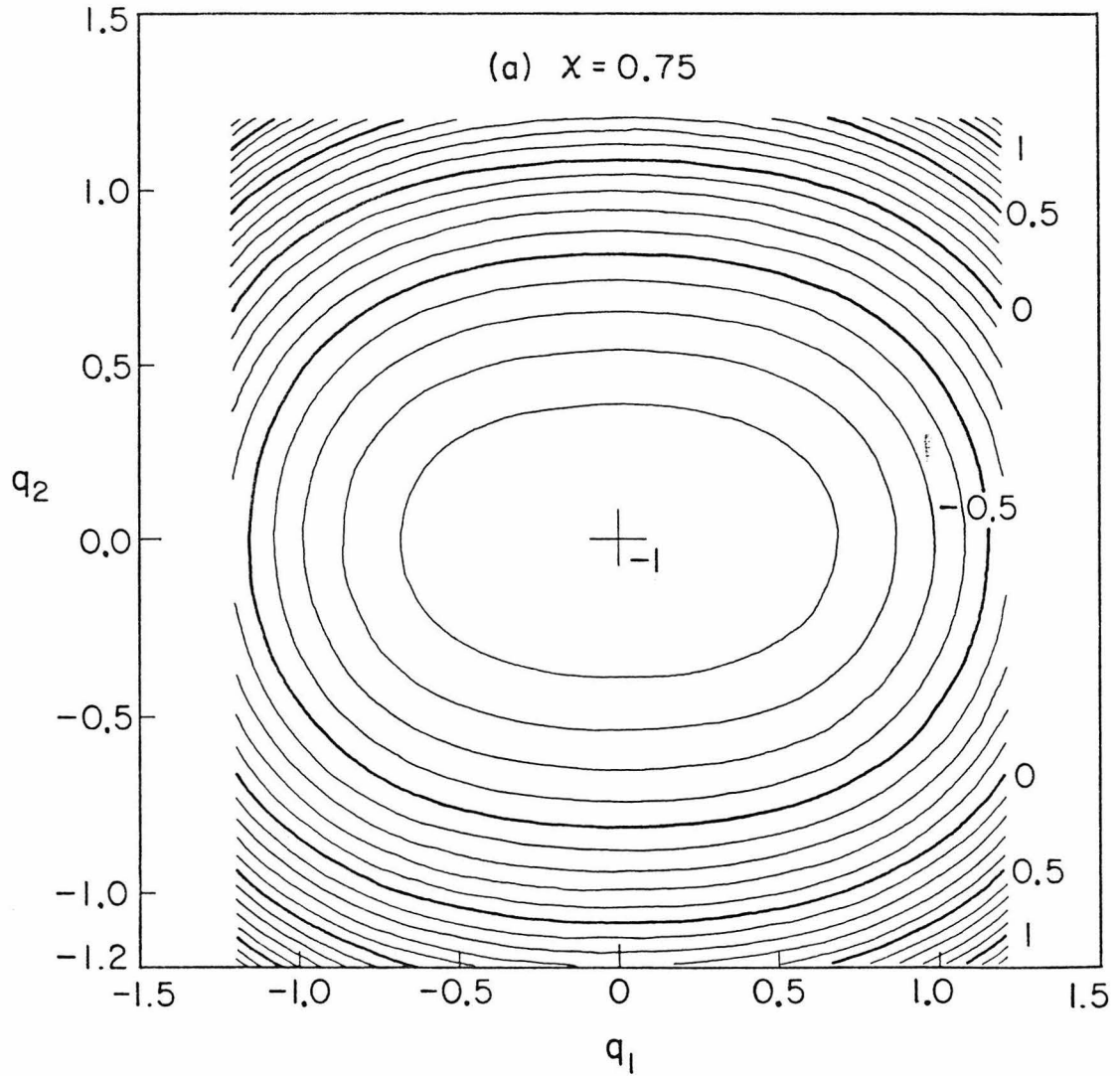
Figure 7

Figure 8.

Contour plot of the static Hamiltonian H($\mathbf{q},\mathbf{p} = 0$), for the SU(3) model. $\chi = 2$, with two minima.
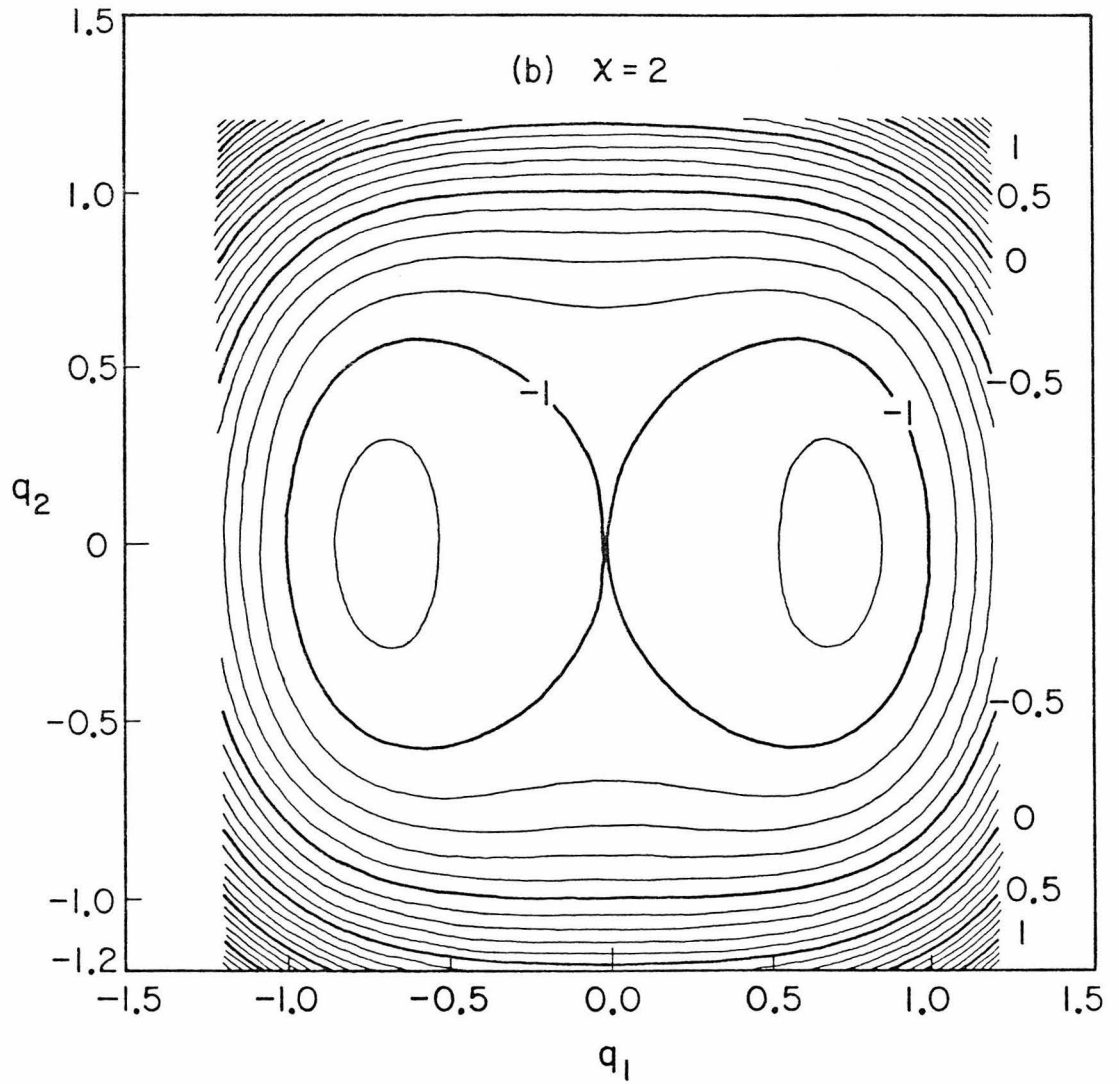
Figure 8

Figure 9.

Contour plot of the static Hamiltonian $H(\mathbf{q}, \mathbf{p} = 0)$, for the SU(3) model. $\chi = 10$, with four minima.

(c). $X = 10$
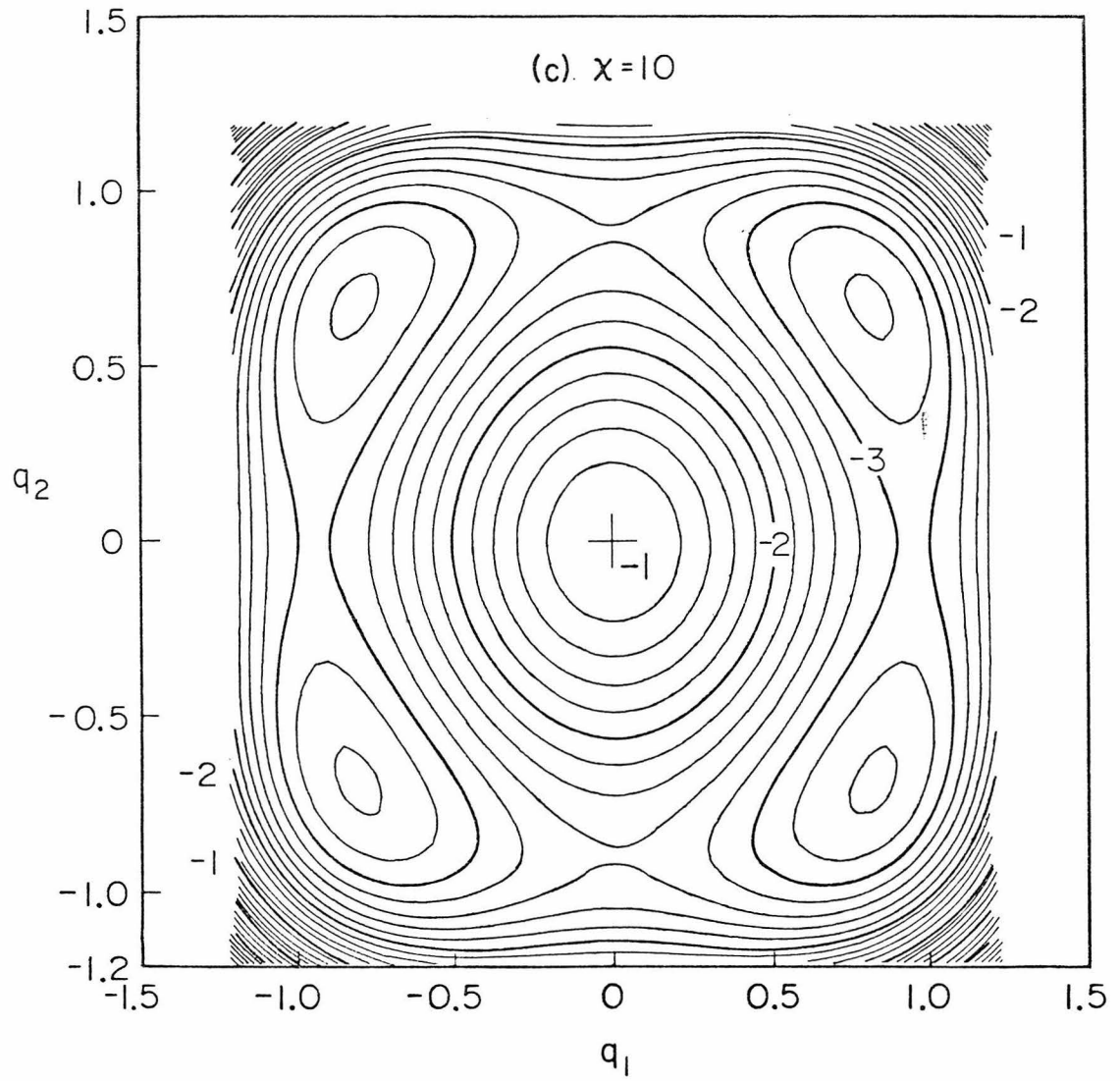
Figure 9

Figure 10. (2 pages)

Trajectory in **q** space (left) and surfaces of section (center and right) for the SU(3) model with $\chi = 10$ for a progression of excitation energy. (a) Harmonic, (b) Quasiperiodic, measurable by plane surface of section, (c),(d) Quasiperiodic, unmeasurable by plane surface of section, (e),(f) Stochastic. Note change of scale in (f).
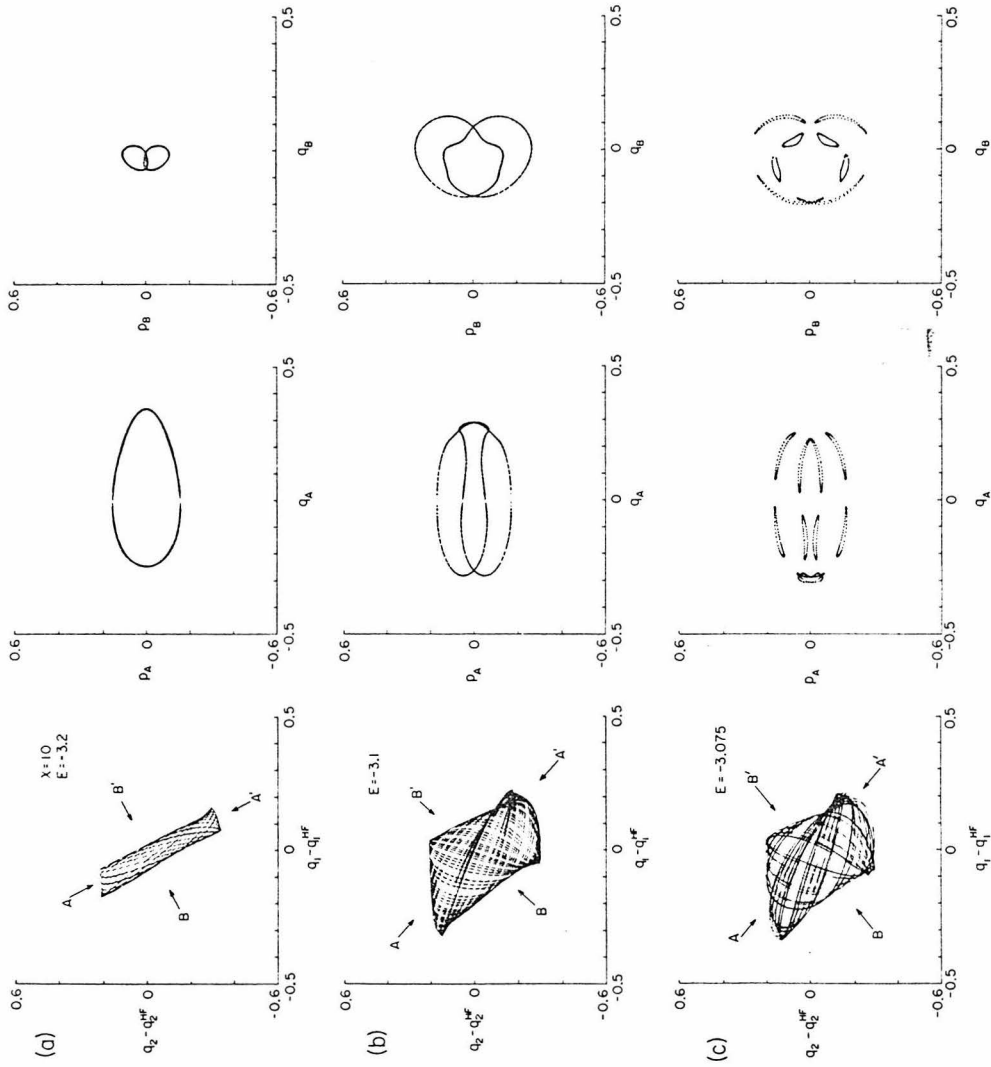
Figure 10
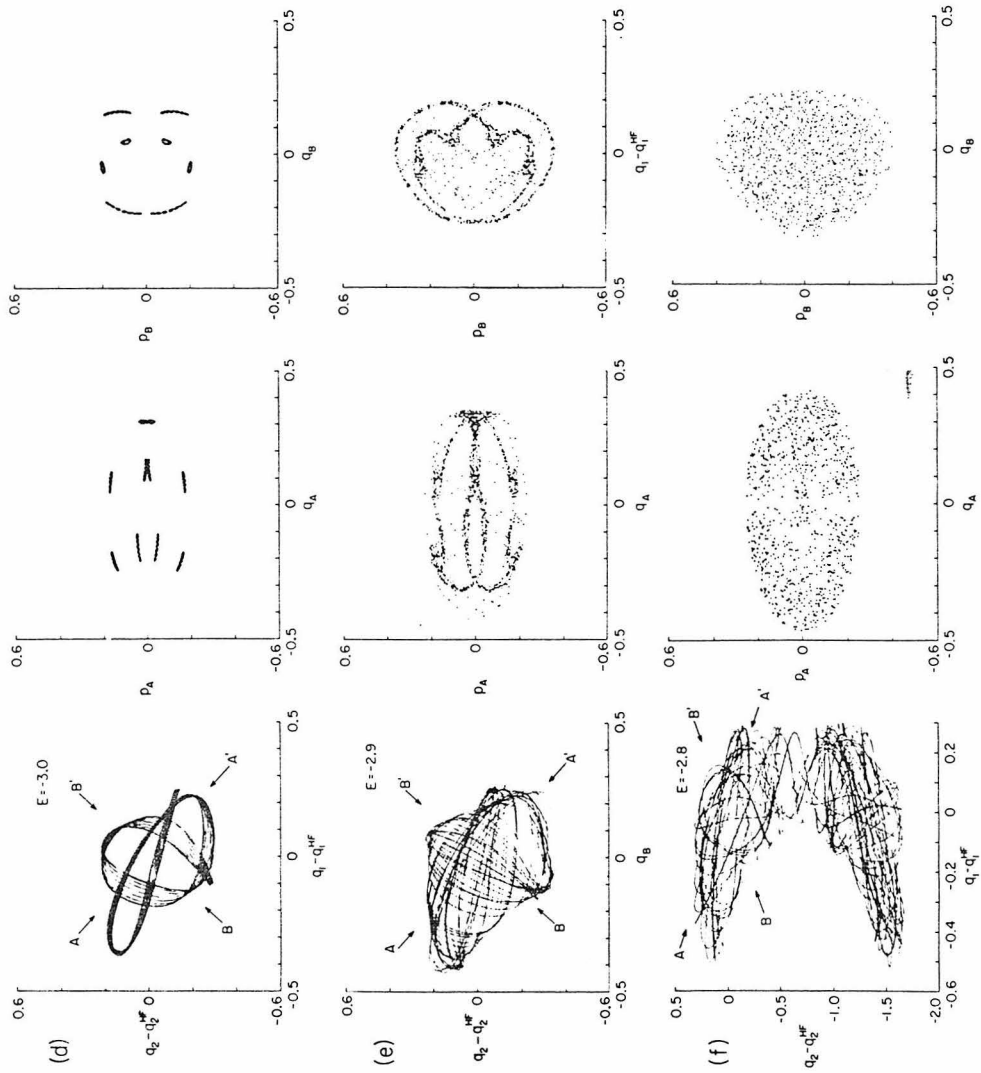
Figure 10 (cont'd)

Figure 11.

Energy contours in action space for the SU(3) model with $\chi = 10$. Solid lines from surfaces of section, and dashed lines from the Birkhoff-Gustavson power series (Table 4). Semiclassical energy levels lie at the grid points marked, which have coordinates that are half integers divided by the number of particles $N = 60$. The shaded region and the top left of the figure were ergodic or unreachable.
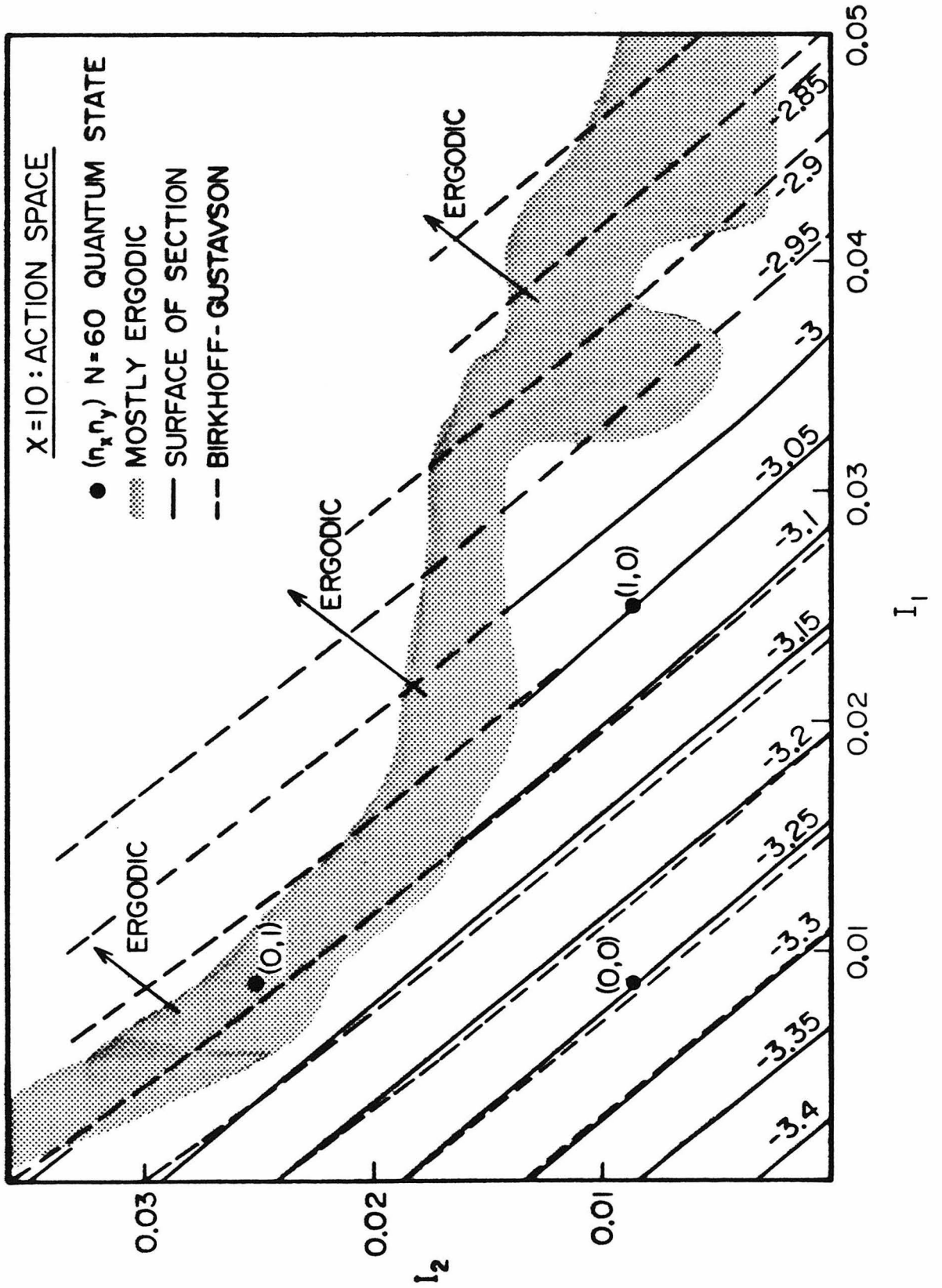
Figure 11

Figure 12.

Energy levels for the SU(3) model, $\chi = 0.75$. There are eight sets of four columns; each set corresponds to a particular number n_1 of oscillator quanta (0-7) while n_2 increases vertically. The four columns are: SE, shifted exact levels (to remove zero-point energy); SS, surface of section method; BG, Birkhoff-Gustavson method; RPA. The (shifted) Hartree-Fock energy is marked, and also the (shifted) saddle energy where it becomes energetically possible for the trajectory to cross into another basin of attraction.
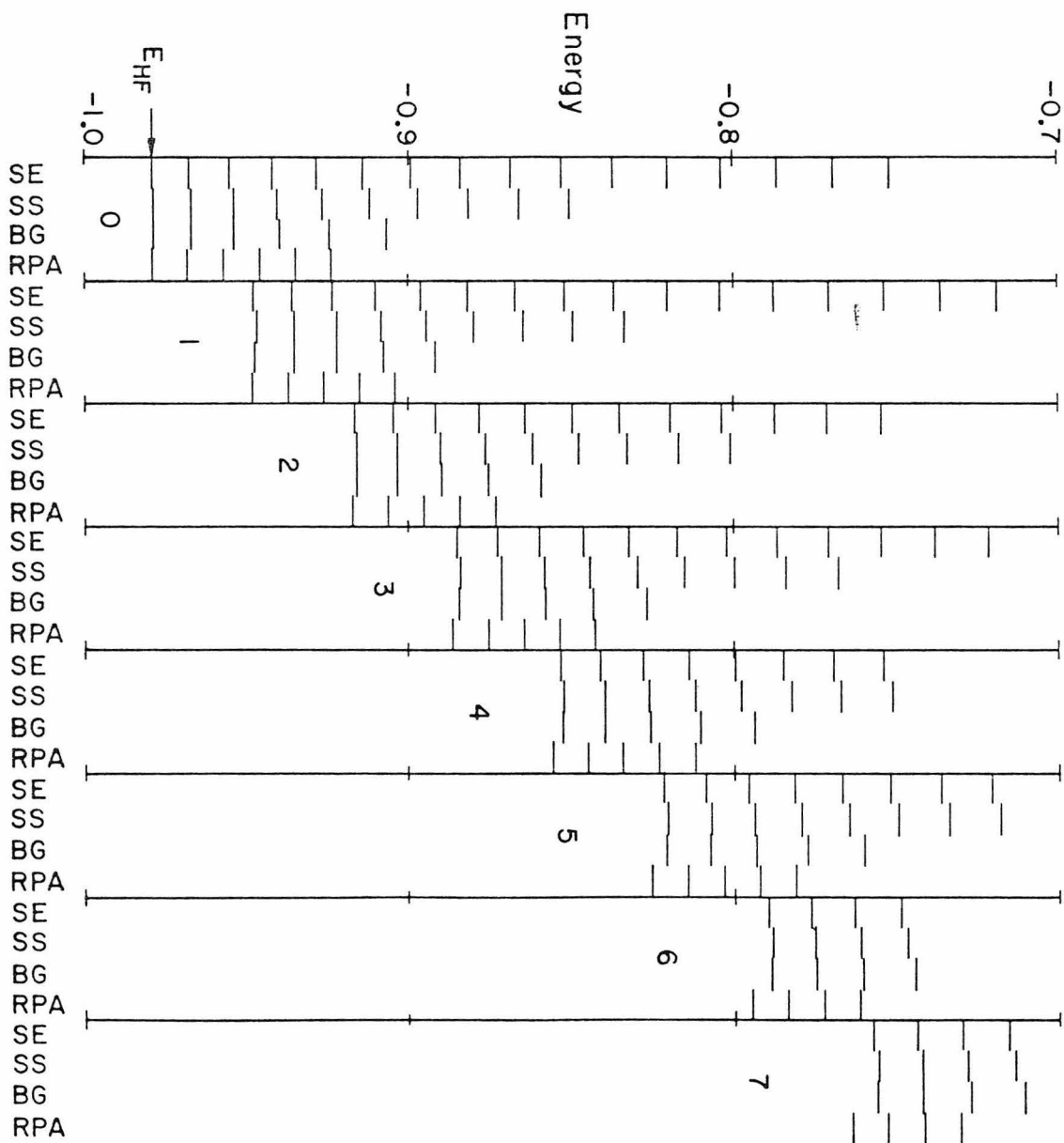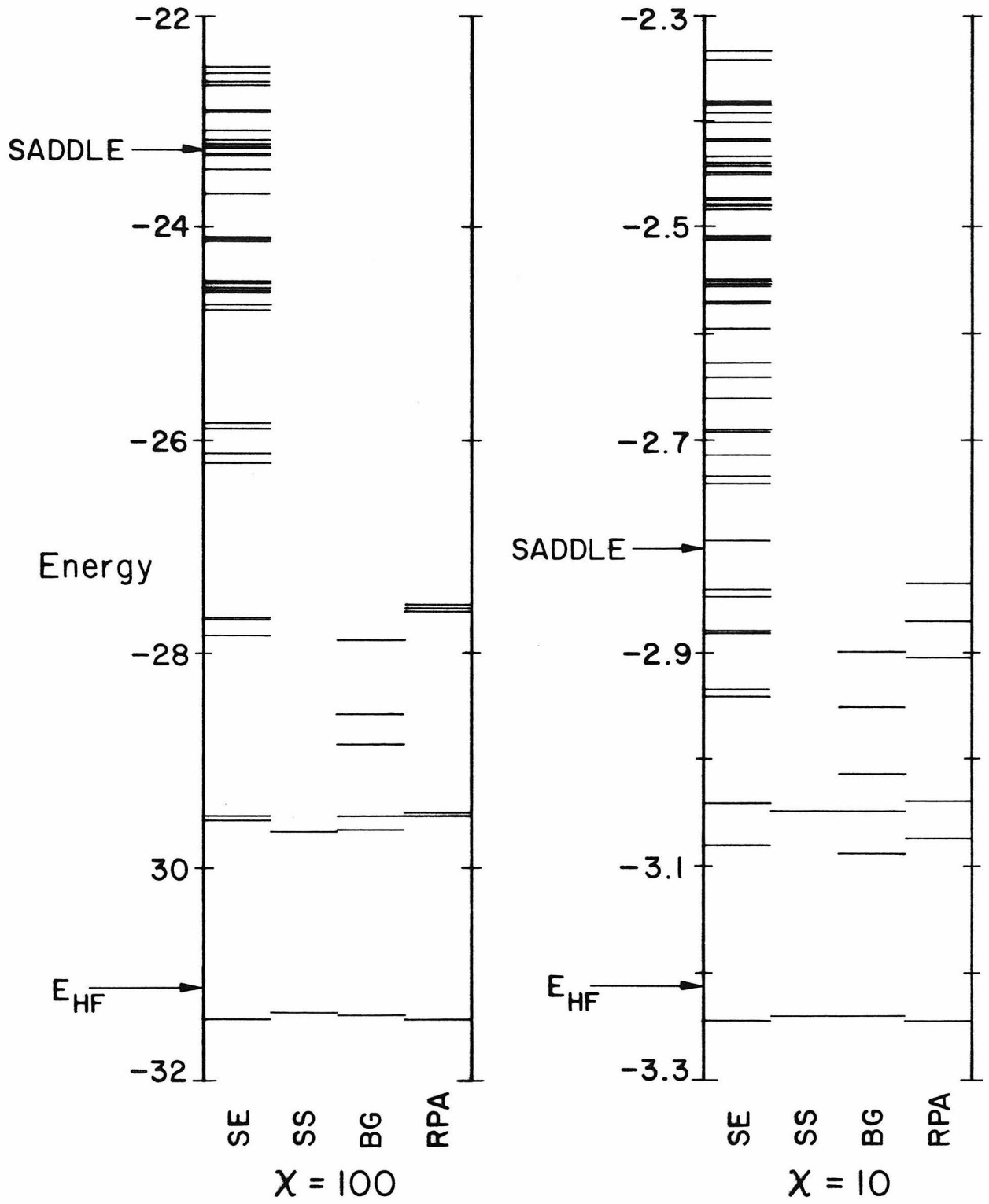
Figure 12

Figure 13.

Energy levels for SU(3) model, $\chi = 10$ and $\chi = 100$. Each set of four columns is as in Figure 12. The (shifted) Hartree-Fock energy is marked, and also the (shifted) saddle energy where it becomes energetically possible for the trajectory to cross into another basin of attraction.

Figure 13

Figure 14.

Energy levels of the walled Henon-Heiles system against ε. For $\varepsilon = 0$, the spectrum is that of a two-dimensional harmonic oscillator, and for $\varepsilon \to \infty$, it is that of a free particle in a triangular enclosure. The solid lines are perturbation expressions from Table 2, and the dashed lines a freehand interpolation. Levels are non-degenerate unless marked otherwise.
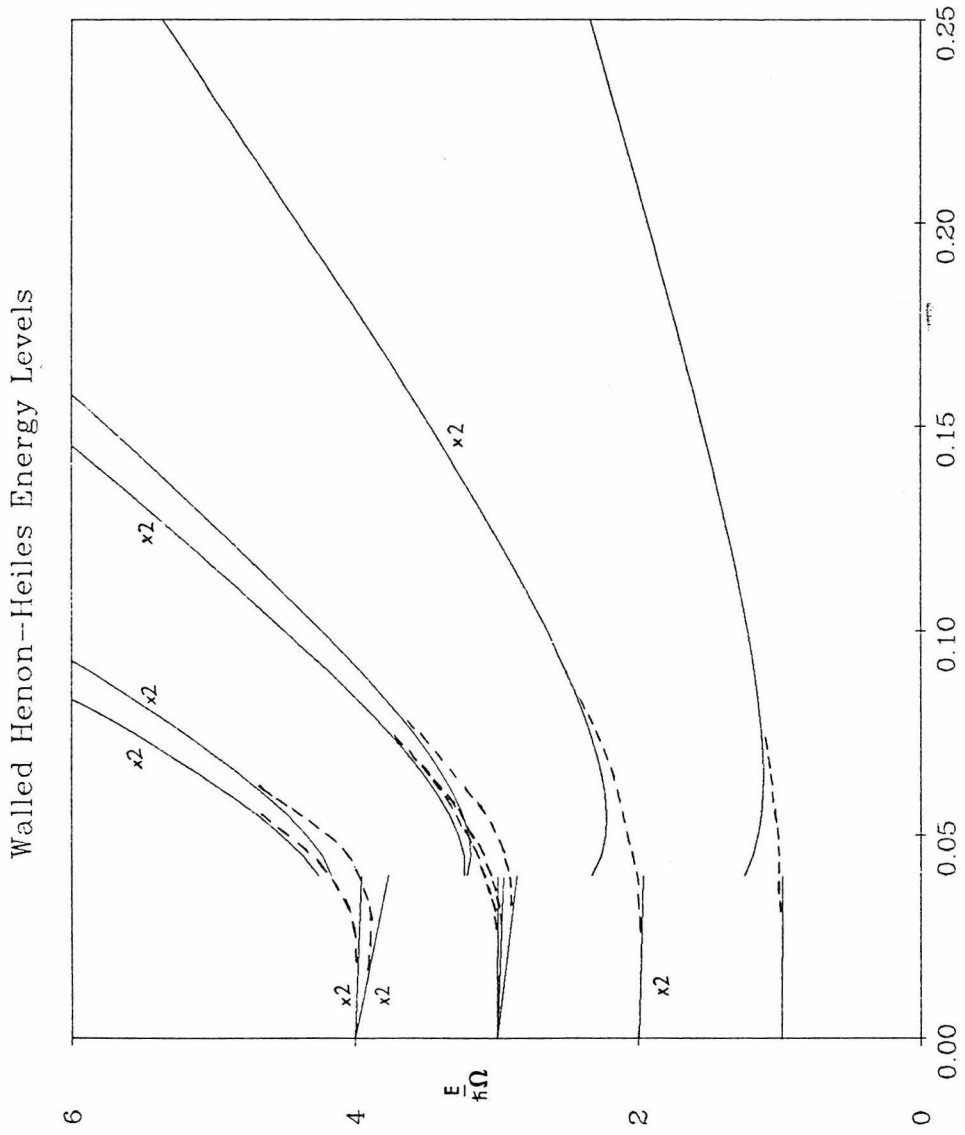
Walled Henon–Heiles Energy Levels

Figure 14

Figure 15.

Periodic trajectories of the Henon-Heiles system. Each point of a solid line is the initial condition for a periodic trajectory, with frequency varying continuously along the line. The thin lines are unstable, the thick lines stable. A very short segment of stability is a blob. The area shown is one sixth of the plane: the rest can be obtained by symmetry operations. The contour $E = 1/6$ is shown by a dashed line. Bifurcations are marked by the rational value of $\nu/2\pi$.
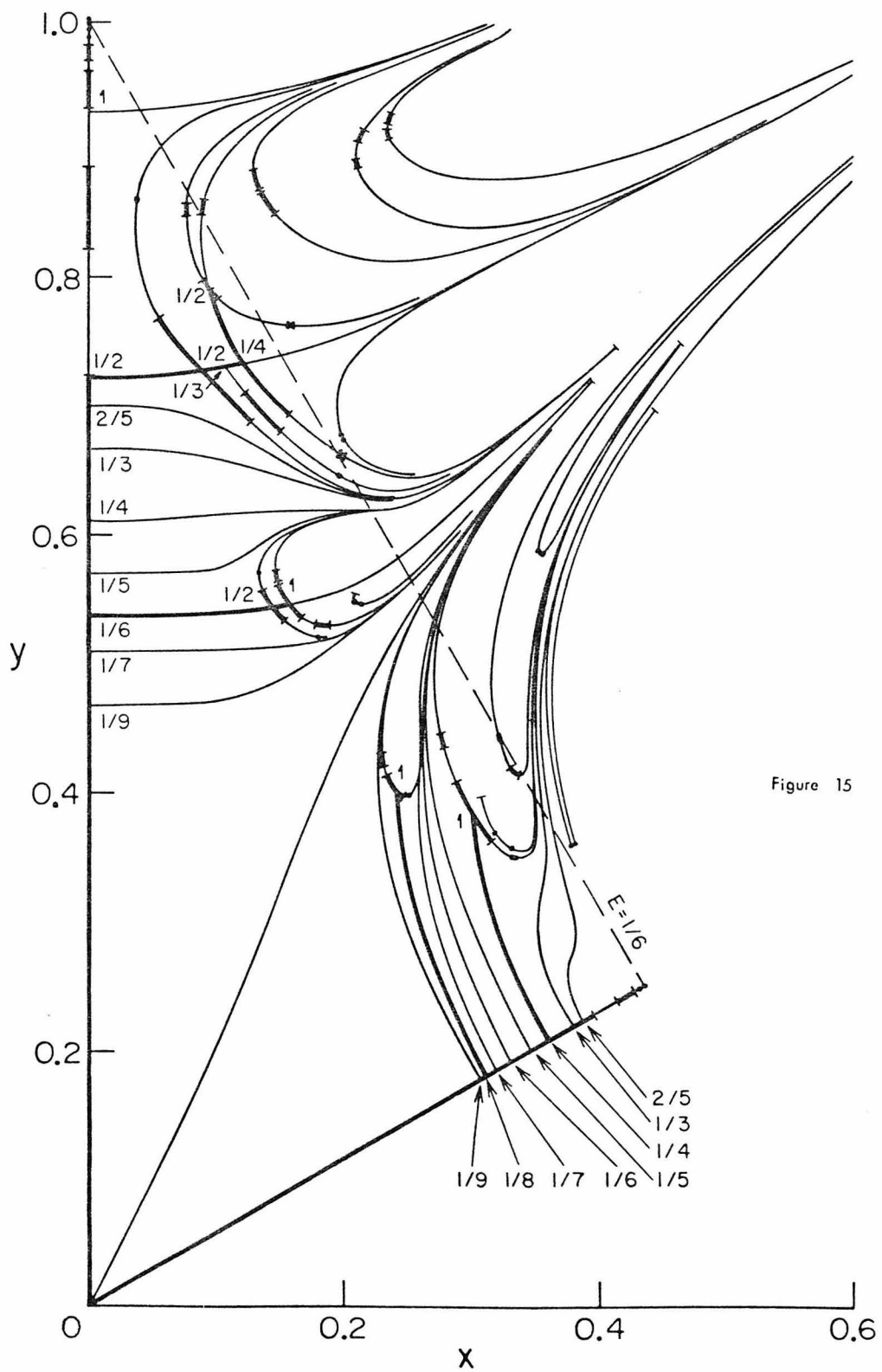
Figure 15

Figure 16.

Detail of a bifurcation sequence. The left part is a copy of part of Figure 15, and defines the points A, B, C, D, E, which are marked as such in Table 5. The abscissa for the side panels is a scaled x or y coordinate, and the frequency and stability are shown. There is period-doubling at B and D, and the same period for the bifurcation C. There is a "Double" bifurcation between B and C (see §13).
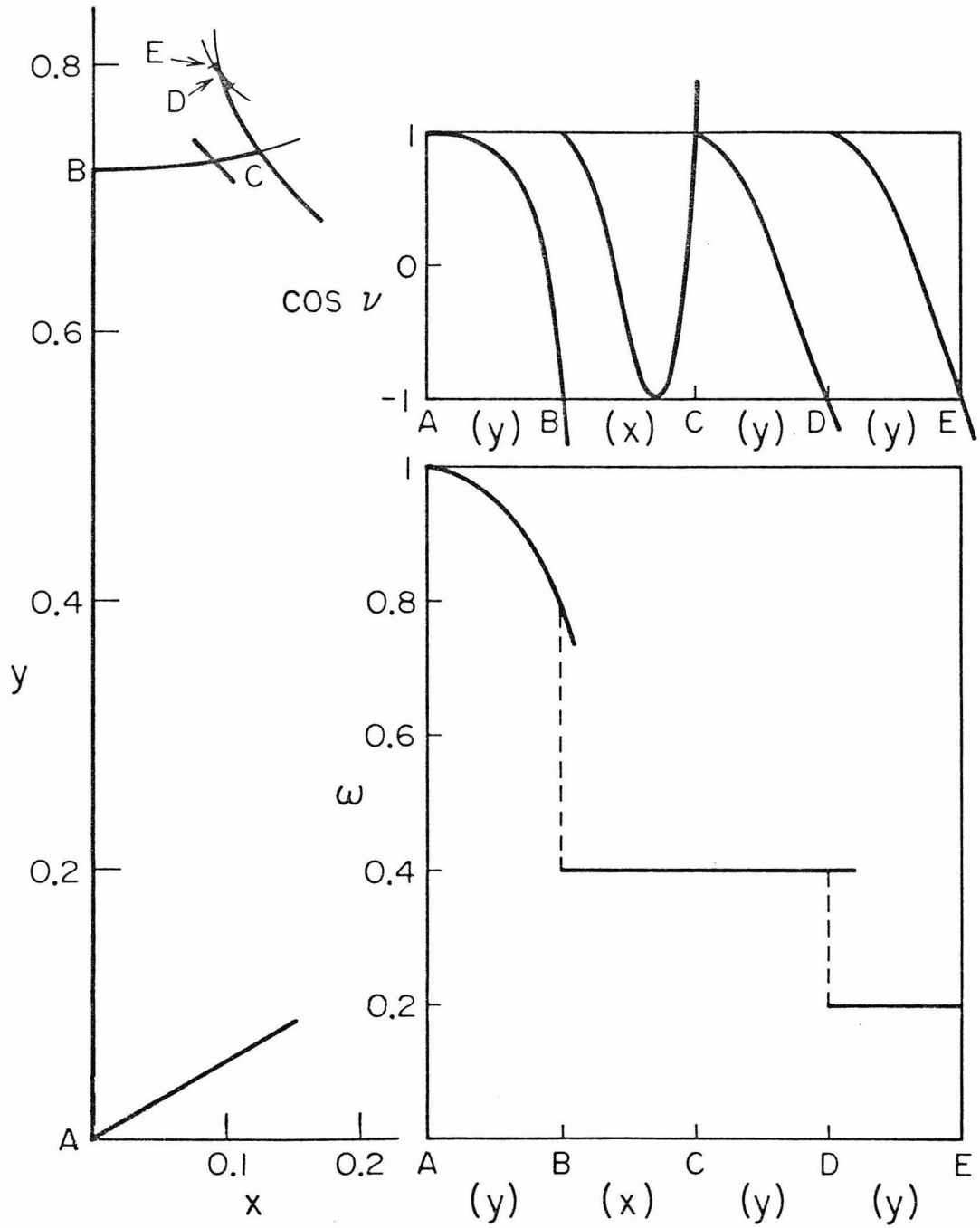
Figure 16

Figure 17.

Zero-point energy of harmonic oscillations transverse to the periodic trajectories, against stability. Quantity plotted is $\left| \frac{\omega^2}{2\pi} \frac{d\nu}{d\omega} \right|$, against $\cos \nu$. Only trajectories on the y-axis have low enough energy to be on this scale.
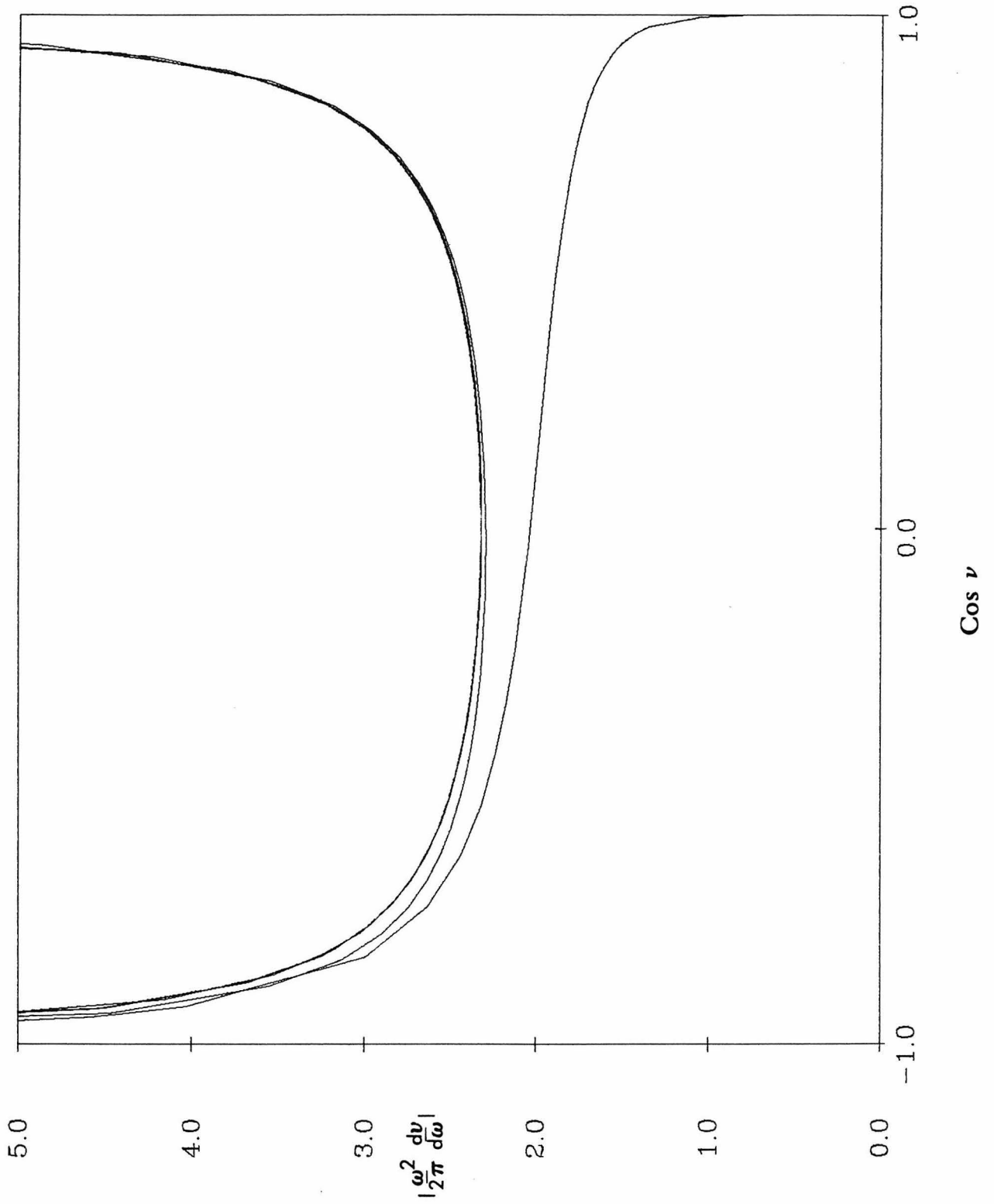
Figure   17